MASTERARBEIT/ MASTER`S THESIS

Titel der Arbeit/Title of the Master`s Thesis

"Sedimentary petrography of Keuper sandstones from the St. Veit Klippenzone of Vienna in comparison to the dislodged slices at the base of the Göller nappe"

verfasst von/submitted from

Martin Hujer BSc.

angestrebter akademischer Grad/in partial fulfilment of the requirements for the degree of

Master of Science (MSc)

Wien, 2018/ Vienna 2018

Studienkennzahl laut Studienblatt/ degree programme code as it appears on the student record sheet	A 066 815
Studienrichtung laut Studienblatt/ degree programme as it appears on the student record sheet	Erdwissenschaften
Betreut von/Supervisor	Ao.Univ.-Prof.Dr. Michael Wagreich

Acknowledgment

First of all, I would like to thank my parents for their support during the last years. Special thanks to my advisor Ao.Univ.-Prof. Dr. Michael Wagreich and to Prof. Mag. Dr. Susanne Gier, Prof. Dr. Michael Götzinger, Prof. Dr. Patrick Meister for their help and advice. My brother Wolfi and his wife Gitti must also be thanked very much at this point. Without them, this thesis would have been not possible in this form. Last but not least, I would like to thank Kathi and Lucy for their help during proofreading.

Contents

1. Abstract

Late Triassic Keuper sandstones from the St. Veit Klippenzone of Vienna, predominantly medium to coarse-grained in composition, were compared in detail with the dislodged slices of Lower Austria, which occasionally crop out along the base of the Göller nappe. These tectonic slices form intercalations of the terrigenous Keuper within the nappe-pile of the Northern Calcareous Alps, which are predominantly characterized by carbonate sedimentation. Taken together, these occurrences represent rare, non-metamorphic and poorly investigated Keuper sediments within the Austrian part of the Eastern Alps.

The petrographic analysis identified the rocks as quartz-rich, moderate to poorly sorted litheranites, sublitharenites, feldspathic litharenites and lithic subarkoses. Rock fragments mainly consist of polycrystalline quartz with inclusions of primary mica. According to their mineralogical maturity index (MMI), the samples can be regarded as submature to mature. In some cases, the samples are heavily quartz-cemented. Sporadic calcite cement was also observed. Geochemically, the rocks were classified as sublitharenites, subarkoses and quartz arenites. All samples show SiO_2-contents above 90%. The CIA-values revealed that the samples are intermediate to extremely weathered. Provenance analysis after Dickinson and Suszeck (1983) identified a recycled orogen as the most probable source of the clastic material. Results clearly indicate a derivation from igneous (granites), metamorphous (gneisses, schists) and sedimentary (sandstones) rocks. Sedimentary processes could be illustrated by e.g. trace element analysis, which indicates high degrees of sorting and recycling due to long, fluviatile transport. The samples were deposited at a passive continental margin. The heavy mineral assemblage mainly consists of zircon, rutile, tourmaline and strong varying amounts of garnet. Monazite, anatase, baryte/celestine and others only occur occasionally.

In general, the samples show much in common with sandstones whose compositions are derived from stable cratonic sources with overlying sediments and long fluvial transport. By considering the “Nordic-Keuper” concept proclaimed by Behrens (1972)

and Köppen and Carter (2000) and the results obtained for this thesis, a long fluvial transport from northern regions, most probably from the Fennoscandian Shield, during Carnian to Norian times must be assumed.

1.2 Zusammenfassung

Mittel bis grobklastische, spät-triassiche Keupersandsteine der St. Veiter Klippen-zone bei Wien wurden mit den sog. Schürflingen, welche an der Basis der Göller-decke stellenweise hervortreten, detailliert verglichen. Diese tektonischen Scherlinge repräsentieren grobklastisch-terrigene Keupereinschaltungen innerhalb der durch überwiegend karbonatische Sedimentation gekennzeichneten nördlichen Kalkalpen. Zusammengenommen stellen diese Sedimentgesteine spärlich auftretende, nicht metamorphe und bis dato wenig untersuchte klastische Keupervorkommen innerhalb des österreichischen Anteils der Ostalpen dar.

Petrographische Analysen identifizierten diese Sandsteine als sehr quarz-reiche, mäßig bis schlecht sortierte Litharenite, Sublitharenite und lithische Subarkosen mit insgesamt hoher mineralogischer Maturität. Fallweise sind die Proben stark quartz-zementiert. Auch sporadisch auftretender Kalkzitzement wurde beobachtet. Die Gesteinsfragmente bauen sich zum überwiegenden Teil aus polykristallinem Quarz mit Glimmereinschlüssen auf. Geochemisch wurden die Proben als Sublitharenite, Subarkosen und Quarzarenite klassifiziert. Alle Proben zeigen einen SiO_2-Gehalt von über 90%. Eine Provenanzanalyse nach Dickinson und Suszeck (1983) ergab ein erodierendes Gebirge („recycled orogen“) als wahrscheinliches Urspungsgebiet des klastischen Materials. Als Liefergesteine konnten eindeutig Magmatite (Granite), Metamorphite (Gneise, Schiefer) und Sedimentite (Sandsteine) ausgemacht werden. Sedimentäre Prozesse konnten anschaulich durch z.B. Spurenelementanalysen dargestellt werden, welche ein hohes Maß an Sortierung aufgrund von langem, fluviatilem Transport andeuten. Die Proben wurden in einem passiven, tektonischen Regime abgelagert. Die Schwerminalzusammensetzung setzt sich zum über-wiegenden Teil aus Zirkon, Rutil, Turmalin und stark variierenden Gehalten von Granat zusammen. Untergeordnet kommen auch Monazit, Anastas, Baryt bzw.

Cölestin und andere vor.

Insgesamt zeigen die Proben große Gemeinsamkeiten mit Sandsteinen, deren Zusammensetzung von stabilen Kratonen mit auflagernden Sedimenten und langem fluviatilem Transport abgeleitet werden kann. Unter Berücksichtigung des „Nordischen Keuper"-Konzeptes, welches von Behrens (1972) und Köppen und Carter (2000) vorgestellt wurde und den Ergebnissen dieser Arbeit, muss als wahrscheinlichstes Urspungsgebiet die ursprünglich nördlich des Germanischen Beckens gelegene Fennoskandische Hochzone angenommen werden.

2. Introduction

This study aims for a better understanding about Late Triassic Keuper sediments, more precisely about the characteristic sandstones or conglomerates, which are part of the stratigraphic succession of the St Veit Klippenzone of West Vienna. Although a recent investigation has taken place during the ÖBB`s Lainz Tunnel project in 2012 (Pfersmann 2013), that clarified some controversies, the geological origin, depositional history, tectonic setting and modal composition of these sediments remained unclear. Additionally, a detailed comparison between samples from the Lainz tunnel section and rare surface outcrops of Keuper sediments, which are also referred to the St. Veit Klippenzone (e.g. at Ober St. Veit, Vienna), is still missing.

The St. Veit Klippenzone of Vienna is currently interpreted as a western extension of the Carpathian Pieniny Klippenbelt (Pfersmann 2013). The quartzite Keuper sandstones and conglomerates form its oldest sedimentary units and have been, as the Klippenzone itself, interpreted differently throughout the time of geological research. During the nineteenth and twentieth century, several authors either assumed a Liassic or Late Triassic age by referring these rocks to the Gresten beds (e.g Trauth 1930, 1950, Janoschek 1956) or to Carpathian Keuper formations (e.g. Wessely 1967, Prey 1975). Due to the absence of index fossils, the exact age of these characteristic rocks is rather inaccurately defined and mostly results from their stratigraphic context. According to Pfersmann (2013), a Late Triassic age is very probable but he also considered the possibility of an early Jurassic age. In general, it is accepted as a whole that these sediments represent Upper Triassic Keuper deposits (e.g. Wessely 1967, Prey 1975, Wessely 1975), although a valid clarification by modern data is still pending.

Additional occurrences of coarse-grained, quartz-dominated Late Triassic Keuper sandstones, the “off thrusts” of the Northern Calcareous Alps, were included and also compared to the Keuper sandstones of the St. Veit Klippenzone. These rocks were dislodged from their original position during orogenic, nappe-building processes and represent an extra alpine facies within the nappe-pile of the Northern Calcareous

Alps (Hertweck 1961). It is assumed that Keuper sandstones of the St. Veit Klippen-zone and the dislodged slices are very similar or even identical in terms of their age, geological background, tectonic setting and composition. Also, these rocks are believed to represent a western continuation of the Westcarpathian Keuper (e.g. Wessely 1967, 1975, 1992, Kröll et. al 1993 etc.).

These facts together give the following objective for this study:

1. To establish a detailed comparison between presumed Keuper sandstones of the Lainz Tunnel section and samples from different surface sources, which are also referred to the St. Veit Klippenzone. As examples may be mentioned: Ober St. Veit (Gemeindeberg), Lainz Tiergarten (Hermes Villa) and Roter Berg (Nothartgasse).
As a result, these sporadic occurrences are to be definitively assigned to the St. Veit Klippenzone.

2. To also include different rare occurrences of Keuper (?) sandstones, the dislodged slices (germ. “Schürflinge”) of the Northern Calcareous Alps into this study. Strong similarities to the St. Veit Klippenzone sandstones and Western Carpathian units are considered, and furthermore, any actual data for these rocks are completely missing. A clarification could provide new information about Keuper sediments within the Austrian Eastern Alps and their relation to Westcarpathian Keuper units.

3. To get more information about the age of these rocks. A number of authors assumed a Liassic or Late Triassic age, so this work additionally compares Keuper sandstones with chosen samples of Gresten sandstones to obtain differences in terms of composition, maturity, tectonic setting, etc.

3. Geological background

3.1 Keuper sediments of the Austrian Eastern Alps and surrounding units

After the deposition of the carbonate Muschelkalk sediment series in Middle and Western Europe, which were induced by an overall sea-level rise of the western Tethys during the Middle Triassic, a significant sea-level drop, beginning at the Carnian, led to the development of the clastic-evaporitic Germanic Triassic Keuper. The mainly fluvial-terrigene Keuper facies, with its main depositional areas situated within the Germanic and Carpathian basin, also occupied northern shelf areas of the Western Tethys consisting of shallow marine sediments (Alpine domain). Deposition mainly occurred under semi-arid to semi-humid conditions. It is assumed, that transportation of clastic material mainly occurred from the north, the Fennoscandian Shield, and the east, the Vindelician – Bohemian High (Fig.1). Due to the strong clastic influx, accompanied by a reduced rate of subsidence, the marine connections to the Western Tethys were closed (Brandner 1984, Faupl 2003, Al – Jaboury 2007).

For the Alpine-Carpathian realm of the Triassic, two main facies zones are present: a continental and shallow-marine carbonate platform development at the northern European margin (today within Pennine, Lower- and Middle Austroalpine units and Tatric, Fatric, Veporic units of the Western Carpathians) and a local pelagic slope facies in southern regions (Northern Calcareous Alps, Hronic slilicic nappes of the Western Carpathians) (Häusler et. al 1993). In the south, this sector was bordered by the Hallstatt-Meliata Ocean, which closed during the Jurassic (Mandl 2000).

The clarification of the Eastern Alpine-Carpathian connection was preceded by long-lasting controversial debates, which are primarily caused by the existence of distinctive differences between Eastern Alpine- and Carpathian tectonics. The covering of the Eastern Alpine-Carpathian junction by the Neogene sediment series of the Vienna Basin has not made research easier in recent decades. Therefore it must be noted, that parallelizations are primarily based on stratigraphic-facial rather than structural similarities. However, characteristic Keuper sediments, which are

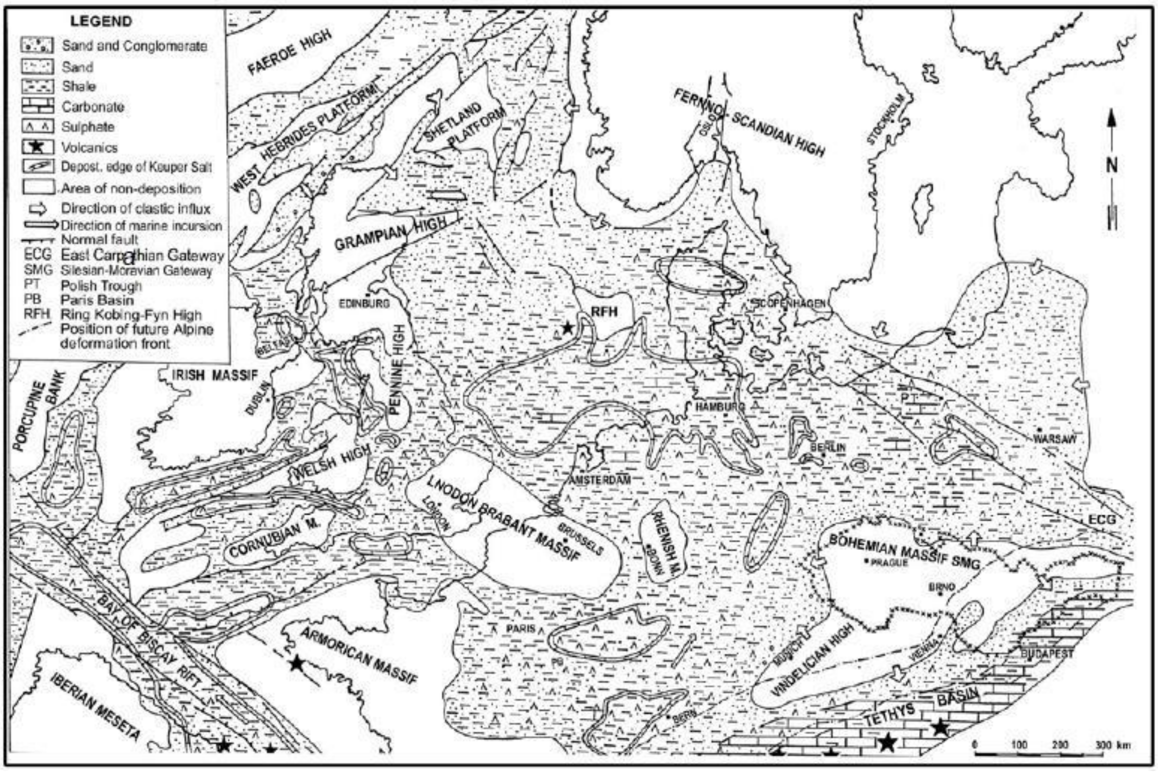

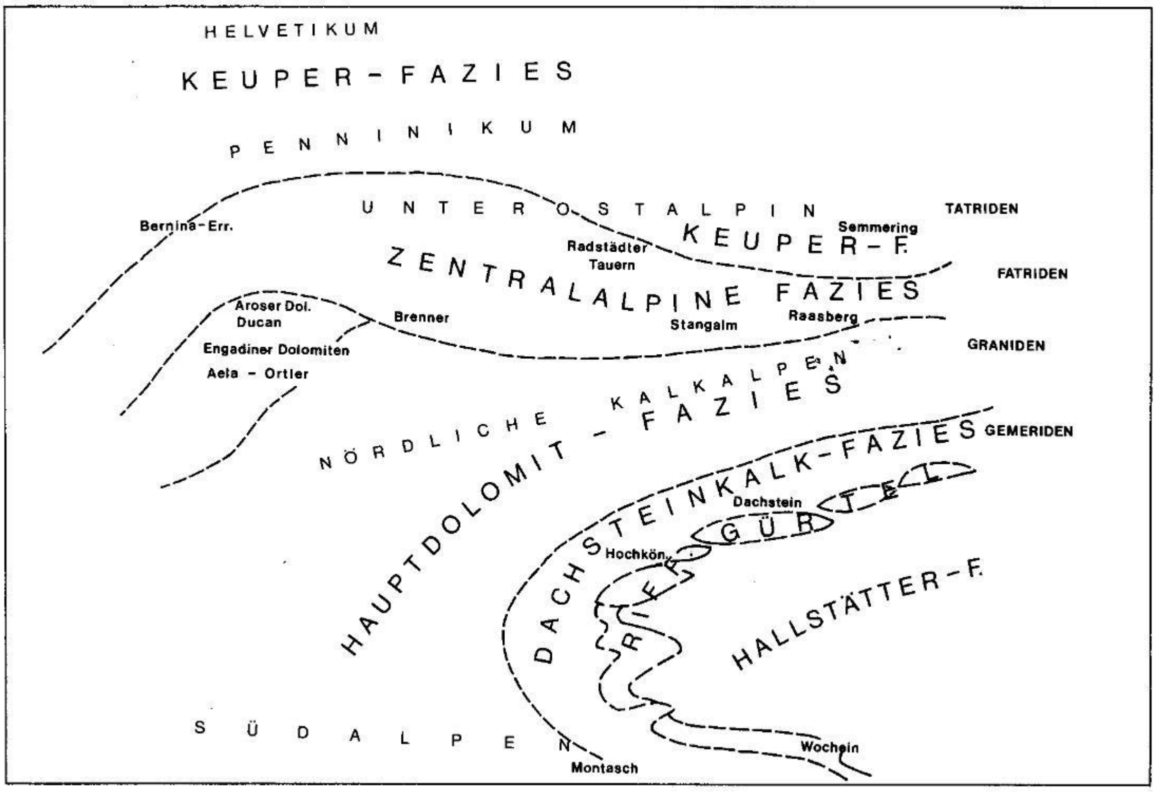

Fig.1 Upper fig.: Keuper sediment distribution during the Carnian – Norian (from Al – Juboury 2007); lower fig.: Paleogeographic sketch of Keuper sediments within tectonic units of the Alps

fragmented on various tectonic units within the Alpine-Carpathian belt, have been often regarded as an indicator for equivalence of certain Eastern Alpine and Western Carpathian units (e.g. Tollmann 1965, 1971, Wessely 1992, Kröll et. al 1993, Häusler et. al 1993, Pfersmann 2013). Originally, it was assumed that there was no continuation of the Westcarpathian Pieniny Klippenbelt in the west of the Vienna basin (e.g. Golonka and Picha 2006). According to Pfersmann (2013), the St. Veit Klippenzone represents a western tectonic continuation of the Pieniny Klippenbelt, which therefore clearly continues below the Vienna Basin to the west of Vienna. Large facial similarities were observed in Lower Australpine units (Semmering, Radstädter Tauern) and northern units of the Northern Calcareous Alps, mainly expressed by common occurrences of Keuper sandstones, Rhaetian Limestones and Jurassic sediments. Also, e.g. due to their characteristic Keuper facies, both of these units (Lower Austroalpine of the Semmering area, the Frankenfels-Lunz nappe system) show strong facial affinity to the Križna nappe system of the Western Carpathians (e.g. Tollmann 1971, Wessely 1992, Kröll et. al 1993).

Generally, Keuper sediments in Austria form occurrences within Penninic- (central and western Tauern Window) and Lower Austroalpine units (Semmering) consisting of metamorphous colored shales, quartzites, gypsum, dolomites, sandstones and conglomerates (Oberhauser 1980). Sporadic occurrences of dolomite, clay and sandstones also occur as intercalations within northern units of the Northern Calcareous Alps, whereas clays and sandstones represent terrigenous input from the European hinterland during the carbonate sedimentation of the Late Triassic. (e.g. Fuchs 1985, Wessely 1989, 1992, 2014, Mandl 2000). For the Austrian Helvetic units no Triassic formations are known (e.g. Faupl 2003). In general, it is believed that Austrian Keuper formations are facially closely linked to Western Carpathian Keuper units (e.g. Tollmann 1965, Wessely 1975, Häusler 1993 etc.).

Clastic Keuper sediments within the Northern Calcareous Alps only occur sporadically and are represented by thin-layered intercalations of shales and sandstones within the Frankenfels nappe (e.g. Wessely 1992, 2014) and by so called “dislodged slices” at the base of the Göller nappe (e.g. Wessely 1975, Plöchinger 1979). These sandstones were dislodged from the Frankenfels nappe and incorporated within the Tirolic nappe system during orogenic processes (Hertweck 1961). Strong similarities between these occurrences, the Keuper sandstones of the St. Veit Klippenzone and Western Carpathian units (e.g. Drietoma unit of the Pieniny Klippenbelt) are assumed (e.g.Wessely 1967, 1975, Pfersmann 2013).

The Western Carpathians can be divided into two major zones tectonically: 1. the **Outer Carpathians**, consisting of the Carpathian Flysch belt and the Pieniny Klippenbelt; 2. the **Inner or Central Carpathians**: the “core mountain” belts, the Vepor and Gemer belts. The main units are the Tatricum, which includes the Variscian crystalline basement and its “Envelope” (the Late Paleozoic to Mesozoic sedimentary cover), the Mesozoic Križna nappe system (Fatricum), the Choč and higher nappe systems (Hronic-Silicic nappes). Upper Cretaceous and Tertiary post-nappe complexes are also involved (e.g. Plasienka et. al 1993).

Keuper deposits within the Western Carpathians can be found in Tatric (Envelope), Fatric, Veporic units, as well as in the Pieniny Klippenbelt consisting of a characteristic variegated shale-claystone complex with alternations of sandstones, conglomerates and dolostones (e.g. Al – Jaboury 2006). Clastic Keuper deposits are preferably exposed within the Mesozoic cover (Envelope) of the Tatricum, whereas in Fatric units carbonate sedimentation (dolomite, Kössen beds) is dominant (e.g. Plasienka et. al 1993). Due to the lack of index fossils, Keuper sediments are considered as rather stratigraphically inaccurately defined (e.g. Rychlisnki 2008, Jaglarz 2010). In general, a continental (littoral, shallow marine, lagoonal) palaeo-enviroment is assumed for the Keuper sediments of the Western Carpathians, whereas the sandstones and conglomerates are believed to represent fluvial deposits (e.g. Turnau-Morawska 1953, Al – Jaboury 1992, 2006, Rychlisnki 2008). Al – Jaboury (2006) classified Keuper sandstones of the Western Carpathians as quartzose litharenites, sublitharenites, subarkoses and quartz arenites, interpreting the metamorphic and igneous rocks of the crystalline cores of the Western Carpathians and the foreland of the Bohemian Massif as provenance. Subordinate contributions of feldspar were also observed by Rychlisnki (2008).

3.2 The Klippenzone of St. Veit and its Keuper sandstones

3.2.1 The Klippenzone of St.Veit

The St. Veit Klippenzone of West Vienna comprises Upper Triassic to Lower Cretacerous beds and is, based on actual data, currently regarded as the western succession of the Westcarpathian Pieniny Klippenbelt (Pfersmann 2013). Paleogeographically, a northern Austroalpine plate position is assumed. The stratigraphic succession, beginning with the oldest units, consists of:

1. **Upper Triassic** quartzite Keuper sandstones /conglomerates**:** colored, coarse-grained sandstones with kaolinitic matrix accompanied by colored clay
2. **Upper Triassic** dolomites
3. **Upper Triassic (Rhaetian)** fossil-bearing marls and limestones (Kössen Formation)
4. **Lower to Middle Jurassic** fossil-bearing sandstones, sandy and marly limestones, marls (Gresten Formation)
5. **Lower to Middle Jurassic** (“Posidonia”) marls and siltstones
6. **Middle Jurassic** sandstones, sandy limestones, shales and fossil-bearing limestones (Hohenauer Wiese Formation)
7. **Upper Jurassic,** red crinoid-bearing limestones of the Kimmeridgian
8. **Upper Jurassic,** coloured radiolarites (Rotenberg Formation)
9. **Upper Jurassic to Lower Cretacerous** aptychus limestones with cherts (Fasselgraben Formation)

Due to the low number of poorly exposed outcrops, which is caused by constant urban development, the tectonic position of the St. Veit Klippenzone was a subject of long-held discussions. Originally, a Helvetic/Ultrahelvetic (Gresten Klippenzone) or Penninic (Ybbsitz Zone) position was also considered. Some outcrops, which were discovered during construction work, vanished completely and were never investigated. Especially occurrences of e.g. Keuper sandstones of the Wienerwald area (e.g. at Hermesvilla) and Roter Berg do not exist anymore (see chapter 4). So the Lainz tunnel project in 2012 was a great opportunity to gain more information about the sedimentary strata of the St. Veit Klippenzone. This tunnel, constructed by the ÖBB to connect southern and western parts of the Viennese infrastructure, has a length of 3350 meters and cuts through rocks of the Rhenodanubian Flyschzone (Kahlenberg nappe) and the St. Veit Klippenzone, whereas Klippenstones outcrops within the tunnel show a total length of 1097 meters (Pfersmann 2013).

3.2.2 The Keuper sandstones and conglomerates (a historical review)

Griesbach (1869) described in detail quartz-dominated conglomerates, sandstones and other different rocks, which he referred to the St. Veit Klippenzone within the Wienerwald area around Ober St. Veit. According to Griesbach, the conglomerates and sandstones were mostly accompanied by Gresten limestones, therefore a Liassic age seemed very probable. Hochstetter (1897) and Trauth (1930) confirmed this observation. Janoschek (1975) mentioned outcrops of “Gresten arkoses” and marlstones at Roter Berg (approx. 1 km east of Gemeindeberg), which were exposed during construction work. In general, the rocks were described as hard, coarse-grained, bright, poorly sorted quartzite sandstones/conglomerates with white or brownish argillaceous matrix. Various amounts of colored quartz grains with diameters of 1 – 2 centimeters were investigated. In many cases, relations to coal-bearing Liassic Gresten beds had been established.

Wessely (1967) firstly referred these quartzites to the Upper Triassic Keuper. He mentioned strong correlations with similar occurrences of the Northern Calcareous Alps (dislodged Keuper sandstones) and the Drietoma unit of the Pieniny Klippenbelt. Prey (1975) followed this interpretation by comparing his samples to the Carpathian Drietoma unit. After all, Pfersmann (2013) completed this development in his conclusion about the Keuper sediments of the Lainz tunnel project.

The Keuper sediments of the Lainz Tunnel section are part of the stratigraphic succession of the St. Veit Klippenzone (Pfersmann 2013): medium to coarse-grained quartzite sandstones, moderate to poorly sorted, accompanied by greenish or reddish clay, have been found within the tunnel section of 1200 and 1300 meters (from entry LT31). The mineralogy of these rocks was very rich of quartz with lesser amounts of feldspar and kaolinite. However, the modal composition is based only on visual estimation. Heavy mineral analysis showed a strong dominance of zircon (56%) and monazite (16%) and lesser amounts of rutile (9%), garnet (6%) and tourmaline (3%). No contents of index-fossils could be found. Sporadic amounts of calcite cementation were observed. Due to similarities to earlier published data (e.g. Prey 1975) a Late Triassic age was assumed.

3.3 The dislodged slices – "Schürflinge"

Due to successive north-trending tectonic thrusting during the Lower Tertiary alpidic orogeny, these rocks were dislodged from their original nappe, lifted up and deposited between the partial nappes of the Oetscher nappe system. Hertweck (1961) firstly recognized these rocks as a strong indicator for the distances of over-thrusting between the nappes of the Northern Calcareous Alps. He described Upper Triassic to Lower Cretaceous occurrences of "dislodged slices" (germ. "Schürflinge") at the basis of the Reisalpen nappe, Göller nappe and the Unterberg nappe: Kössener beds, "Gresten arkoses", Gryphaeen limestones (Liassic Gresten limestones, Kalksburger beds, marls, aptychus limestones). He interpreted the Frankenfels nappe as the original nappe.

For the coarse-grained, mainly of quartz and feldspar composed "arkoses", which were found within the surrounding area of Nöstach, Rehgras and Agsbach (Lower Austria) Hertweck (1961) mentioned strong correlations to the Gresten Klippenzone. Therefore he assumed a Liassic age. The rocks were found as spotty occurrences, partially overlying on agricultural fields. Wessely (1965), at first, interpreted these rocks as Werfen quartzites of the Oetscher nappe.

During the next years, Wessely compared fine to coarse-grained dislodged quartzites from the area nearby Groisbach (Wessely 1967), Hinterbrühl – Enzersdorf, Nöstach and Heiligenkreuz (Wessely 1975) to the "Liassic Gresten sandstones" of the St. Veit Klippenzone. By recognizing strong similarities to Carpathian Keuper sediments of the Pieniny Klippenbelt he assumed a Late Triassic age. Since then the interpretation of these rocks as a westernmost succession of western Carpathian

Keuper units is overall accepted and can be found in several publications. E.g. Plöchiner (1979) gave following stratigraphic succession of the dislodged slices of Hinterbrühl of Lower Austria:

1. **Upper Triassic** Keuper quartzites and variegated shales around the area of the “Grillenbühel” and the “Hühnerkogel”
2. **Liassic** marls (“Fleckenmergel”) and siliceous marls of the same area as the Keuper quartzites
3. **Lower Cretacerous** grayish, coal-bearing marls

Outcrops of dislodged Keuper sandstones, which are located within the so called “Schürflingszone” of Lower Austria, follow the WSW-NEN striking base of the Göller nappe at following spots (beginning at western areas): between Rehgras and Agsbach, Groisbach, Mayerling, Steinfeld (south of Mayerling), Heiligenkreuz, Hinterbrühl – Maria Enzersdorf at the “Grillenbühel” (e.g. Tollmann 1967) (fig.2).

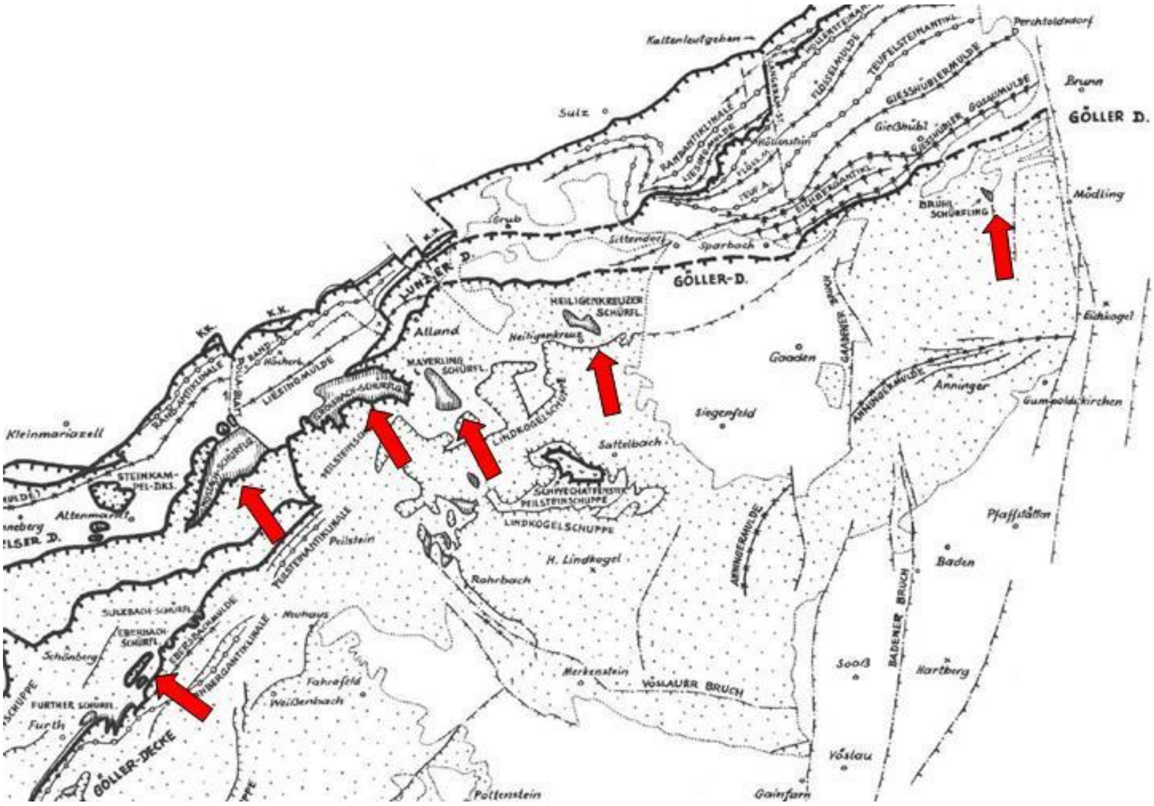

Fig.2 Outcrops of dislodged slices within the eastern part of the Northern Calcareous Alps (from Tollmann 1967).

4. Setting and sampling

4.1 Geographical and geological setting

4.1.1 The St. Veit Klippenzone

The Lainz tunnel, with its two main entries (LT33: Auhof, LT31: Lainz), is located in the western area (13th district) of Vienna and strikes with NW – SE heading direction through rocks of the Kahlenberg -, Hütteldorf Formation and the St. Veit Klippenzone (fig.3).

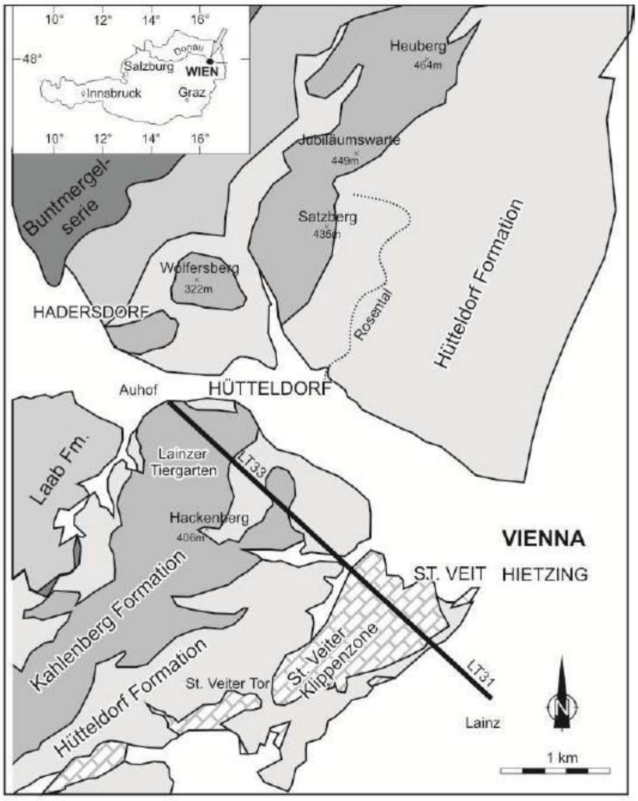

Fig.3 Geographical and geological position of the Lainz tunnel of western Vienna (from Pfersmann 2013)

Outcrops of the St. Veit Klippenzone, which are exposed at the surface, are rare, located at e.g. Roter Berg – nearby Nothartgasse, Ober St. Veit – Gemeinde-berg and the Lainz Tiergarten area nearby Hermesvilla (e.g. Trauth 1930, Janoschek 1956, Prey 1975).

Sampling of Keuper sandstones from the Lainz tunnel section occurred in 2012 by

Pfersmann. The rocks used in this study were taken from the archived collection of the Department of Geodynamics and Sedimentology of the University of Vienna including following samples: LT31/1164.5m, LT31/ 1200m, LT31/ 1215.5m, LT31/1277.2m (fig.4).

For searching and collecting of Keuper sandstones of the Klippenzone the geological map sheet “58 Baden” (1:50 000, Geological Survey of Austria) was used.

At Hermesvilla (Lainz Tiergarten) and Roter Berg no outcrops could be found. Therefore, sampling mainly took place at the **Gemeindeberg** of Ober St. Veit, where these rocks crop out in large numbers along paths and trails (e.g. at the crossroad Gemeindeberggasse – Hanschweg) what made them easy to find and to collect.
The rocks appeared very rich of quartz and often included colored quartz grains with a size of 1-2 centimetres. The size of the rock pieces was mostly once or twice of a human fist. A coarse (seldom medium) grained, overall poorly sorted, composition was investigated (fig.4).

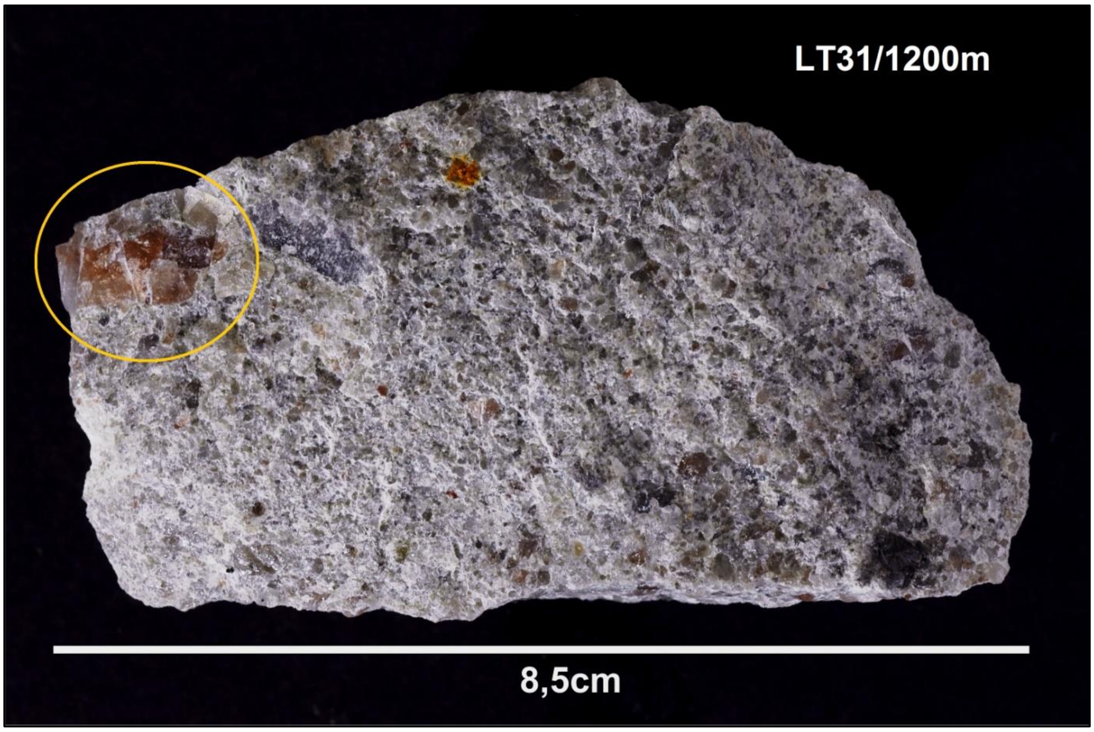

Fig.4 Samples, which are currently regarded as Keuper sandstones of the St. Veit Klippenzone,

LT31/1200m (previous page): coarse grained and poorly sorted; note the large, colored quartz grains; LT31/1215m: a medium grained, overall better sorted sample indicates a range of medium to coarse grained composition for the Keuper sandstones of the Lainz tunnel section; Ober St. Veit: coarse grained; poorly sorted; samples from the Gemeindeberg are mainly strongly weathered

4.1.2 Dislodged slices (Keuper?)

The sampling was carried out using the geological map sheets **"**58 Baden" (1:50 000) and "75 Puchberg am Schneeberg" (1:50 000) at Rehgras, Mayerling, Groisbach, Heiligenkreuz and Hinterbrühl – Maria Enzersorf within the "Schürflingszone" (locations, where these rocks are preferably exposed) of Lower Austria.

At the "Grillenbühel" of **Hinterbrühl**, next to Badgasse, tightly packed, greenish to grayish quartz-rich sandstones (fig.5) were found within small creeks, which were located inside a park. By following the Fürstenweg, east of Badgasse, reddish coarse-grained samples were found within an old bomb (?) crater.

North of **Heiligenkreuz**, overlying on agricultural fields, medium to coarse-grained grayish sandstones form a large occurrence ("Lesesteine"). Seemingly these loose stones were dug out by the use of farming machines. Red-colored quartz grains were also detected (fig. 6, 7).

At **Mayerling,** only a small number of samples were found. A single quartzite sandstone cropped out along a trail at the "Kritschenkogel" approx. 400 meters western of Mayerling and one more stone along a trail within the adjacent forest.

Near the road between Alland and **Groisbach,** fine-grained, grayish, partially strongly weathered sandstones ("Groisbach Schürfling") were found (fig.8).

Rehgras actually constitutes a breeding farm of the Viennese University of Veterinary Medicine. Samples of coarse-grained sandstones/conglomerates were found as outcrops along a trail and as a large occurrence within an adjacent forest several hundred meters east of the farm (fig.8, 9). The rocks appeared very rich of quartz partially with grain sizes up to approx. 1 cm. Colored quartz grains, very similar to the samples of the Lainz tunnel section, were observed very often.

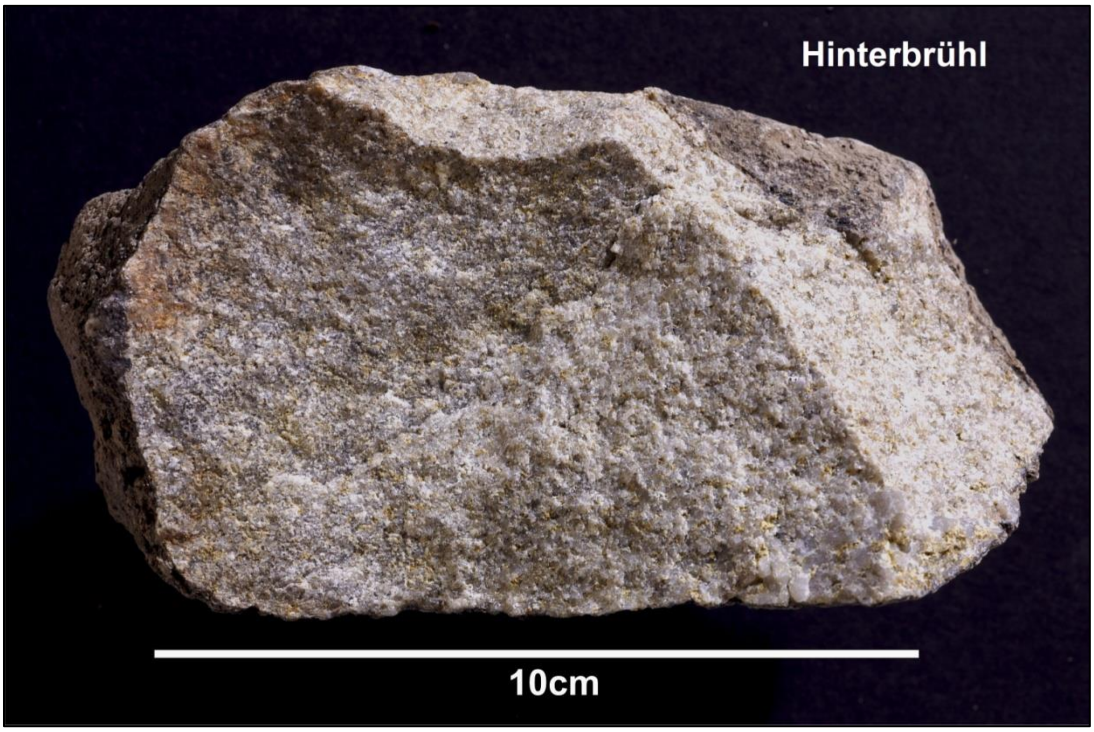

Fig.5 Dislodged slices of Hinterbrühl, currently regarded as Keuper sandstones

bright color; solid and tightly packed; taken western of the “Grillenbühel”; a dark crust surrounds the rocks (see upper picture, top right)

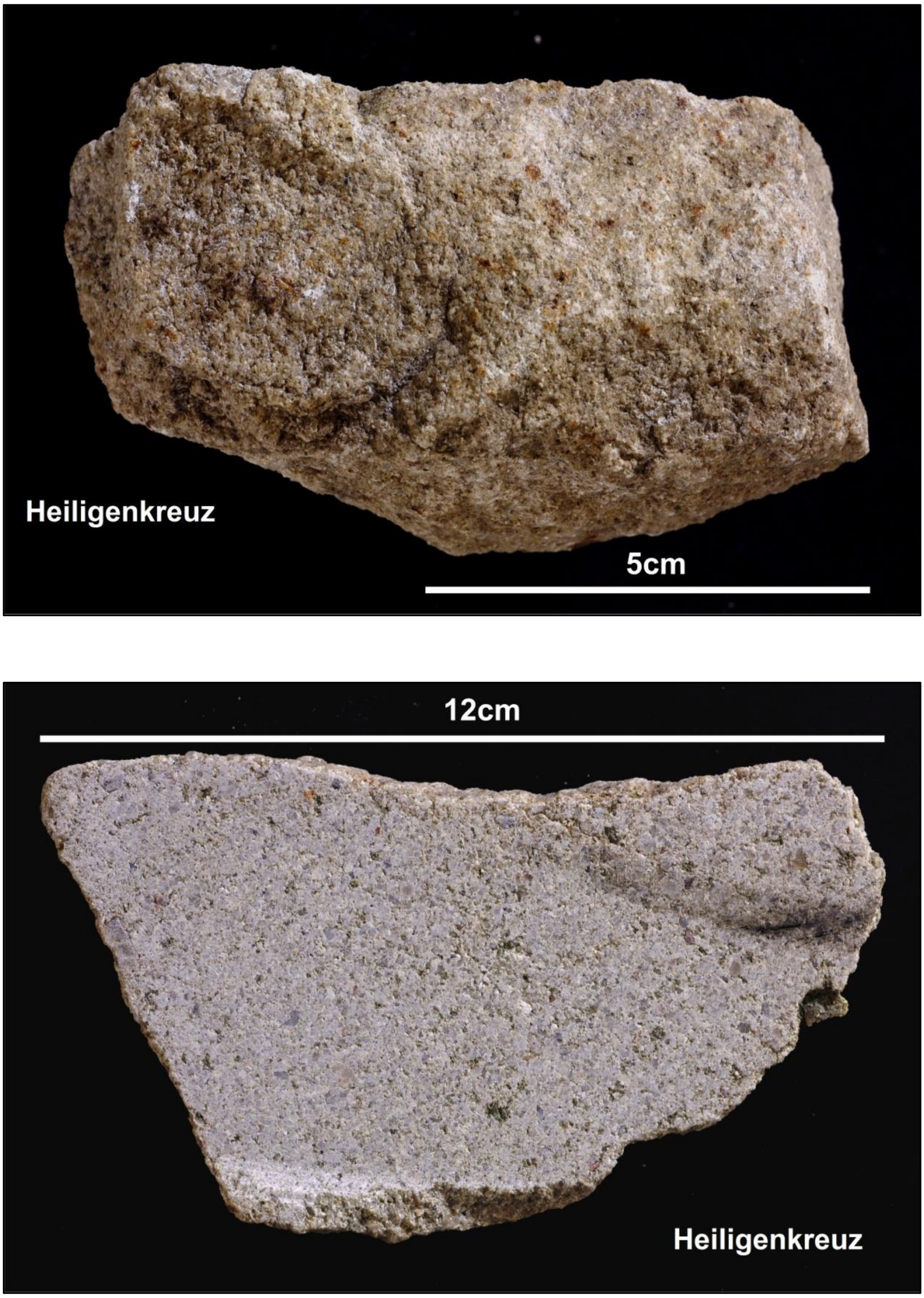

Fig.6 Dislodged slices of Heiligenkreuz; currently regarded as Keuper sandstones

overlying on fields; medium to coarse grained; often with colored quartz grains; iron oxides on the crust can be seen quite often (upper picture);

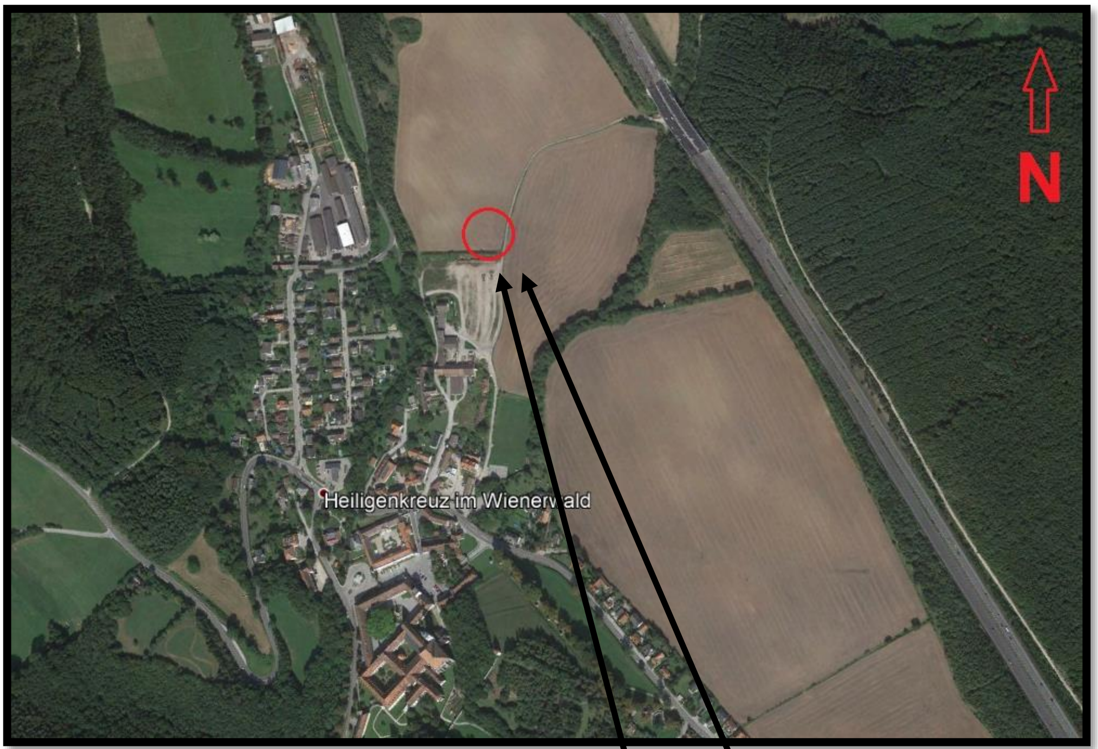

Fig.7 Outcrops of disl-odged slices north of Heiligenkreuz

The rocks cover agricultural fields; ploughing by farming machines brought these stones to the surface; the German term “Lesesteine” implies the easy picking up of these stones

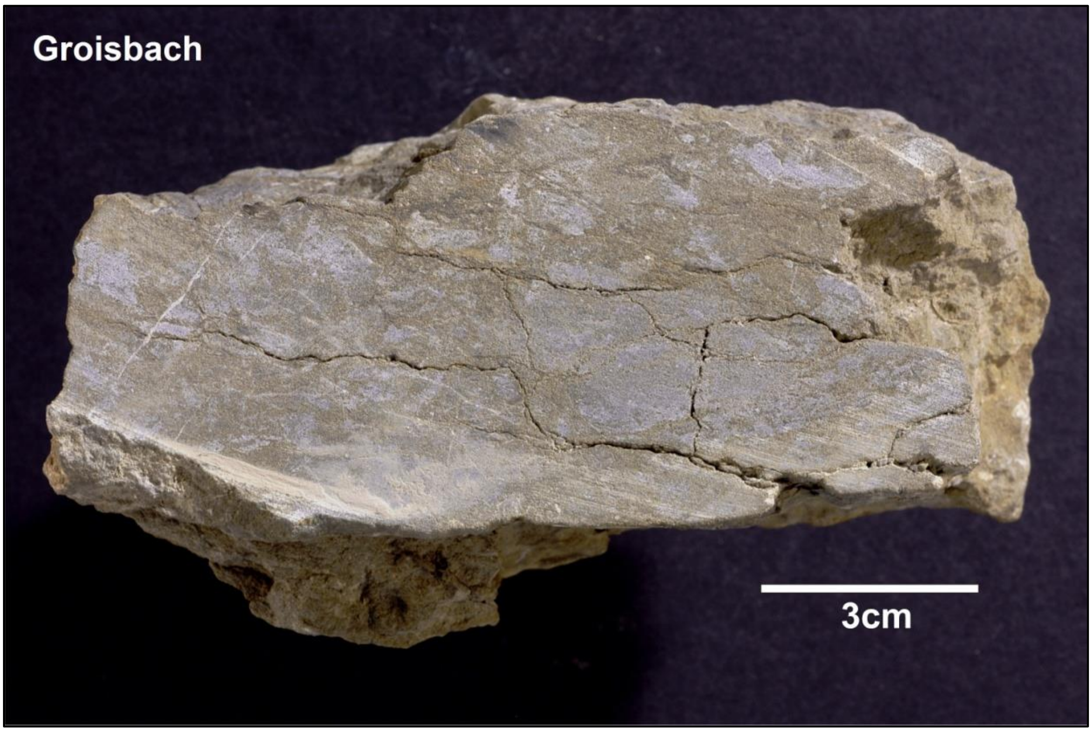

Fig.8 Dislodged slice of Groisbach: fine grained, strongly weathered, appears good sorted, grey-brownish color; dislodged slice of Rehgras: currently regarded as Keuper sandstone; coarse grained, poorly sorted rock with a greyish-brown crust;

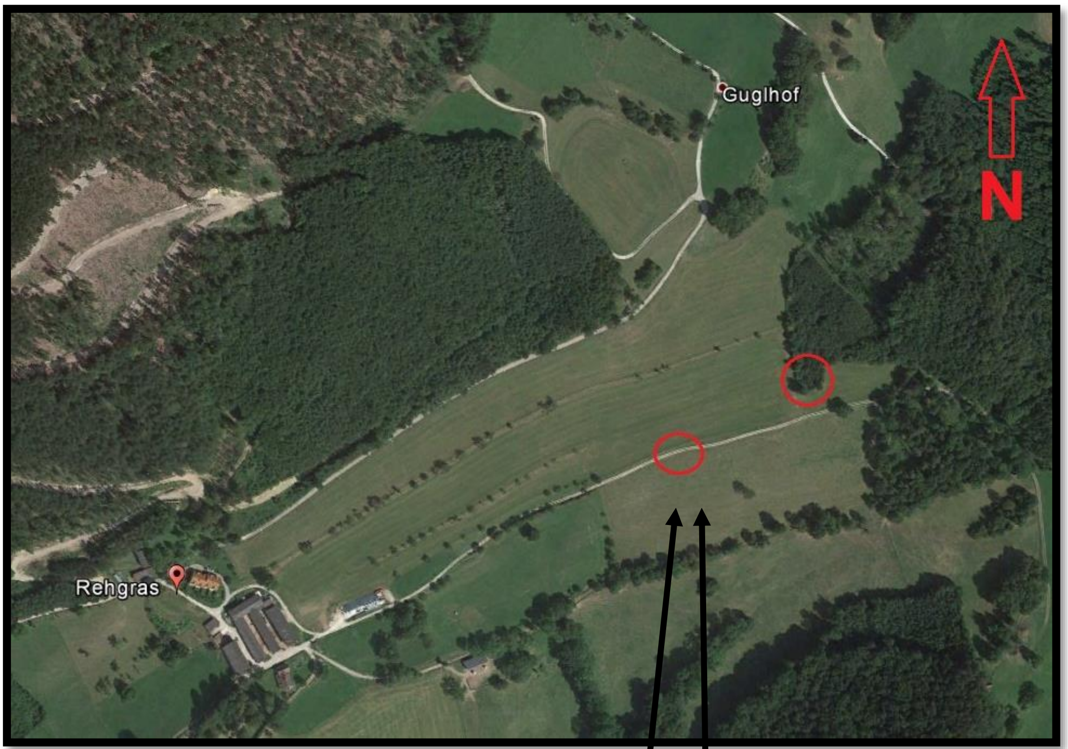

Fig.9 Outcrops of dislodged slices of Rehgras

The rocks were found as out-crops along a path and within an adjacent forest east of the farm

4.1.3 Reddish, fine-grained intercalation within the Hauptdolomit (Keuper?)

In the northeasternmost nappes of the Northern Calcareous Alps fine-grained, colored Keuper shales form eye-catching intercalations within the Hauptdolomit (e.g. Plöchinger and Salaj 1991, Mandl 2000). Reddish, fine-grained rocks, intercalated within the Hauptdolomit of the Reisalpen nappe at **Hafnerberg** are reminiscent of comparative Keuper occurrences of the northern Bajuvarikum or the St. Veit Klippen-zone. (fig.10,11). Plöchinger and Salaj (1991) described these rocks as pelitic calcareous arenites and assumed a Late Cretaceous age. However, since there is no modern data of these conspicuous rocks, samples were taken for clarification if a Late Triassic age is probable.

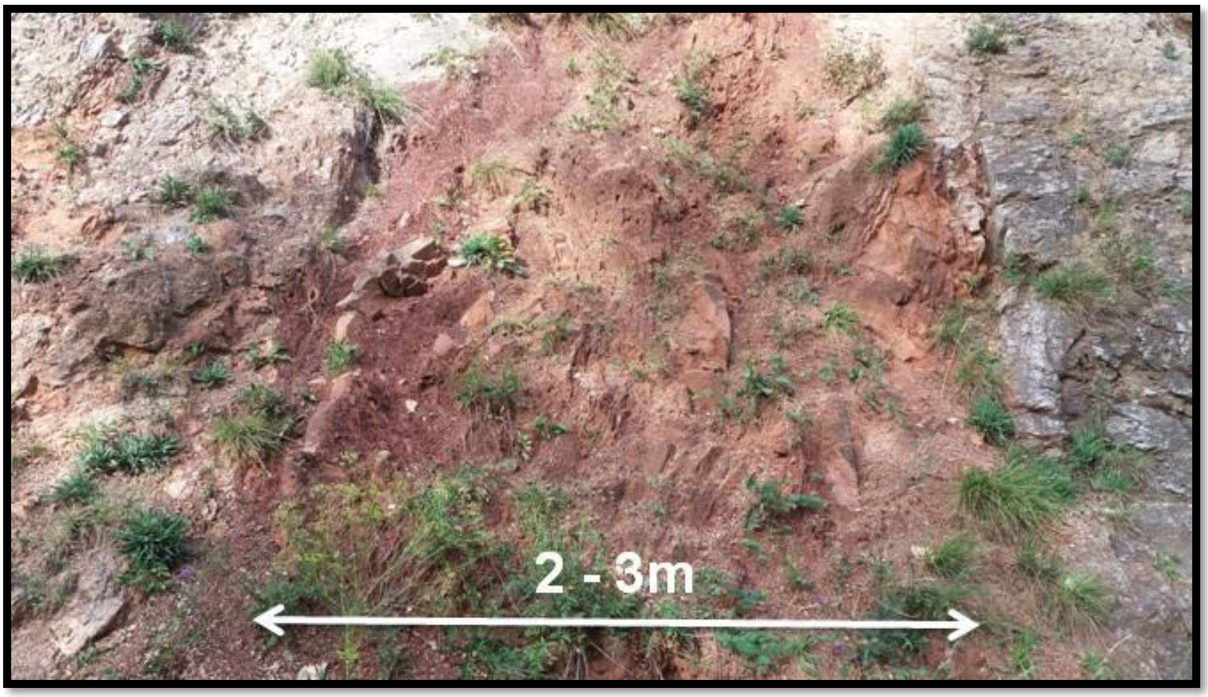

Fig.10 Reddish fine-grained intercalation within the Hauptdolomit; along a street western of Hafner-berg, width of outcrop: approx. 2,5m

Fig.11 Reddish fine grained rocks, intercalated within the Hauptdolomit of the Reisalpen nappe wester of Hafnerberg (Keuper?)

4.1.4 Liassic Gresten sandstones

Liassic sandstones and arkoses of the Gresten Klippenzone were provided by the OMV E & P Laboratory Gänserndorf including following samples:

1) Liassic Gresten arkose of **Waidhofen/ Ybbs** (Fig.12, A)

2) Liassic Gresten conglomerate/ porphyry of **Waidhofen/ Ybbs** (Fig.12, B)

3) Coal-bearing, Liassic – Dogger sandstone nearby the area of **Ybbsitz** (Fig.12, C)

4) Coal-bearing, Liassic Gresten arkose of the **Pechgraben area/Weyer** (Fig.12, D)

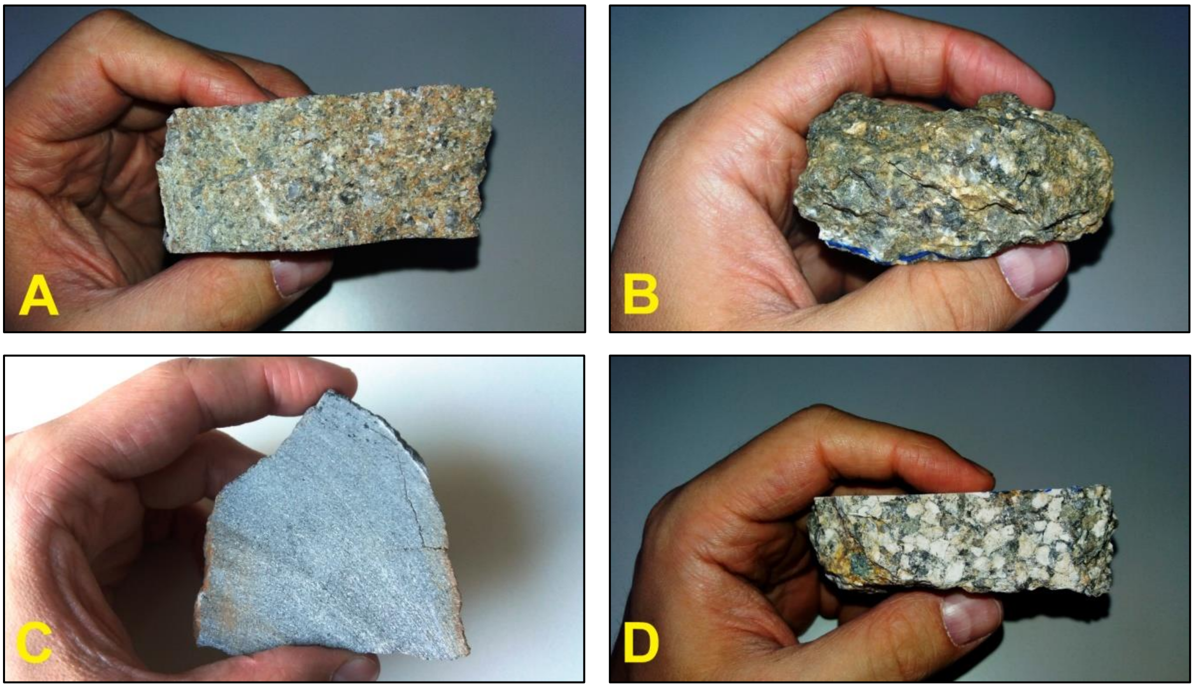

Fig.12 Liassic-Doggerian sandstones of the Gresten Klippenzone

A: Gresten arkose (Waidhofen/Ybbs, Collection: Wessely), B: Gresten conglomerate, porphyry (Waidhofen/Ybbs, Collection: Wessely), C: Coal-bearing, fine to medium grained Gresten sandstone (Ybbsitz, Collection: Kölbl), D: Coal-bearing Gresten arkose (Pechgraben/Weyer, Collection: Rosenberg)

4.2 GPS – Data

No.	Sample site	Correlation	Coordinates
1	Gemeindeberg	St.Veit Klippenzone	48°10'41.40"N 16°15'27.11"E
2	Gemeindeberg	St.Veit Klippenzone	48°10'40.78"N 16°15'26.41"E
3	Rehgras	dislodged slice	47°58'50.85"N 15°59'27.16"E
4	Rehgras	dislodged slice	47°58'53.30"N 15°59'31.50"E
5	Mayerling	dislodged slice	48° 2'26.86"N 16° 5'19.19"E
6	Mayerling	dislodged slice	48° 2'33.42"N 16° 5'13.52"E
7	Groisbach	dislodged slice	48° 2'54.69"N 16° 3'46.33"E
8	Heiligenkreuz	dislodged slice	48° 3'36.38"N 16° 7'41.73"E
9	Hinterbrühl - Grillenbühel	dislodged slice	48° 5'26.50"N 16° 15'9.23"E
10	Hinterbrühl - Grillenbühel	dislodged slice	48° 5'28.20"N 16°15'18.78"E
11	Hafnerberg	Reisalpen nappe	48° 1'9.10"N 16° 0'34.84"E

Tab. 1 GPS - coordinates of sample sites

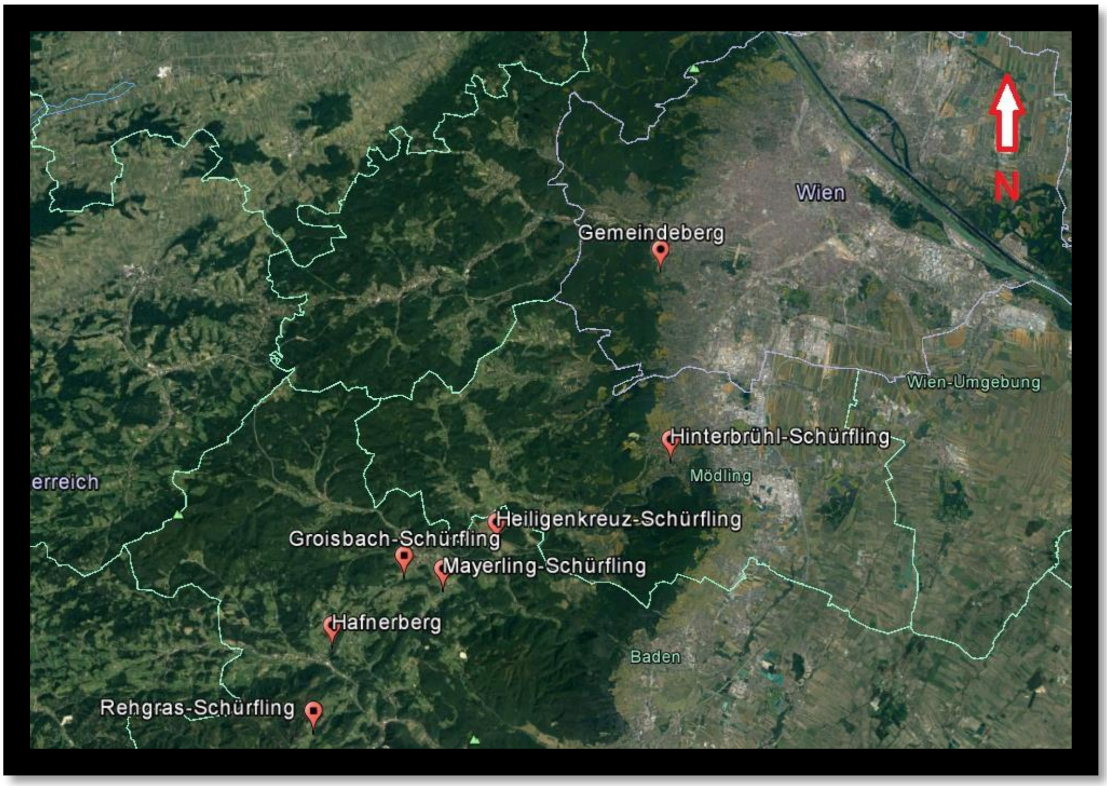

Fig.13 Geographic sketch of sample sites

5. Methods

5.1 X-ray powder diffraction (whole rock)

For the mineralogical analysis of the samples, a PANalytical X´Pert Pro (CuKα: 40kV, 40 mA) with a step size of 0.0167 (5 seconds for each step) was used. For peak identification and comparison the programs "X´Pert High Score Plus" (Version 2.2e) and X´Pert Data Viewer (Version 1.2f) were used. Altogether 26 samples were analyzed including:

- 9 samples of the St. Veit Klippenzone (4 samples of the St. Veit tunnel section + 5 samples of Ober St. Veit, Gemeindeberg)
- 11 samples of dislodged slices (2 samples each of Rehgras, Heiligenkreuz, Mayerling, Hinterbrühl + 3 samples of Groisbach)
- 2 samples of colored, intercalated shales (Hafnerberg)
- 4 samples of Gresten arkoses/sandstones

5.2 Thin section microscopy (Gazzi – Dickinson point counting)

The Gazzi Dickinson point counting technique (e.g. Ingersoll et al. 1984) is a common used method to quantify the mineralogical content of medium to coarse-grained sandstones. Altogether 17 thin sections were counted including:

- 8 samples of the St. Veit Klippenzone (4 samples of the Lainz tunnel section (LT31/1164.5m, LT31/ 1200m, LT31/1215.5m, LT31/1277.2m) + 4 samples of Ober St. Veit - Gemeindeberg)
- 9 samples of the dislodged slices of Lower Austria (4 samples of Hinterbrühl + 4 samples of Heiligenkreuz+1 sample of Rehgras)

To minimize the influence of grain size on composition only sand-sized grains (300 counts minimum) were counted. Only samples with similar grain sizes should be compared for provenance analysis (e.g. Dickinson and Suszek 1983). Another way in which this technique differs from traditional methods is that polymineralic grains were not primarily counted as rock fragments, but as the intersected mineral (if sand-sized), which occurs within the larger rock fragment. This leads to a diminution of rock fragments within the counted sample. Polycrystalline quartz and chert, if pure silica, were finally treated as quartz for ternary QFL-plotting. There are different approaches for differentiation of polycrystalline quartz grains during counting procedure. Using the Gazzi Dickinson point counting technique, only microcrystalline quartz (e.g. chert) is counted as Qp, whereas coarse-grained subgrains within composite quartz were finally treated as Qm. However, due to the wide range of different appearances of polycrystalline quartz within the counted samples (e.g. elongated subgrain-fabric, irregular subgrain-fabric with barely visible subgrain boundaries), this treatment of composite quartz grains becomes nonpractical. Therefore, composite quartz was finally counted as Qp during counting procedure. Dividing between different types of subgrain-fabrics (more or less than 3 subgrains, subgrain-boundaries, subgrain-orientation) within polycrystalline quartz crystals was an important way of distinction. Inclusions of primary mica within polycrystalline quartz classify the grain as a metamorphic rock fragment (Ingersoll et. al 1984). Only detrital grains are counted using the Gazzi Dickinson method. Cement and matrix are ignored during the counting procedure.

5.3 Geochemical analysis (Major-, minor- and trace elements)

The geochemical analysis includes major-, minor- and trace element distribution and was done by the TPA (Technische Prüfanstalt) - STRABAG AG Vienna. As analytical technique, an AXIOS – sequential high power X-ray fluorescence spectrometer (Dual Multi Channel Analyzer, 20-60 kV, 10-100 mA) was used. Altogether, a limited number of 12 samples was analyzed including:

- 2 samples of the St. Veit Klippenzone (2 samples of the Gemeindeberg quartzites)
- 6 samples of dislodged slices (1 sample of Hinterbrühl+ 2 samples each of Heiligenkreuz and Rehgras + 1 sample of Groisbach)
- 2 samples of Hafnerberg (reddish, fine grained sediments)
- 2 samples of quartz-rich Gresten sandstones (Gr.S.01, Gr.S.04)

5.4 Heavy mineral analysis

Heavy mineral studies are of an immense importance for determining the provenance and maturity of sandstones (e.g. Hubert 1962). Heavy minerals were counted by a minimum range of 200 counts and subdivided by their shape (zircon) and color (rutile, tourmaline, yellow zircon). It is already mentioned here, that in only 9 samples significant amounts of heavy minerals were found, including:

- 3 samples of the St. Veit Klippenzone (Ober St. Veit, Gemeindeberg)
- 6 samples of dislodged slices (3 sampls of Rehgras + 3 samples of Heiligen-kreuz)

5.5 Carbonate content determination

To determine the content of calcium carbonate, the sample-powder was treated with HCL (25%) by the use of a Müller-Gastner bomb (Müller and Gastner 1971). Altogether 22 samples were analyzed by this method including:

- 6 samples of the St. Veit Klippenzone (4 samples of the Lainz tunnel secion + 2 samples of Ober St. Veit, Gemeindeberg),
- 8 samples of dislodged slices (1 sample of Rehgras, Heiligenkreuz, Mayerling, Hinterbrühl + 4 samples of the Groisbach)
- 4 samples of colored, intercalated shales (Hafnerberg)
- 4 samples of Gresten arkoses/sandstones

6. Results

6.1 X-ray powder diffraction (whole rock)

6.1.1 St. Veit Klippenzone sandstones

Samples of the Lainz tunnel section (LT31/1164,5m, LT31/1200m, LT31/1215,5m, LT31/1277,2m) are compared to samples of Ober St. Veit (Gemeindeberg), which are also referred to the St. Veit Klippenzone (GeB.1, Geb.3, Geb.Kr.1, Geb.Kr.2) (fig.14).

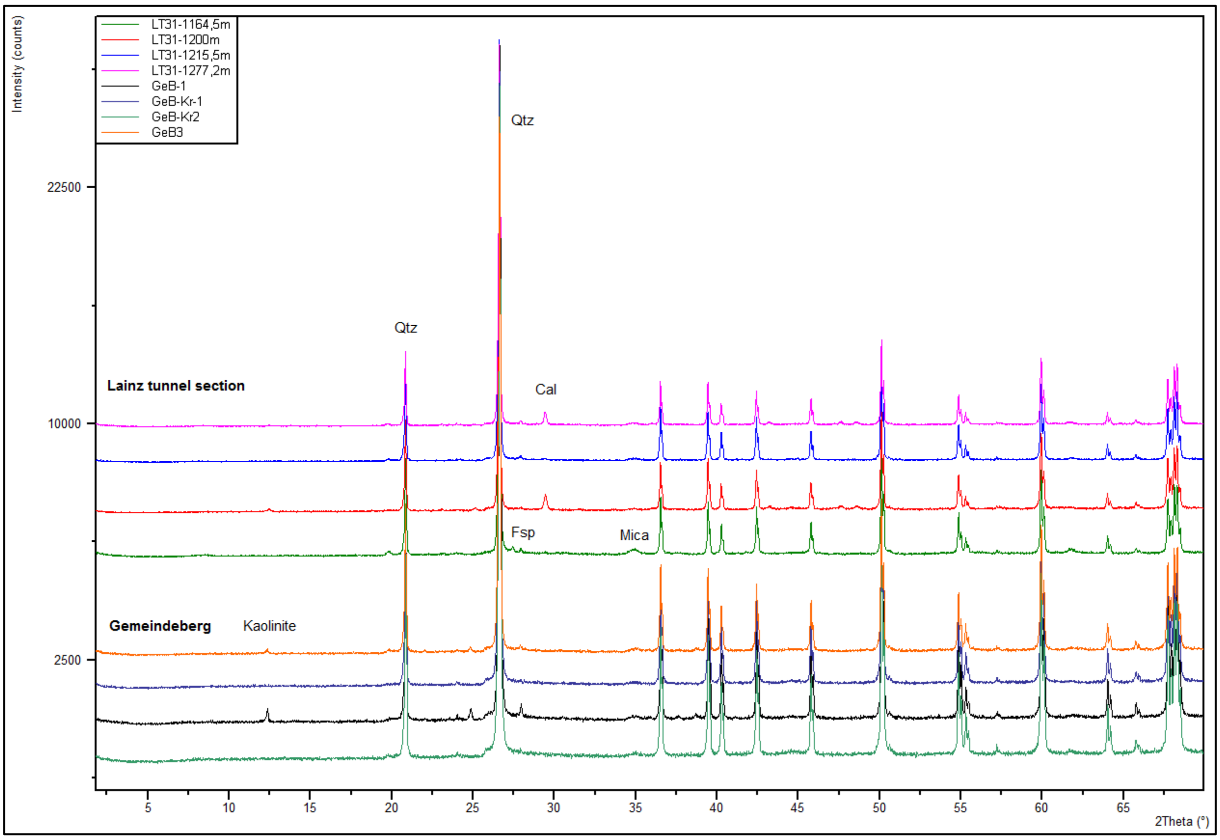

Fig.14 X-ray patterns of selected samples of St. Veit Klippenzone quartzites

Quartz, as the main phase, shows high intensity peaks (e.g. 2Θ=26,64˚, d=3,342; 2Θ=20,87˚, d=4,256) for all samples. Two samples of the Lainz tunnel section (LT31/1200m, LT31/1277,2m) show significant amounts of calcite (e.g LT31/1200m: 2Θ=29,45˚, d=3,03) which are completely missing in the samples of Ober St. Veit. Low amounts of feldspar, kaolinite and mica (muscovite) are also involved.

6.1.2 Dislodged slices

Figure 5 shows a comparison of selected samples of Rehgras (Rehgr.02), Mayerling (May01_W), Heiligenkreuz (Hkr.02), Groisbach (Gr.3) and Hinterbrühl (Hb.Gb-3).

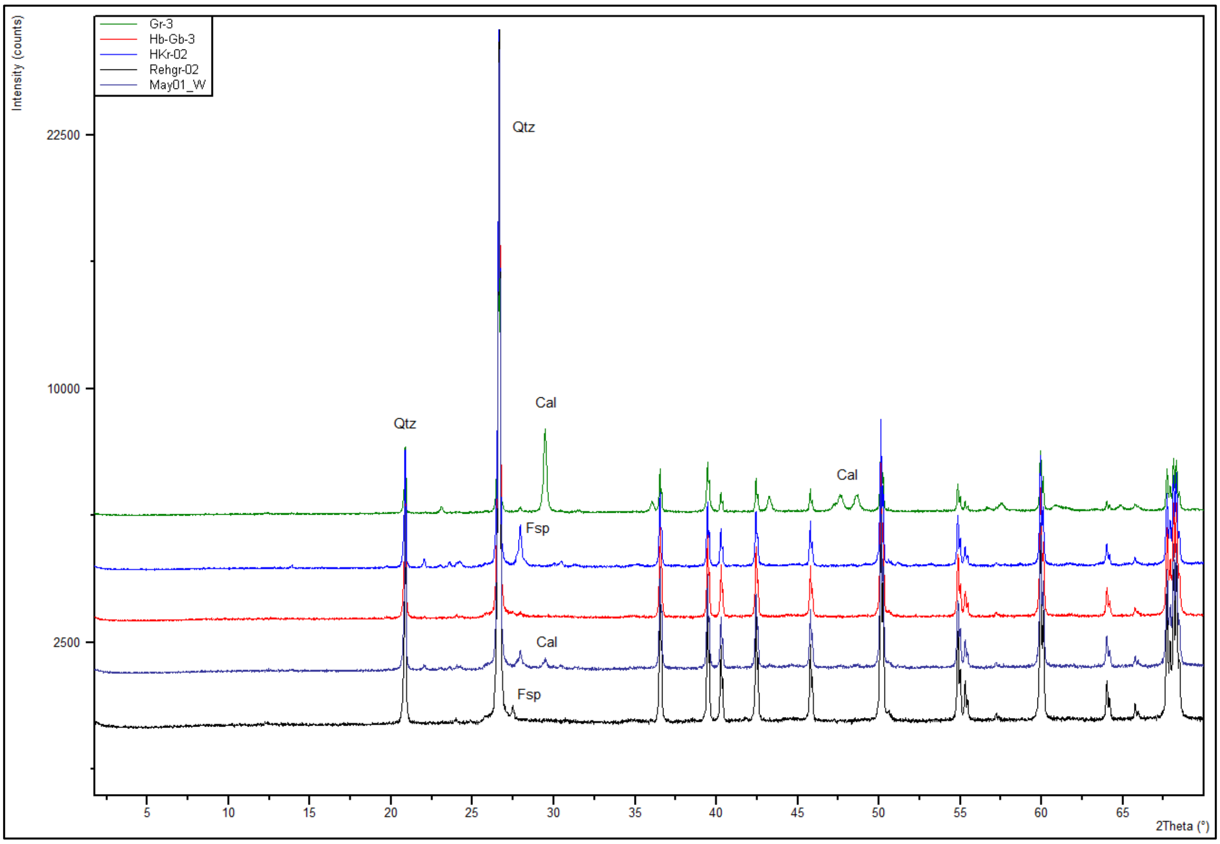

Fig.15 X-ray patterns of the dislodged slices of Lower Austria

Quartz is the main phase in all the samples, whereas the sample of Groisbach additionally shows significant peak intensities for calcite. Feldspar is also present in almost all samples. Higher peak intensities for feldspar are visible especially for the sample of Heiligenkreuz and (in smaller amounts) of Mayerling. The Mayerling – "Schürfling" also shows a peak that was identified as calcite (2Θ=29,478˚, d=3,027). Peaks for muscovite (Heiligenkreuz, Hinterbrühl) and kaolinite (Rehgras) were also identified, but are barely visible in the graph.

6.1.3 Reddish, fine grained samples of Hafnerberg

The samples of Hafnerberg (reddish, fine-grained rocks intercalated within the Haupt-dolomit), and the dislodged slices of Groisbach show high amounts of carbonate minerals. Therefore, these samples are combined for comparison in one figure (fig.16).

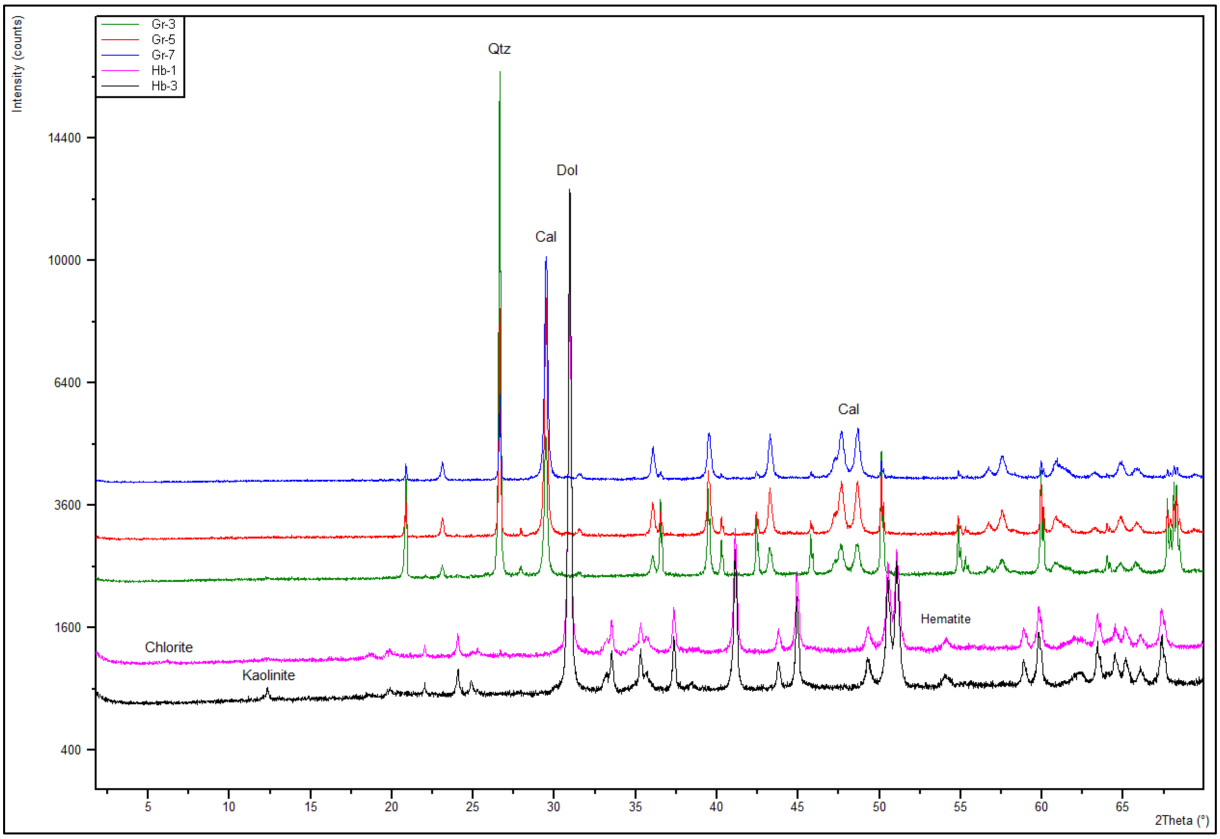

Fig.16 X-ray patterns of intercalated colored shales and dislodged slices of Groisbach

Dolomite constitutes the main mineralogical phase within the samples of Hafnerberg, which is shown by very high peak intensities. Hematite is also identified (e.g. 2Θ=33,115˚, d=2,703). Kaolinite and quartz (in very low amounts) are also involved. One sample (Hb.1) also might show low amounts of chlorite (2Θ=6,115˚, d=14,35).
Quartz and calcite are the main phases within the dislodged slices of Groisbach but also low peak intensities for kaolinite and feldspar are visible.

6.1.4 Liassic Gresten sandstones/conglomerates

The results of the samples of Waidhofen (Gr.S.01, Gr.S.02), the fine-grained sandstone of Ybbsitz (Gr.S.03) and the sample of Pechgraben (Gr.S.04) are combined as a comparison in one graph (fig.17).

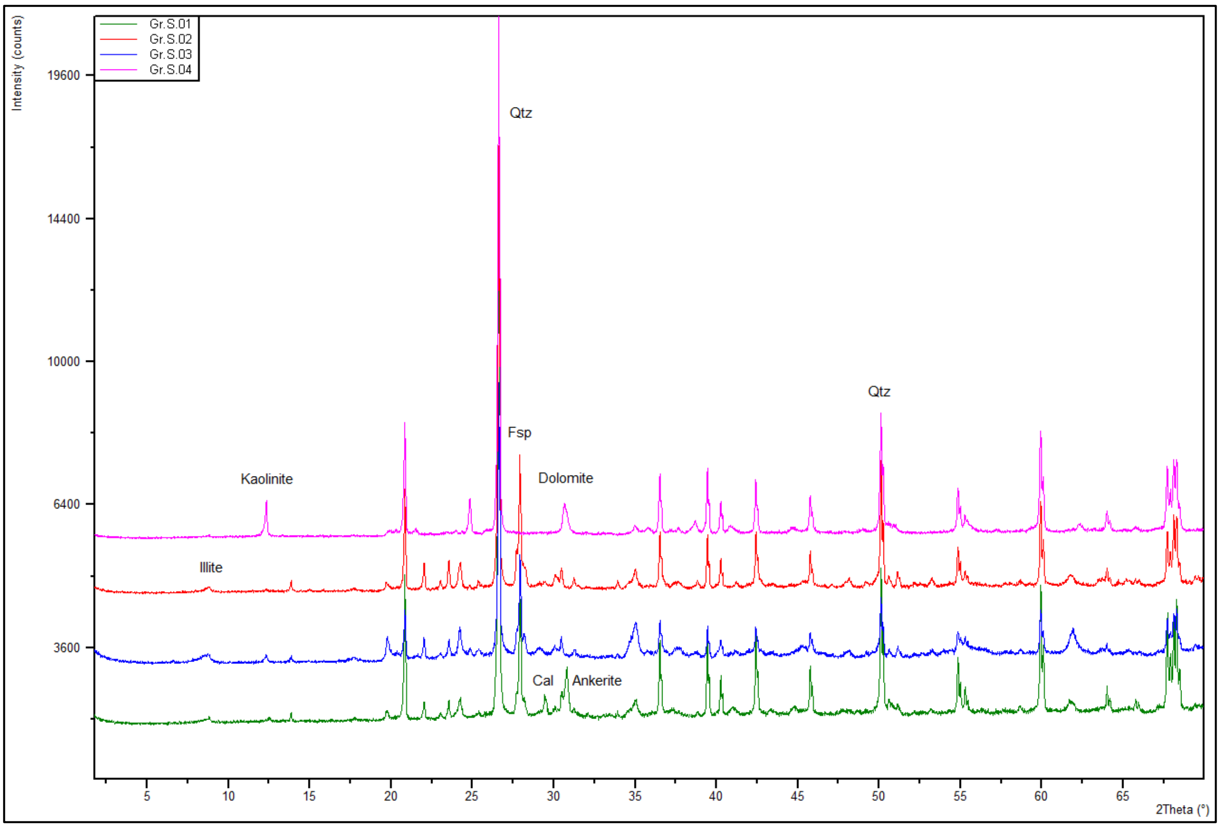

Fig.17 X-ray patterns of Liassic Gresten sandstones

All samples show high-intensity peaks for quartz. Feldspar also constitutes a main phase within 3 samples (Gr.S.01, Gr.S.02, Gr.S.03). Calcite is also present, especially within the sample of Waidhofen (2Θ=29,43˚, d=3,03) The sample of Pechgraben (Gr.S.04) shows very notable peak intensities for kaolinite (2Θ=12,345˚, d=7,17) and dolomite (2Θ=30,67, d=2,91) but no feldspar seems to be present. Illite is also present in all samples (e.g. 2Θ=8,822˚, d=10,023 for Gr.S.03).

6.1.4 Combined graph and table

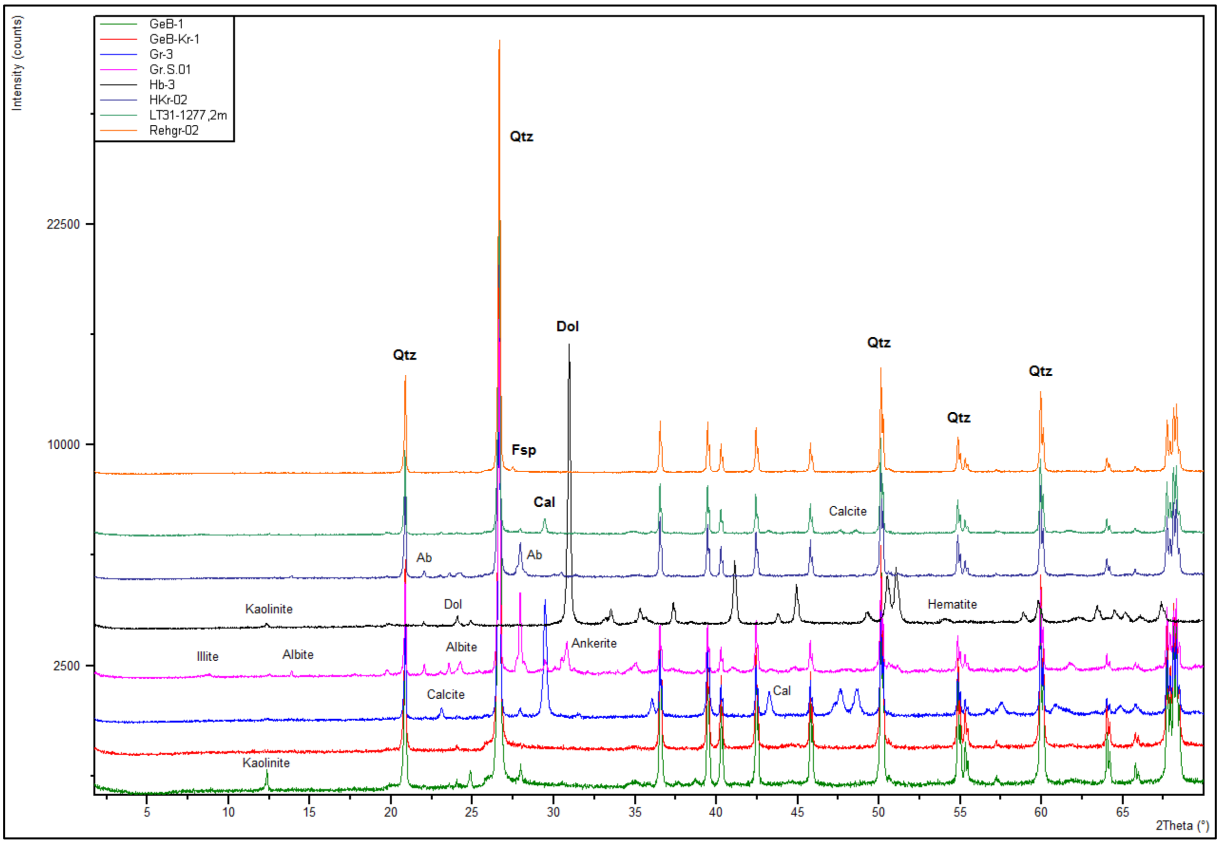

Fig.18 Combined x-ray patterns of chosen samples

Sample site	Correlation	Mineralogical content
Lainz tunnel	St. Veit Klippenzone	Quartz, Feldspar (Albite), Calcite, Mica, Kaolinite
Gemeindeberg	St. Veit Klippenzone	Quartz, Feldspar (Albite), Mica, Kaolinite
Hinterbrühl - Grillenbühel	dislodged slice	Quartz, Feldspar (Albite), Mica
Heiligenkreuz	dislodged slice	Quartz, Feldspar(Albite), Mica
Groisbach	dislodged slice	Quartz, Calcite, Ankerite, Feldspar (Albite), Kaolinite
Mayerling	dislodged slice	Quartz, Calcite, Feldspar (Albite), Kaolinite
Rehgras	dislodged slice	Quartz, Feldspar(Anorthoclase), Kaolinite, Mica
Hafnerberg	Reisalpen nappe	Dolomite, Hematite, Kaolinite, Chlorite, Quartz
Sample	**Correlation**	**Mineralogical content**
Gr.S.01 (Waidhofen)	Gresten Klippenzone	Quartz, Feldspar(Albite), Calcite, Ankerite, Illite, Kaolinite
Gr.S.02 (Waidhofen)	Gresten Klippenzone	Quartz, Feldspar(Albite), Calcite, Illite
Gr.S.03 (Ybbsitz)	Gresten Klippenzone	Quartz, Feldspar(Albite), Calcite, Kaolinite, Illite
Gr.S.04 (Pechgraben)	Gresten Klippenzone	Quartz, Kaolinite, Dolomite (Ankerite?), (Illite)

Tab.2 Results for XRD-analysis

6.2 Thin section microscopy (Gazzi Dickinson point counting)

6.2.1 St.Veit Klippenzone sandstones (Lainz tunnel section)

Thin section analysis shows moderately well to poorly sorted, medium to very coarse grained samples mainly consisting of mono- and polycrystalline quartz, minor amounts of K-feldspar (partially exsoluted) and lithic fragments. Chert only occurs occasionally. Overall, a subangular to subrounded grain shape dominates. Single grains also form a rounded shape. Dissolution of feldspar led to a significant amount of secondary porosity within 2 of the counted samples (e.g. fig.19 A, B). The grain contacts appear convex to concave. In general, Keuper sandstones of the Lainz tunnel section are tightly packed. No matrix was detected. Quartz and calcite cementation is common. The amount of grains with sizes over 2 mm is varying within the samples, also depending on sorting. Partially, poorly sorted samples show high amounts of such grains. However, these grains were ignored by using the Gazzi-Dickinson point-counting technique.

Quartz: Monocrystalline quartz occurs within a range of 5.2 – 16.6% (fig.19 E, F). Most of these grains show clear undulatory extinction over 10° (83.7 – 97.6%). Polycrystalline quartz shows a strong dominance of 76.00 – 79.1% within the samples. Different kinds of subgrain-fabrics can be divided. 2.1 – 11.9% of all Qp-grains show characteristic triple-grain junctions with straight and sutured subgrain boundaries. Elongated subgrains, a strong stress-indicator within the former rock, form frequencies of 0.8 – 3.3%. In general, Qp with more than 3 subgrains (Qp>3) is the most common type: 82.5 – 92.6%. Qp2 (e.g. fig. 19, G) and Qp3 show ranges of 5.00 – 11.5% and 2.3 – 6.4%. Overall, most Qp-grains are characterized by an irregular arrangement of subgrains, expressed by the absence of any preferred orientation (e.g. fig.19, H). Chert shows frequencies of 0 – 1.9% (fig.19 M, N).

Fig.19 (next page), A (PPL), B (XPL): medium to coarse grained sandstone from the Lainz tunnel section, dissolution of feldspar led to the formation of sec. porosity; C (PPL), D (XPL): poorly sorted, quartz and calcite cemented sample; E (XPL): Qm with embayment (very rare, F (XPL): zircon inclusion wihtin Qm, G (XPL): Qp with 2 subgrains, H (XPL): Qp with irregular shaped subgrains

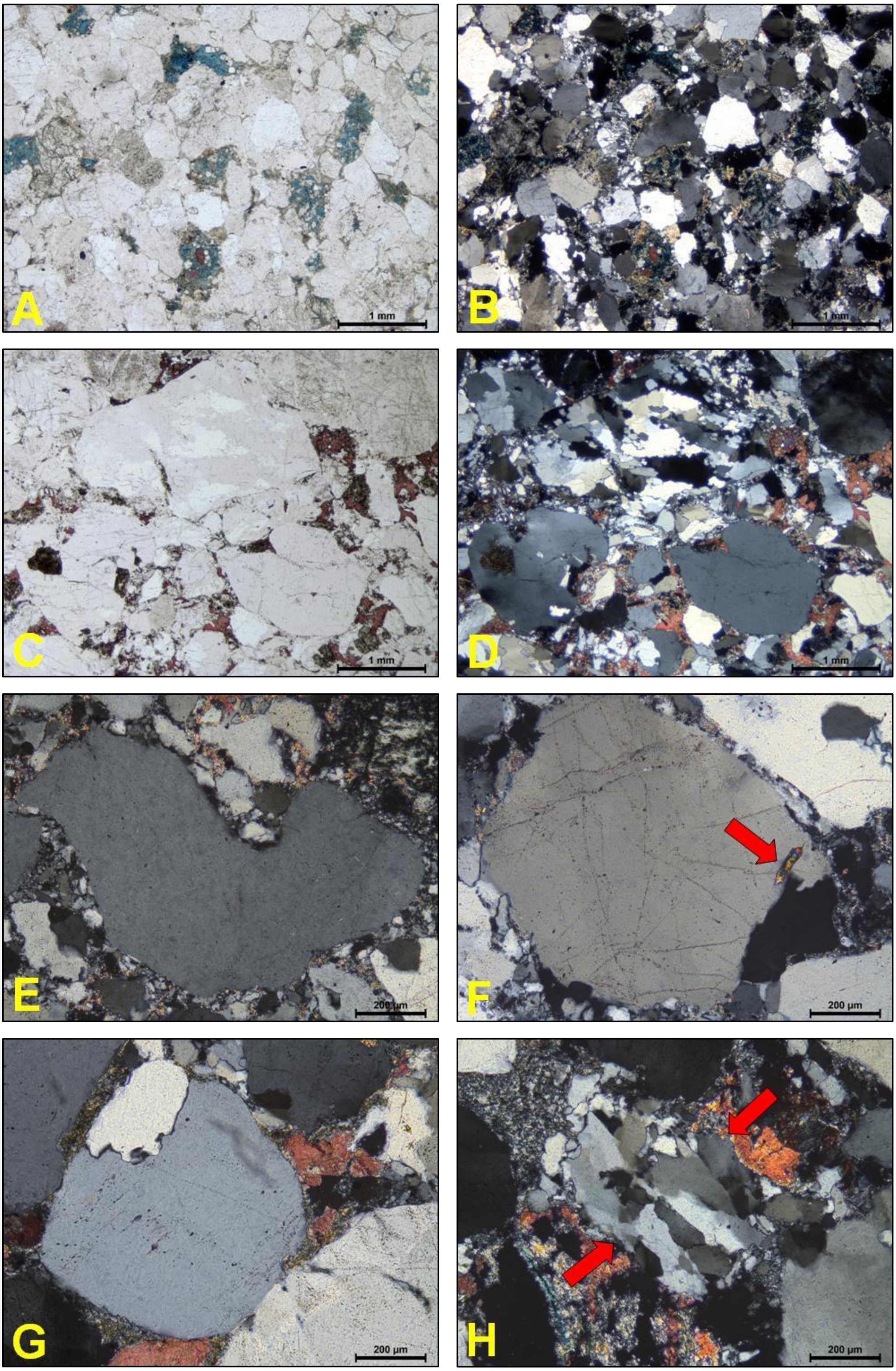
A
1 mm
B
1 mm
C
1 mm
D
1 mm
E
200 µm
F
200 µm
G
200 µm
H
200 µm

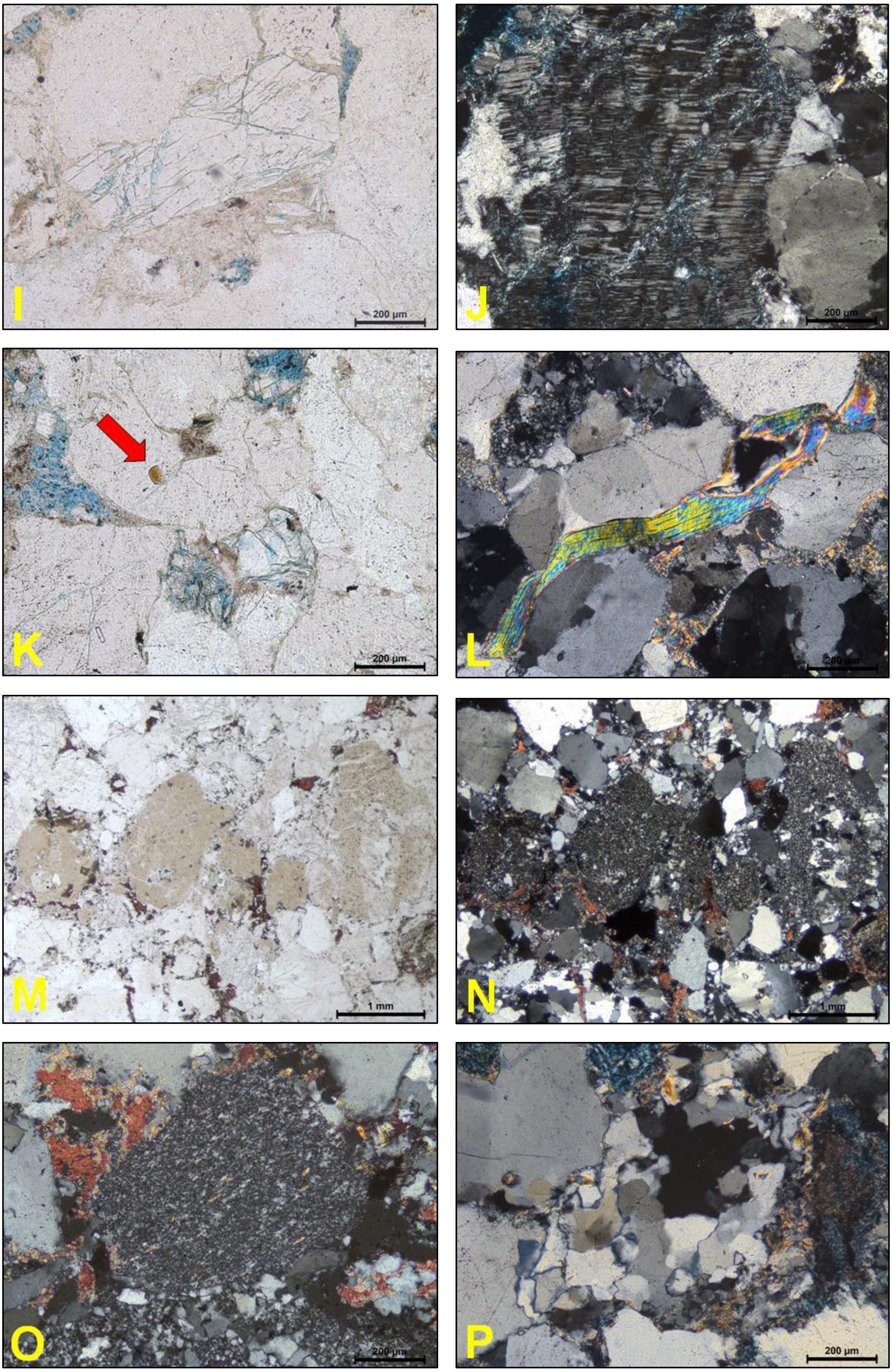
I
200 µm
J
200 µm
K
200 µm
L
200 µm
M
1 mm
N
1 mm
O
200 µm
P
200 µm

Inclusions within Qm and Qp are common mainly consisting of mica (mostly muscovite, rarely biotite and chlorite) and heavy minerals like zircon, tourmaline and others (fig. 19, F, K, P). According to Ingersoll (1984) Qp with inclusions of mica is defined as a metamorphic rock fragment (Lm).

Feldspar: K-feldspar forms occurrences of 0.3 – 7.3% within the samples (fig.19, I, J). No plagioclase was detected. The grains are often strongly weathered, leading to significant amounts of secondary porosity of 0.6 – 4.5% (fig.19, A, B). Perthitic exsolution is common (fig.19, J). According to Dickinson (1985), perthitic feldspar is counted as K-feldspar. By combining counted feldspar and secondary pores, an original feldspar content of 0.3 – 9.7% can be calculated.

Lithic fragments: 17.1 – 31.0% of Qp-grains show inclusions of mica, which leads to an amount of 13.0 – 24.6% related to the whole rock. These grains represent, by definition, the majority of lithic fragments within the samples (fig.19, P). Different, mainly unstable fragments occur within a range of 0.6 – 6.1% and are represented by sedimentary silt or shale clasts, felsic rock fragments (mainly composed of several grains of feldspar, sometimes with quartz) and other metamorphic fragments (e.g. Fig. 19, O).

In summary, the average framework composition of 4 counted samples of the Lainz tunnel section consists of 12.1% monocrystalline quartz, 59.0% polycrystalline quartz, 17.9% polycrystalline quartz with inclusions of mica (counted as Lm), what makes 76.9% polycrystalline quartz grains in total, 4.7% K-feldspar, 0.6% chert, 3.3% of different rock fragments and 1.9% of sand-sized secondary porosity due to the dissolution of feldspar. The average original feldspar content was calculated as 6.6% (fig.20).

Fig.19 (previous page), I (PPL) K-feldspar; J (XPL): perthitic exsoluted K-feldspar; K (PPL): inclusion of tourmaline (red arrow) within quartz; L (XPL): detrital mica (very rare); M (PPL), N (XPL): several grains of chert; O (XPL): microcrystalline quartz with mica (counted as Lm), probably from a schist; P (XPL): Qp with mica (Lm)

Lainz tunnel section Average composition (%)	
Qm (slight u.ex), <10°	1,42
Qm (undul. ex.), >10°	10,66
Total	**12,07**
Qp2	7,23
Qp3	3,49
Qp>3	66,13
**Qp elong.*	1,17
**Qp tripple. gr. b.*	3,82
**(+mica (Lm))*	17,84
Total	**76,85**
Fsp.	0,70
Fsp (exsolution l.)	0,54
Sec. Por. (Relicts of F.)	3,47
Total	**4,71**
grain replacive kaolinite	0,00
Chert	0,55
Mica	0,23
Sec. Porosity	1,88
Lithic fragments	
***Felsic fr.**	0,93
***Ls**	2,24
***Lm**	0,54
Total	**3,25**
Total 322 counts	**99,54**

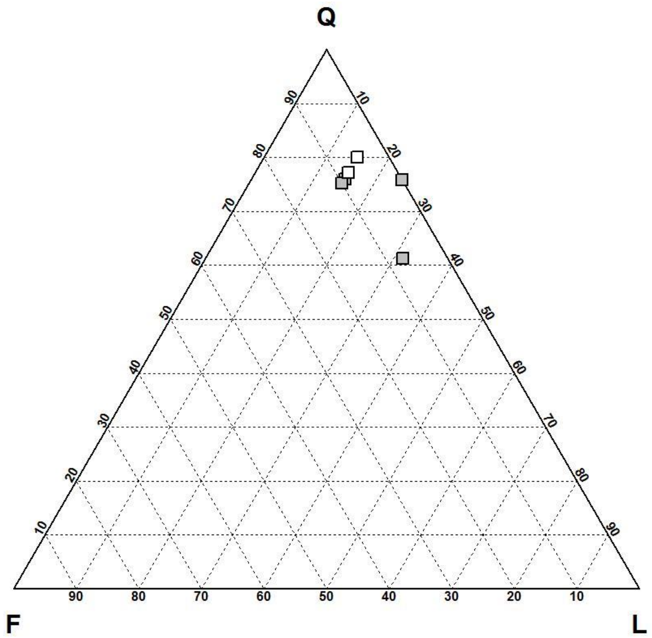

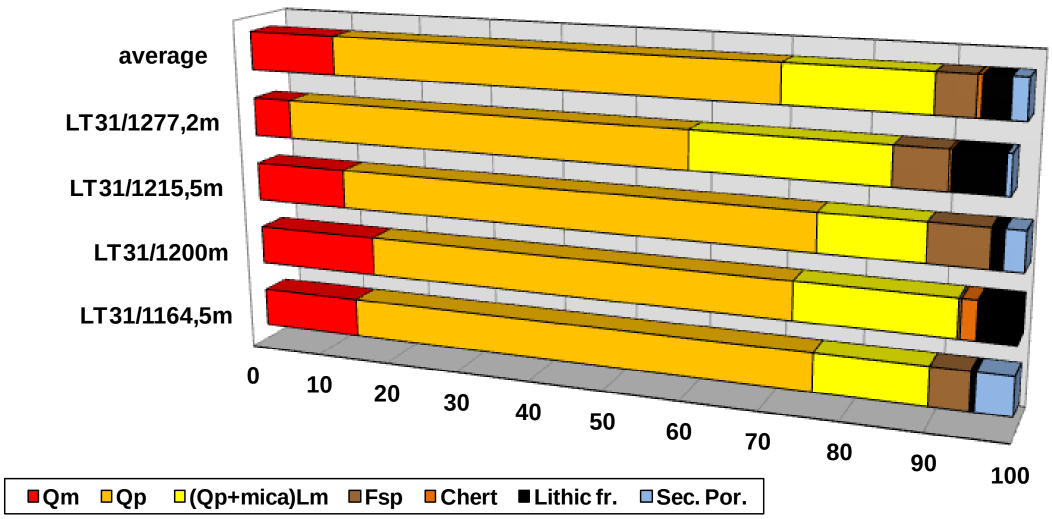

Fig.20 Upper left: average composition of 4 counted sandstones/conglomerates of the Lainz tunnel section (* different categories of Qp, related to the whole rock) upper right: ternary QFL-plot; grew squares represent samples with calculated, original feldspar content, lower fig.: results of four counted samples of the Lainz tunnel section

6.2.2 St. Veit Klippenzone sandstones (Ober.St Veit, Gemeindeberg)

Thin section analysis shows moderately well to poorly sorted, medium to very coarse grained samples mainly consisting of mono- and polycrystalline quartz, minor amounts of relictic K-feldspar, kaolinite and lithic fragments. Chert is rare. Overall, the grains show a subangular to subrounded shape. Rounded grains only occur occasionally. Dissolution of feldspar led to a significant amount of secondary porosity (fig.21, A, B). Synsedimentary clay coatings can also be observed (e.g. fig.21, C). The grain contacts appear convex to concave. Depending on sorting and grain size, grain sizes over 2mm are very common.

Quartz: Monocrystalline quartz shows a frequency between 2.5 – 7.3% within 4 counted samples (fig.21, G). Undulatory extinction over 10° was investigated within 87.5 – 95.8% of the grains. Polycrystalline quartz show high amounts of 78.8 – 84.3%, whereas 89.4 – 93.4% of these grains include more than 3 subgrains (Qp>3). Qp2 and Qp3 occur within a range of 2.7 – 5.5 and 3.0 – 5.1%. The subgrain boundaries mostly appear irregular to sutured. A characteristic fabric of triple grains junctions can be observed within a range of 1.9 – 14.3%. Triple grain junctions show straight to sutured subgrain boundaries. 0.4 – 2.2% of polycrystalline quartz grains show elongated subgrains. Most Qp-grains form irregular subgrain fabrics. Only 2 grains of chert (0.3%) in total were counted.

Inclusions within quartz are common, mainly consisting of mica (muscovite). Biotite is rare. Isolated grains might show inclusions of former, weathered feldspar. Zircon, tourmaline and other heavy minerals can also be detected. For the final classification of the sample, polycrystalline quartz with inclusions of mica was treated as a metamorphic rock fragment.

Fig.21 (next page), A (PPL), B (XPL): moderately well sorted sandstone of Gemeindeberg, C (PPL), D (XPL) secondary posority with relicts of feldspar and brown clay coatings, E (PPL), F (XPL): grain-replacive kaolinite, G (XPL): rounded, monocrystalline quartz, H (XPL): Qp with mica (Lm)

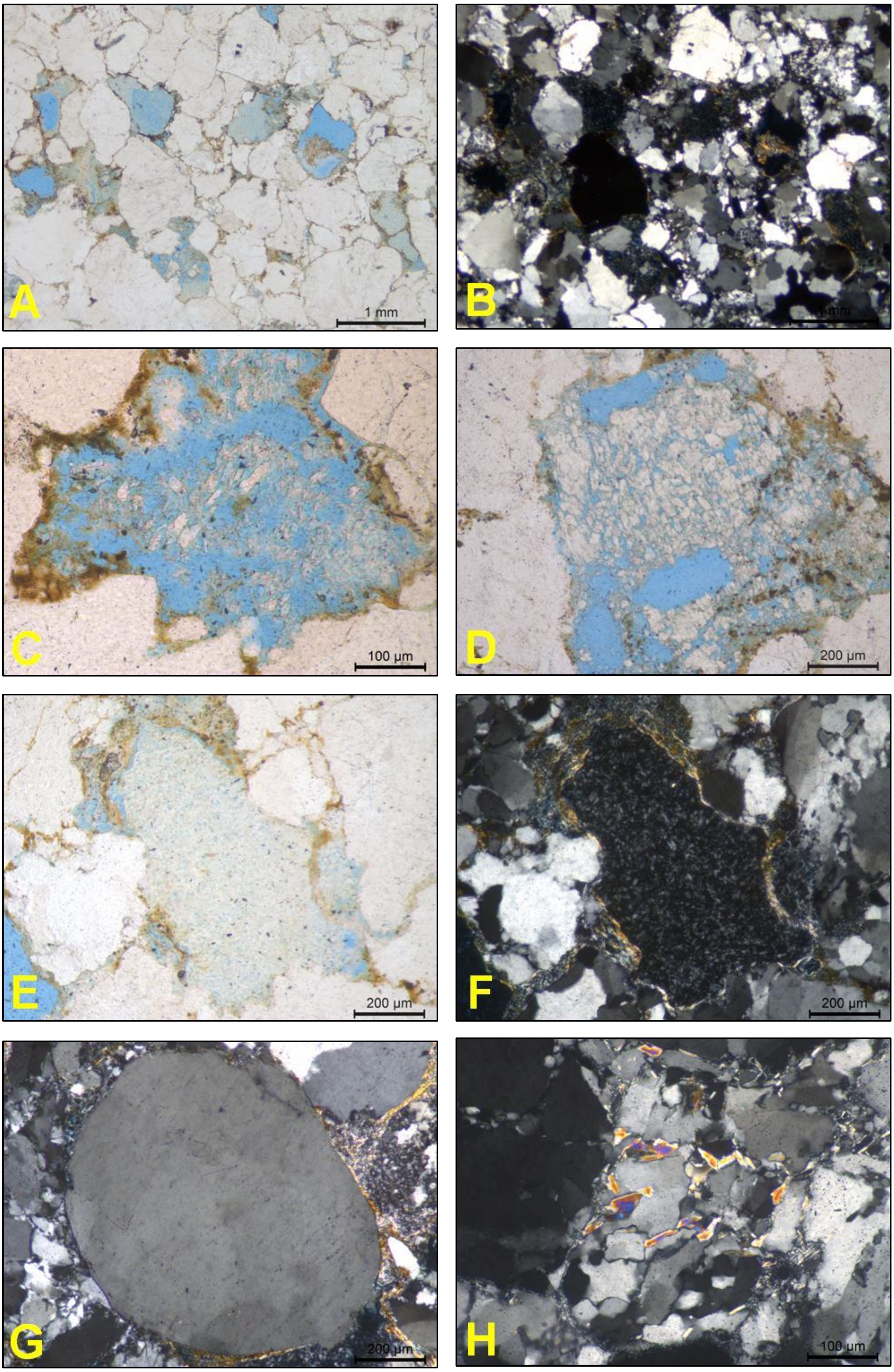
A
1 mm
B
C
100 µm
D
200 µm
E
200 µm
F
200 µm
G
200 µm
H
100 µm

Feldspar: Grains of K-feldspar are strongly weathered or completely dissolved (fig. 21, C, D). K-feldspar or relicts of feldspar show frequencies 3.0 – 6.1%. Exsolution lamellae (perthitic?) are partially visible. No contents of plagioclase were observed. Secondary porosity occurs within a range of 4.2 - 6.1%. Chemical weathering of feldspar led to the formation of authigenic kaolinite: 0.6 – 6.0% (fig.21, E, F). By combining this values, an original feldspar content of 8.2 – 15.5% can be estimated.

Lithic fragments: 23.1 – 47.5% of polycrystalline quartz grains include traces of primary mica and therefore were classified as metamorphic rock fragments (fig.21, H). That accounts for 18.2 – 38.1% of the whole rock composition. Coarse to very coarse-grained samples show significantly higher amounts of such grains. Sedimentary and different metamorphic rock fragments only occur occasionally by showing a range of 0.60 – 3.6% related to the whole rock.

In summary, the average framework composition of 4 counted samples of Gemeindeberg quartzites consists of 4.6% monocrystalline quartz, 50.2% polycrystalline quartz, 31.4% polycrystalline quartz with inclusions of mica (Lm), what makes 81.7% polycrystalline quartz grains in total, 4.6% relicts of K-feldspar, 2.1% grain-replacive kaolinite, 1.9% different rock fragments and 4.8% of sand-sized secondary porosity due to the dissolution of feldspar. The average original feldspar content was calculated as 11.5% (fig.22).

St.Veit Klippenzone (Gemeindeberg) Average composition (%)	
Qm (slight u.ex), <10°	0,38
Qm (undul. ex.), >10°	4,23
Total	4,62
Qp2	3,53
Qp3	3,47
Qp>3	74,66
Qp elong.	1,00
Qp tripple. gr. b.	6,53
(+mica (Lm))	31,42
Total	81,66
K-feldspar	0,94
K-Feldspar exsoluted	0,39
Sec. Porosity. within Fsp.	3,30
Total	4,62
grain replacive kaolinite	2,11
Chert	0,15
Mica	0,15
Sec. Porosity	4,79
Lithic fragments	0,00
*Felsic fr.	0,00
*Ls	1,18
*Lm	0,71
Total	1,89
323,5	100,00

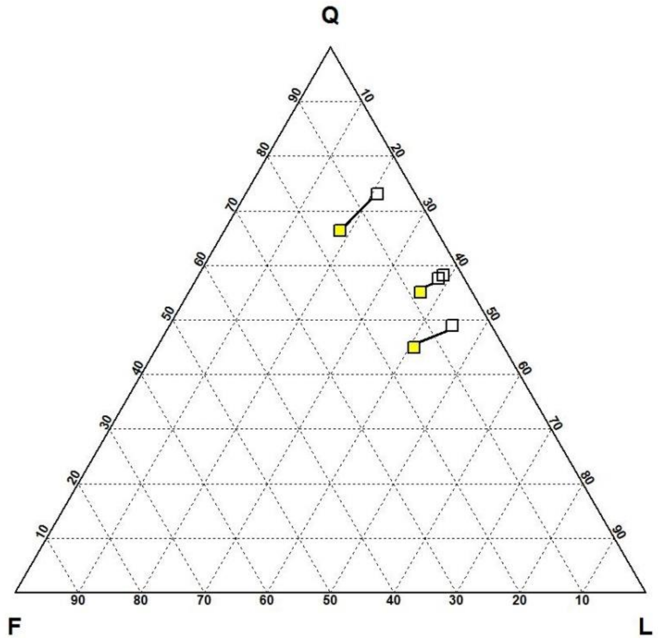

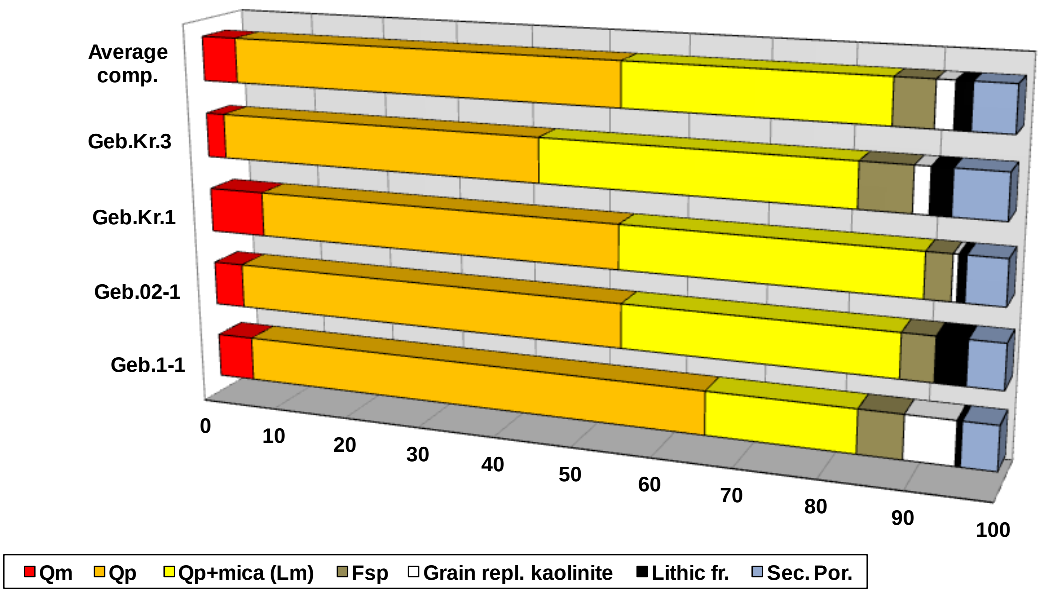

Fig.22 Upper left: average composition of 4 counted Gemeindeberg quartzites, upper right: QFL-plot ot 4 counted Gemeindeberg quartzites (yellow squares: samples with calculated, original feldspar content), lower fig.: mineralogical and average composition of 4 counted Gemeindeberg sandstones

6.2.3 Dislodged slices of Hinterbrühl ("Grillenbühel")

Thin section analysis shows a moderatety well to moderately sorted, coarse to very coarse-grained, strongly quartz-cemented and tightly packed fabric of mono- and polycrystalline quartz, K-feldspar or relicts of K-feldspar and lithic fragments. Some samples also show calcite cementation. The grain contacts appear convex to concave, partially sutured. A grain shape of subangular to rounded was investigated. No primary porosity was observed. Amounts for secondary porosity due to the dissolution of feldspar are very low and not significant. Isolated grains show a size over 2 mm. (Fig. 23, A, B).

Quartz: Monocrystalline quartz shows a range of 15.6 – 29.7% within the samples. Almost all grains (97.1 – 98.4%) show clear undulatory extinction over 10°.
Polycrystalline quartz occurs within a range of 63.9 – 76.6%. Polycr. quartz with 2 and 3 subgrains (Qp2, Qp3) shows a frequency of 11.4 – 21.9 and 11.8 – 13.5% within all counted Qp-grains. A subgrain-fabric with more than 3 subgrains (Qp>3) is the most common type with 64.8 – 76.7%. The subgrain boundaries are irregular to straight. 4.1 – 10.8% of all counted Qp-quartz grains show triple grain junctions with straight to sutured subgrain boundaries (Fig. 23, M). Polycr. quartz with elongated subgrains occurs within a range of 0.82 – 3.6%.

Due to strong quartz cementation, syntaxial quartz overgrowths can be seen very often (Fig. 23, D, E). Additionally, so-called volcanic resorption channels were also investigated, which occur within 3.7 – 15.4% of all counted quartz grains (Fig.23, F).
Chert is very rare. Single grains were observed but not intersected by the crosshair during counting procedure.

Fig.23 (next page), A (PPL), B (XPL): coarse grained, quartz-cemented dislodged slice of Hinterbrühl, C (PPL), D (XPL): rounded monocrystalline quartz with syntaxial quartz overgrowths, red arrows show primary grain boundaries, E (XPL): syntaxial quartz overgrowth, F (XPL): volcanic resportion channel, G (XPL), H (XPL): sutured grain boundaries

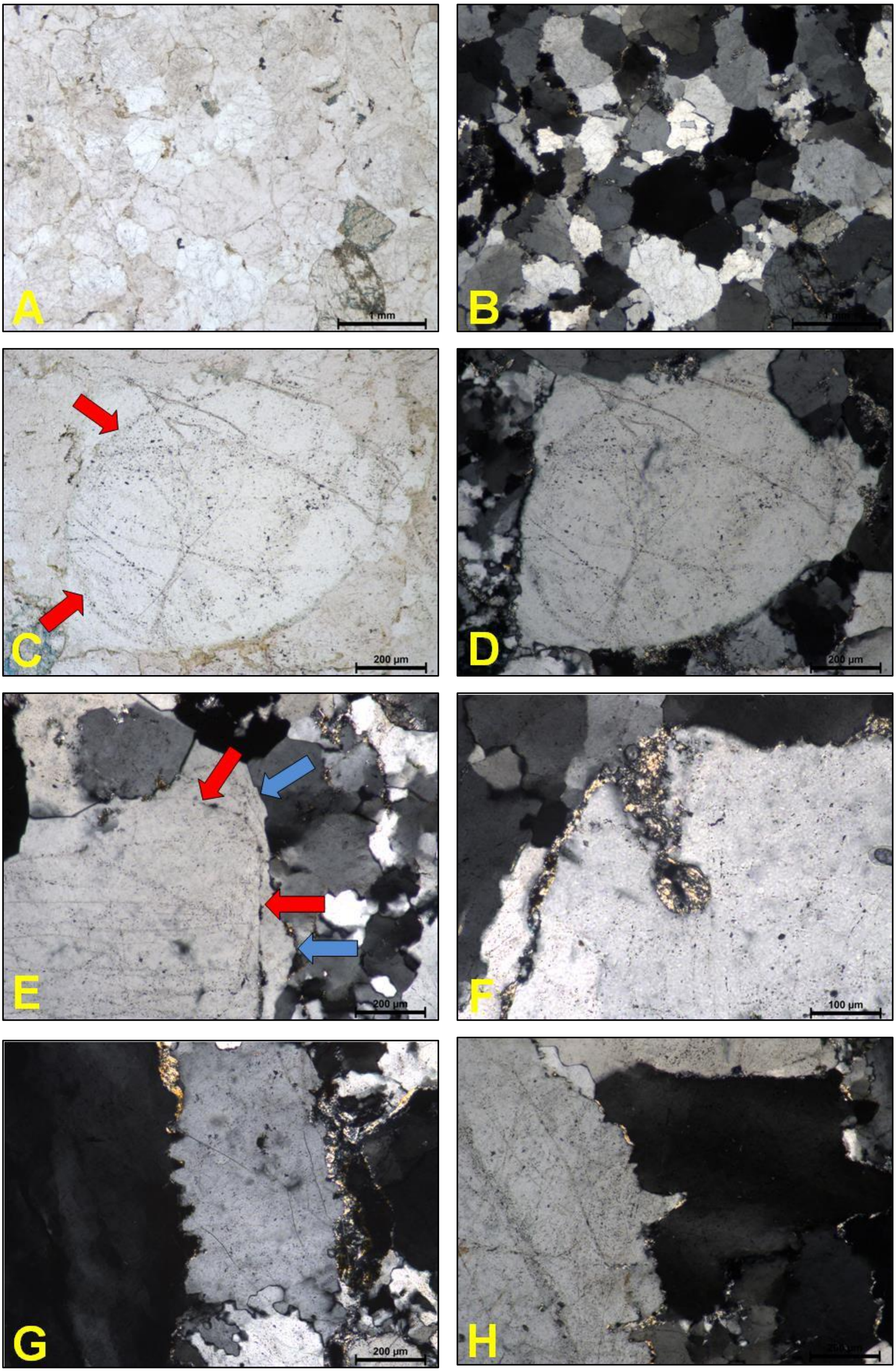
A
1 mm
B
C
200 µm
D
200 µm
E
200 µm
F
100 µm
G
200 µm
H

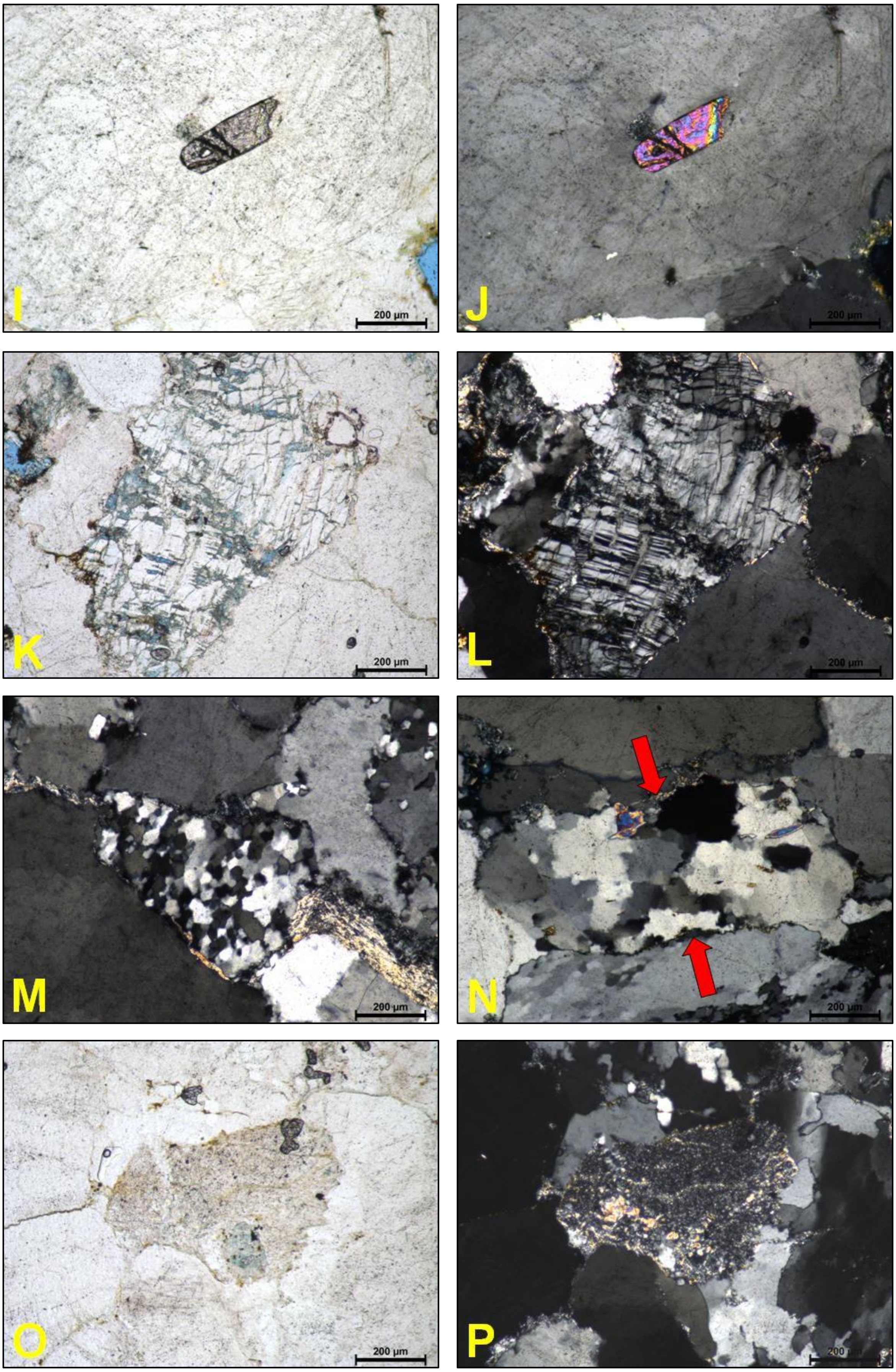
I
200 µm
J
200 µm
K
200 µm
L
200 µm
M
200 µm
N
200 µm
O
200 µm
P
200

Inclusions within quartz are common including mica (mainly muscovite, rarely biotite) (Fig.17 N), feldspar and heavy minerals like zircon or tourmaline (e.g. Fig.23 I, J). For ternary QFL – plotting, polycrystalline quartz grains with inclusions of primary mica were treated as metamorphic rock fragments.

Feldspar: By combining the values of intersected K-feldspar and secondary porosity due to the dissolution of feldspar and original content of 4.1 – 7.1% can be estimated. Intersected feldspar also partly shows strong weathering. Clear visible exsolution was observed within a range of 20.0 – 35.7% of all counted feldspar grains (fig.23, L). Single grains show quartz inclusions. No plagioclase was detected.

Lithic fragments: Lithic fragments occur within a frequency of 19.8 – 31.15%. Metamorphic rock fragments, consisting of polycrystalline quartz and inclusions of mica occur within a range of 18.2 – 30.0% related to the whole rock (fig.23, N). Single grains of felsic rock fragments (mainly composed of feldspar), sedimentary rock fragments (silt and shale fragments) and different metamorphic rock fragments occur within a range of 1.1 – 3.7% related to the whole rock composition.

In summary, the average framework composition of 4 counted dislodged slices of Hinterbrühl consists of 21,2% monocrystalline quartz, 45,9% polycrystalline quartz, 25,5% polycrystalline quartz with inclusions of mica (Lm), what makes 71,4% polycrystalline quartz grains in total, 4,8% feldspar and 2% of different rock fragments (fig.24).

Fig.23 (previous page), I (PPL), J (XPL): heavy mineral (zircon) inclusion within quartz, K (PPL), L (XPL): K-feldspar shows exsolution under XPL, M (XPL): polycrystalline quartz with triple grain junctions, N (XPL): metamorphic rock fragment, O (PPL), P(XPL): metamorphic rock fragment consisting of poly-, microcrystalline quartz and mica

Dislodged slice (Hinterbrühl) (Average composition (%)	
Qm (slight u.ex), <10°	0,46
Qm (undul. ex.), >10°	20,76
Total	21,22
Qp2	11,75
Qp3	9,04
Qp>3	50,61
**Qp elong.*	1,33
**Qp tripple. gr. b.*	5,31
**(+mica (Lm))*	25,52
Total	71,40
K-feldspar	2,85
K-feldspar exsoluted	1,16
Sec. Porosity within Fsp.	0,74
Total	4,75
grain replacive kaolinite	0,00
Chert	0,00
Mica	0,00
Sec. Porosity	0,60
Lithic fragments	0,00
*Felsic fr.	0,46
*Ls	0,77
*Lm	0,79
Total	2,03
322,75	100,00

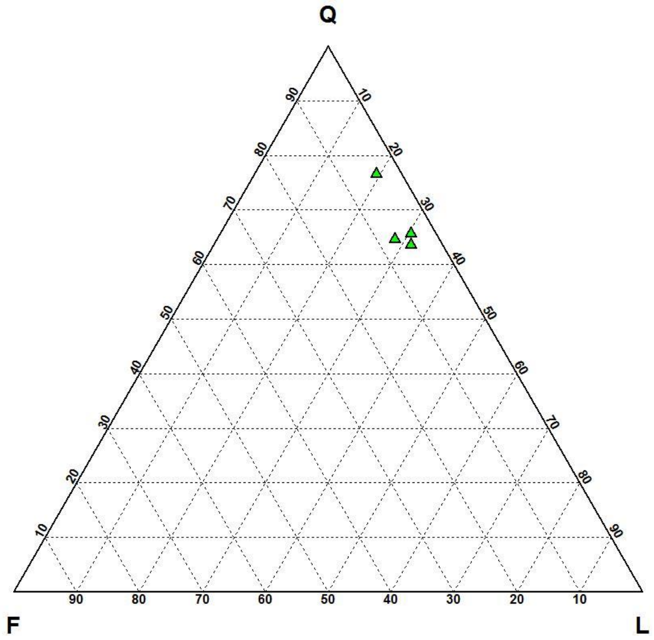

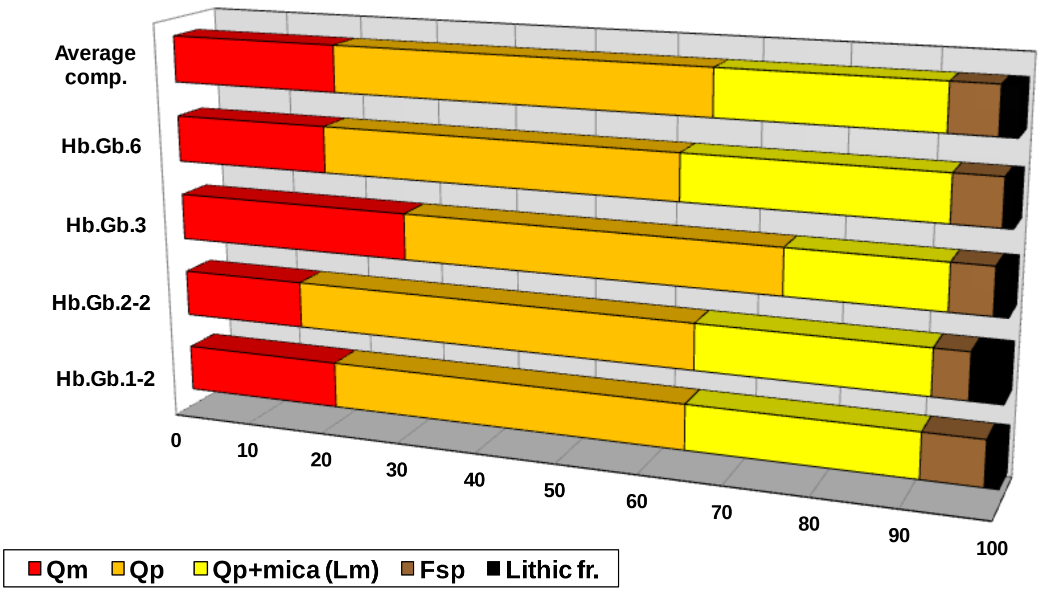

Fig.24 Upper left: average composition of 4 counted samples of Hinterbrühl, upper right: ternary QFL – plot of 4 counted samples of Hinterbrühl. lower fig.: mineralogical composition of 4 counted samples of Hinterbrühl

6.2.4 Dislodged slices of Heiligenkreuz

Thin section analysis shows a moderately well to moderately sorted, medium to (very) coarse-grained fabric of mono- and polycrystalline quartz, feldspar (often weathered) and lithic fragments (fig.25, A, B). Single grains with sizes over 2 mm were also observed. Overall, the grain contacts are predominantly convex-concave and partially sutured. No matrix was detected. Occasionally, quartz overgrowths can be recognized. The grain shape appears subangular to subrounded. Iron oxides are also present.

Quartz: Monocrystalline quartz shows an occurrence of 7.4 – 13.2%. Undulatory extinction over 10° is very common with 85.7 – 92%. Also, bohemian lamellae within monocrystalline quartz can be observed, but are very rare (fig.25, D). Polycrystalline quartz forms a range of 72.2 – 79.1, whereas a subgrain-fabric of more than 3 subgrains (Qp>3) is the most common type within 81.8 – 91.2% of the grains. Qp2 and Qp3 each show frequencies of 2.6 – 9.9 and 4.8 – 8.2%. A subgrain-fabric of characteristic triple grain junctions can be observed within 4.7 – 9.5% of the counted grains. Elongated subgrains show an occurrence of 1.6 – 3.4%. Overall, the subgrain boundaries appear irregular to straight, whereas only polycrystalline quartz with triple grain junctions shows straight (and sutured) subgrain boundaries. Chert is very rare.

Inclusions within quartz are common. Both Qm and Qp show inclusions of mica (muscovite, rarely biotite), feldspar and heavy minerals like zircone, tourmaline and garnet. Polycrystalline quartz grains with inclusions of mica were treated as metamorphic rock fragments for QFL-plotting (fig.25, E).

Fig.25 (next page), 19 A (PPL), B (XPL): moderately sorted, coarse grained dislodged slice of Heiligenkreuz, C (XPL): perthitic feldspar, D (XPL): monocrystalline quartz with bohemian lamellae, E (XPL): metamorphic rock fragment, F (XPL): feldspar with inclusions of quartz (blue arrow) and biotite (red arrow), G (PPL), H (XPL): large subrounded sillimanite

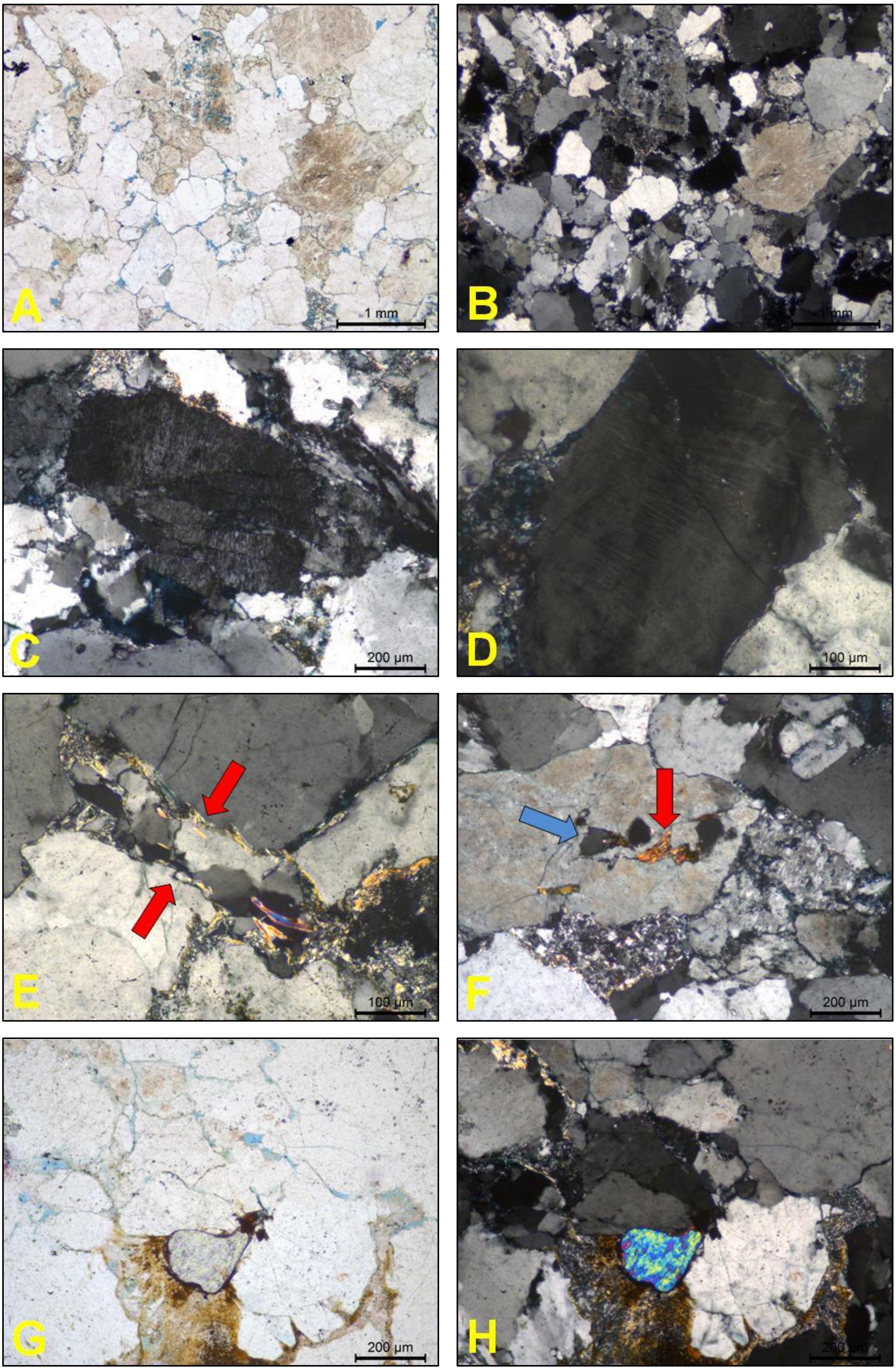
A
1 mm
B
1 mm
C
200 µm
D
100 µm
E
100 µm
F
200 µm
G
200 µm
H
200 µm

Feldspar: Secondary porosity due to the weathering of K-feldspar shows a frequency of 0.31 – 1.27%. By combining this value with the values of intersected feldspar, an original content of 8.8 – 18.21% for K-feldspar can be estimated. Perthitic exsolution is very common (46.6 – 51.7%) (fig. 25, C). Inclusions are common mainly consisting of quartz (fig.25, F). Plagioclase, identified by its polysynthetic twinning, is very rare. 2 grains in total were observed, but not intersected by the crosshair during the counting procedure.

Lithic fragments: 14.0 – 33.0% of polycrystalline quartz grains include traces of primary mica. Therefore, these grains were finally counted as metamorphic rock fragments. In relation to the whole rock composition, this amounts for 10.7 – 23.2%. Shale or silt clasts and other metamorphic fragments show a frequency of 1.3 – 1.9%.

In summary, the average framework composition of 4 counted dislodged slices of Heiligenkreuz consists of 10.7% monocrystalline quartz, 57.7% polycrystalline quartz, 16.9% polycrystalline quartz with inclusions of mica (Lm), what makes 74.4% polycrystalline quartz grains in total, 13.1% feldspar and 1.6% of other different rock fragments (fig.26).

Dislodged slice (Heiligenkreuz) Average composition (%)	
Qm (slight u.ex), <10°	1,09
Qm (undul. ex.), >10°	8,98
Total	**10,07**
Qp2	4,62
Qp3	4,69
Qp>3	65,13
**Qp elong.*	1,80
**Qp tripple. gr. b.*	5,16
**(+mica (Lm))*	16,91
Total	**74,43**
K-feldspar	5,92
K-feldspar exsoluted	6,62
Secondary por. within fsp.	0,55
Total	**13,09**
grain replacive kaolinite	0,00
Chert	0,23
Mica	0,23
Sec. Porosity	0,39
Lithic fragments	0,00
*Felsic fr.	0,23
*Ls	0,86
*Lm	0,47
Total	**1,56**
Total (320,25)	**100,00**

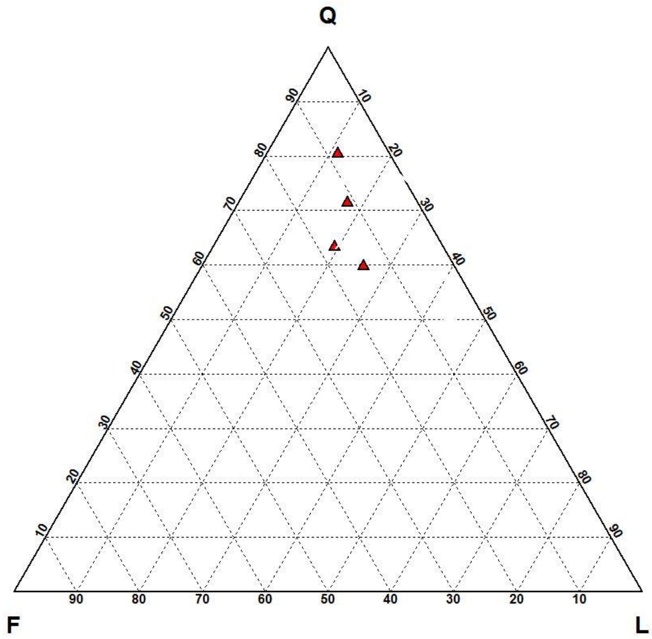

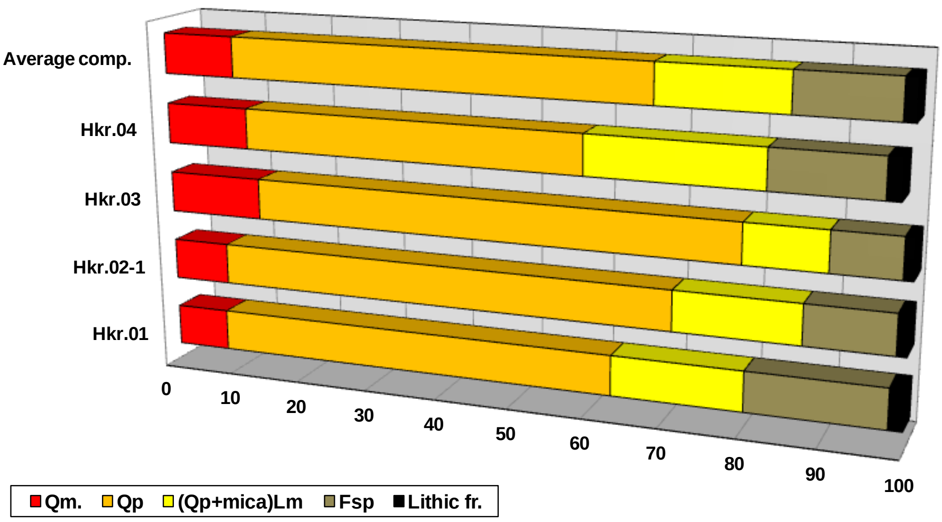

Fig.26 Upper left: average composition of 4 counted samples of Heiligenkreuz, upper right: ternary QFL – plot of 4 counted samples of Heiligenkreuz. lower fig.: mineralogical composition of 4 counted Heiligenkreuz-samples

6.2.5 Dislodged slices of Groisbach

Thin section analysis shows a fine-grained, very well sorted fabric within a sparry cement and very small amounts of bioclasts (e.g. echinoderms) for some of the samples (fig.27, A, B). Monocrystalline quartz constitutes the main mineralogical phase. Grains of polycrystalline quartz, chert, feldspar, flakes of mica and rock fragments (e.g. monocrystalline quartz plus mica) only form single occurrences. Some of the feldspar grains show exsolution. Overall, the shape of the grains appears angular to subangular. Single grains of rounded shape can also be seen. These samples can be regarded as carbonate sandstones.

Amounts of bioclasts vary strongly between the samples (e.g. fig.27, A, C). Samples with high amounts include gastropods, large numbers of echinoderms (e.g. cross sections of stalks of crinoids) and different shell pieces, which in many cases show original substance preservation (fig.27, E). Echinoderm fragments show the characteristic straight exsolution under XPL. Ooids, often with echinoderms or quartz (fig.27, G) as a nucleus, also occur in high amounts. The component distribution appears overall consistent (e.g. fig.27, F, H). Shell fragments indicate a certain orientation (fig. 27, E). Most of the ooids show radial-fibrous laminae (e.g. fig.27, G), which are common for low water energy settings (Flügel 2002). According to Folk (1958, 1962) and Dunham (1962) these sandy limestones can be classified as sandy oo-/biosparites or as bioclastic grainstones.

Microfacies analysis after Flügel (2002) indicates a shallow marine environment like a platform, shelve, oolitic shoal with various amounts of clastic influx due to re-gression and transgression events (SMF-type 15).

Fig.27 (next page), A, B: sand-sized, fine grained sample of Groisbach, C: gastropode (center), ooids, echinoderms and monocrystalline quartz, D: ooids, shell fragments, echinoderms and monocrystalline quartz, E: shell fragments with original substance preservation, F: recrystallized shell fragment (center) and ooids (XPL), G: monocrystalline quartz often form nuclei within ooids (center), H: large echinoderm fragment next to a recrystallized bivalve and non-recrystallized shell fragments,

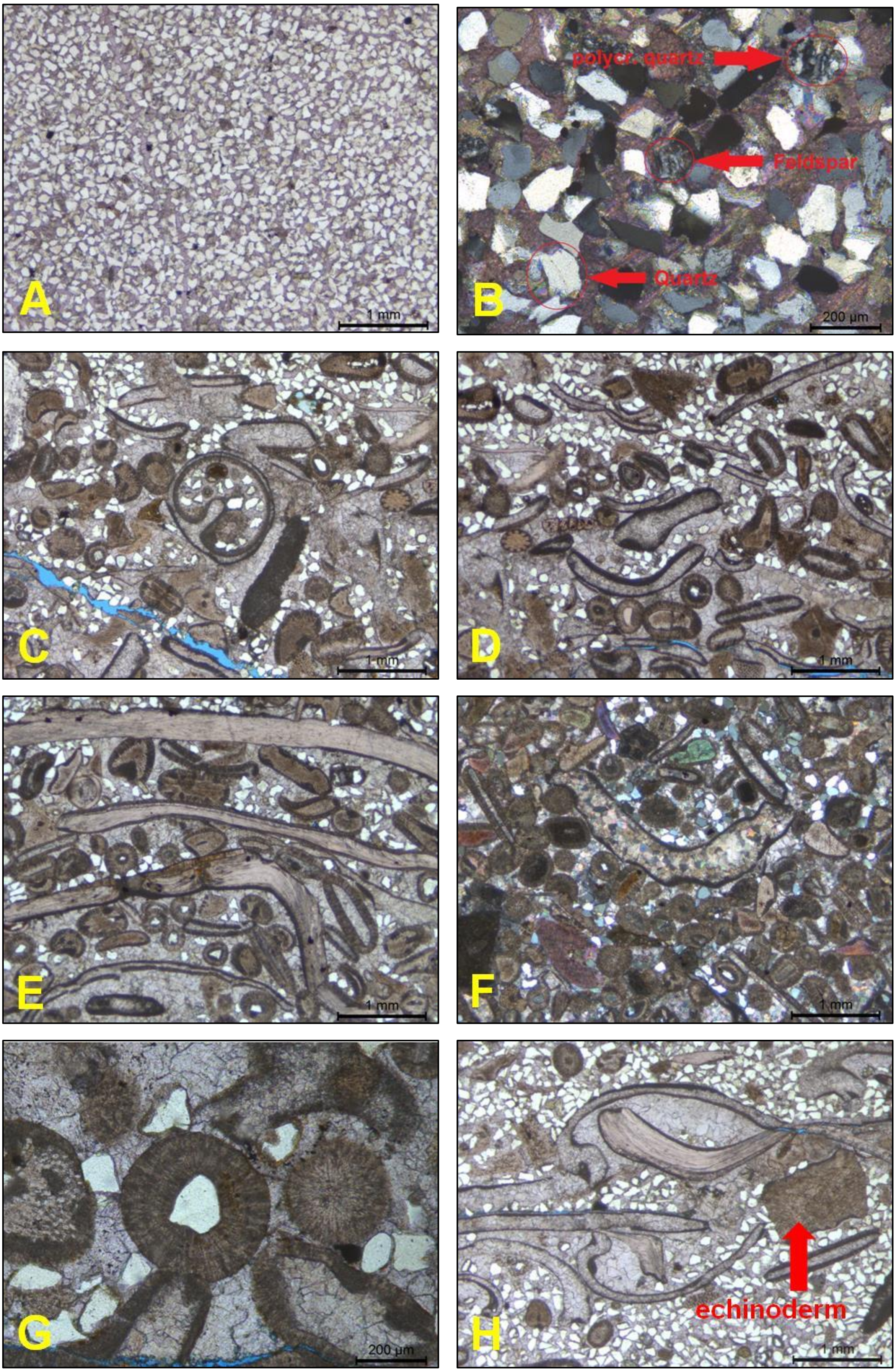
A
1 mm
polycr. quartz
Feldspar
Quartz
B
200 µm
C
1 mm
D
1 mm
E
1 mm
F
1 mm
G
200 µm
echinoderm
H
1 mm

6.2.6 Reddish, fine grained samples of Hafnerberg

Thin section analysis shows an inequigranular mosaic of tightly packed, non-rhombic dolomite within a spotty groundmass of hematite (fig.28). The shapes of the crystals appear anhedral to euhedral with lobate to straight grain boundaries. No intercrystalline porosity was detected. The maximum crystal size is up to 200 µm. According to the crystal size of >10µm, the samples can be classified as dolosparstones (after Friedman 1965). Plöchinger and Salaj (1991) classified these rocks as calcareous arenites.

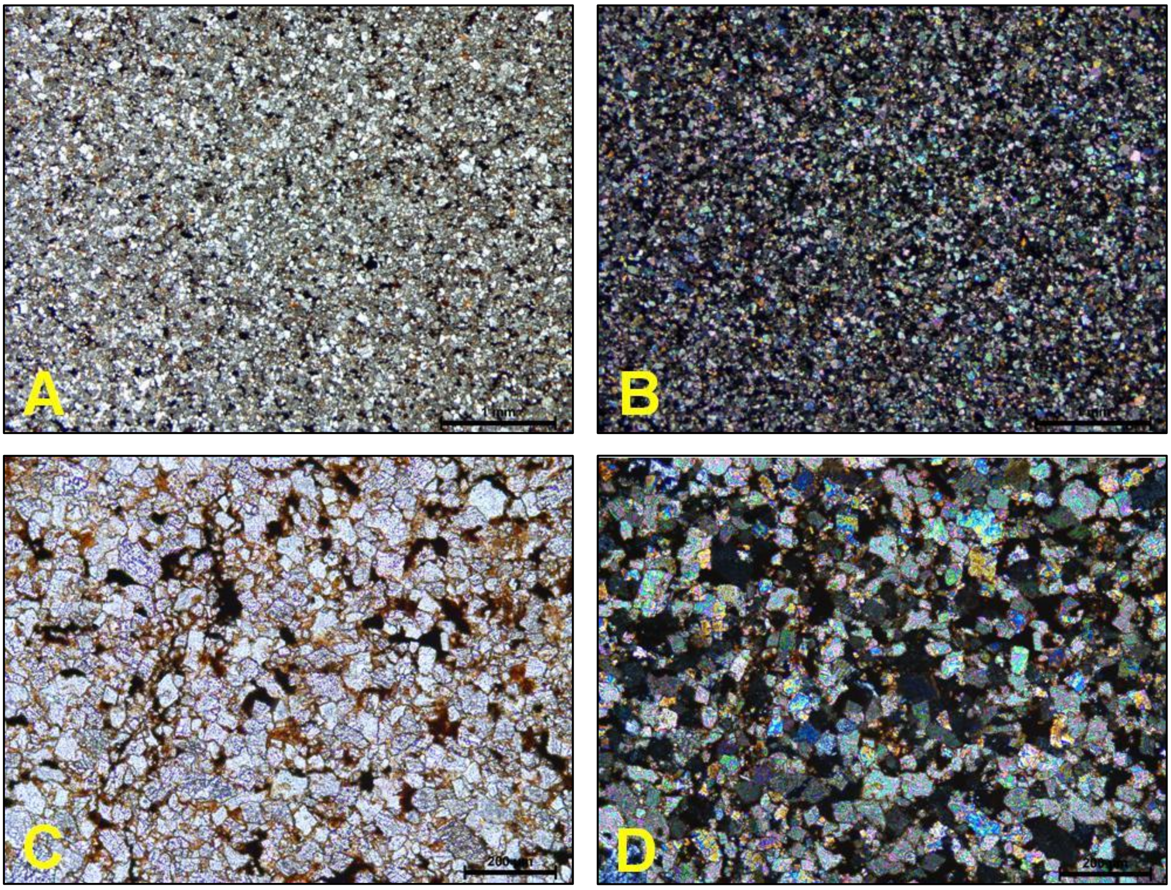

Fig. 28 PPL (left) and XPL (right) images of dolostones of Hafnerberg

6.2.7 Results of Gazzi-Dickinson point-counting

According to the count results, an average mineralogical composition of $Q_{88}F_{10}L_2$ for all samples can be calculated, whereas Q includes all quartzose grains. F for feldspar reflects the original feldspar content of approx. 10%. Amounts of feldspar, kaolinite and secondary porosity were used to calculate the original feldspar content. By adding polycrystalline quartz grains with inclusions of mica to the lithic fraction (as proposed by Ingersoll 1984), the rocks show an average composition of $Q_{65}F_{10}L_{25}$.

Overall, the samples are very similar. Variations between Qm and Qp are primarily caused by grain size effects. Compared to the dislodged slices, the St. Veit Klippenzone sandstones appear more weathered by showing higher amounts of kaolinite and secondary porosity due to postdepositional weathering of feldspar. Average chert values are 0.3 and 0.1%. Lithic fragments, which are predominantly unstable, show low occurrences of 2.6 and 2.2% (tab.3).

Samples	n	Parameters	Qm	Qp (total)	F	Kaolinite
St.Veit Klippenzone		mean	8,3	79,3	4,7	1,1
(Lainz tunnel + Ober St. Veit,	8	range	3,9 - 16,6	76,0 - 84,3	0,3 - 7,3	0 - 6,0
Gemeindeberg)		std. dev.	4,9	3,0	2,1	1,9
Dislodged slices		mean	16,7	71,0	9,2	0,1
(Hinterbrühl, Heiligenkreuz,	9	range	7,4 - 29,7	55,1 - 79,1	4,1 - 18,0	0 - 1,1
Rehgras)		std. dev.	7,2	7,0	4,3	0,4

Samples	n	Parameters	Chert	L	Sec. Por.	L+ (Qp+mica)
St.Veit Klippenzone		mean	0,3	2,6	3,3	27,2
(Lainz tunnel + Ober St. Veit,	8	range	0 - 1,9	0,6 - 6,1	0 - 6,1	14,5 - 40,6
Gemeindeberg)		std. dev.	0,6	1,9	2,0	21,7
Dislodged slices		mean	0,1	2,2	0,6	22,8
(Hinterbrühl, Heiligenkreuz,	9	range	0 - 0,6	1,1 - 5,1	0 - 3,7	11,9 - 31,1
Rehgras)		std. dev.	0,2	1,3	1,1	6,1

Tab.3 Calculated results of Gazzi-Dickinson point counting

sdt.dev. = standard deviation, Qm = monocrystalline quartz, Qp (total) = total polycrystalline quartz grains, F = Feldspar. L = lithic fragments (except Qp+mica), sec. por. = sand-sized secondary porosity, L+(Qp+mica) = lithic fragments in total as defined by Ingersoll (1984)

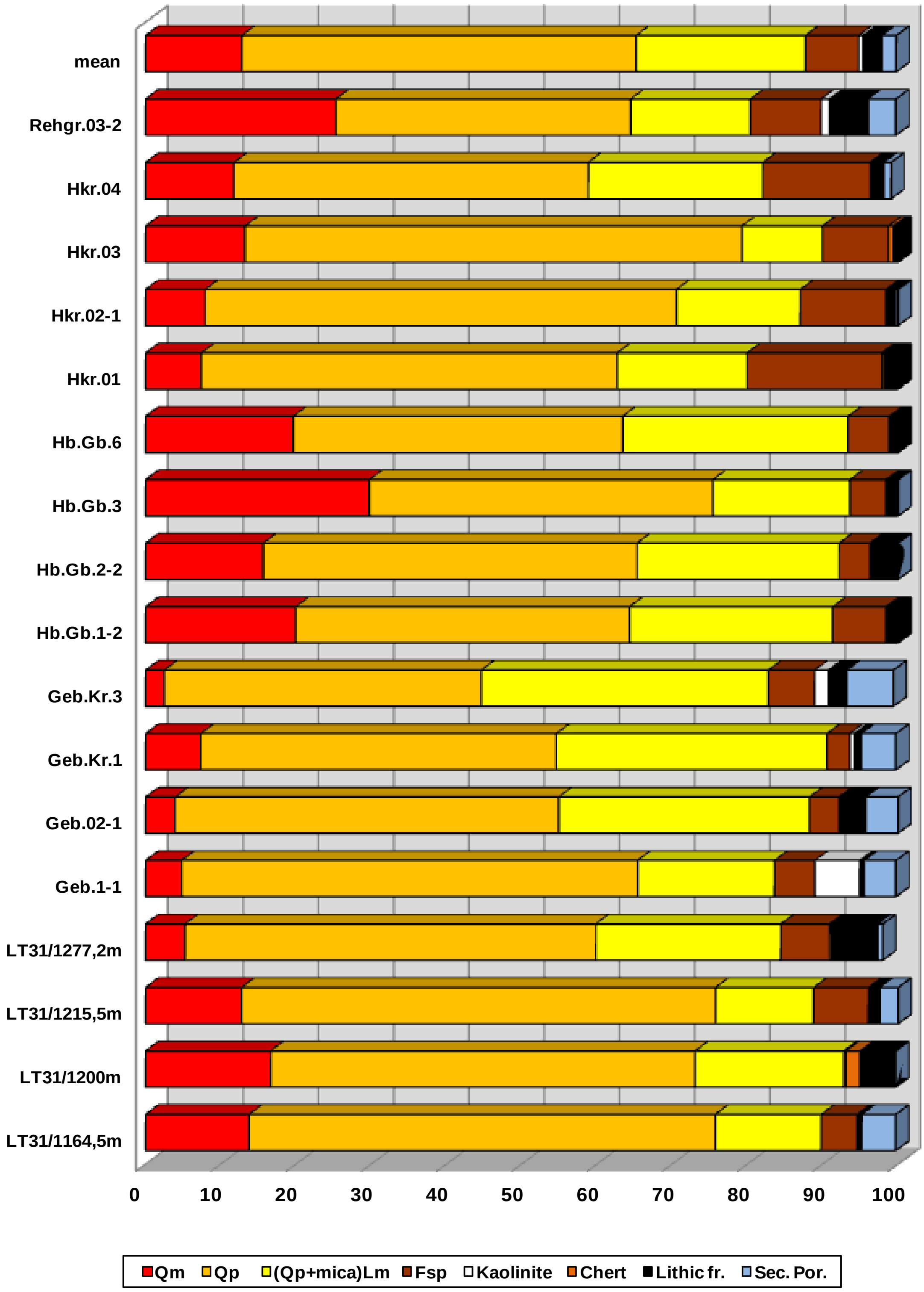

Fig.29 Count results of investigated samples (LT: Lainz tunnel, Geb.: Gemeindeberg, Ober St. Veit, Hb.Gb.: Hinterbrühl ("Grillenbühel"), Hkr.: Heiligenkreuz, Rehgr.: Rehgras)

6.2.8 MMI-Mineralogical maturity index

The MMI uses the proportions of quartz (Qm, Qp, chert) related to the proportions of feldspar and rock fragments to obtain the mineralogical maturity of a sample according to following scale (Nwajide and Hoque 1985):

Q=95%, (F+L)=5%	**MMI≥19 : super mature**
Q=95-90%, (F+L)=5-10%	**MMI=19-9.0: mature**
Q=90-75%, (F+L)=10-25%	**MMI=9.0-3.0: submature**
Q=75-50%, (F+L)=25-50%	**MMI=3.0-1.0: immature**
Q= <50%, (F+L)= >50%	**MMI=≤1: extremly immature**

Tab. 4 Sandstone maturity scale after Nwajide and Hoque (1985)

Sample	sample site	correlation	MMI (Q/(F+L))
LT31/1164,5m	Lainz tunnel	St. Veit Klippenzone	9,1
LT31/1200m	Lainz tunnel	St. Veit Klippenzone	18,9
LT31/1215,5m	Lainz tunnel	St. Veit Klippenzone	7,9
LT31/1277,2m	Lainz tunnel	St. Veit Klippenzone	6,4
GeB.1-1	Gemeindeberg	St. Veit Klippenzone	5,2
GeB.02-1	Gemeindeberg	St. Veit Klippenzone	7,5
GeB.Kr.1	Gemeindeberg	St. Veit Klippenzone	9,9
GeB.Kr.3	Gemeindeberg	St. Veit Klippenzone	5,0
Hkr.01	Heiligenkreuz	dislodged slice	4,0
Hkr.02-1	Heiligenkreuz	dislodged slice	6,7
Hkr.03	Heiligenkreuz	dislodged slice	8,9
Hkr.04	Heiligenkreuz	dislodged slice	4,8
Hb.Gb.1-2	Hinterbrühl	dislodged slice	10,5
Hb.Gb.2-2	Hinterbrühl	dislodged slice	11,8
Hb.Gb.3	Hinterbrühl	dislodged slice	14,6
Hb.Gb.6	Hinterbrühl	dislodged slice	14,1
Rehgr.03-2	Rehgras	dislodged slice	4,4
mean			8,8

Tab.5 Calculated MMI for Keuper sandstones of the St. Veit Klippenzone and dislodged slices

According to Nwajide and Hoque (1985), the quartzite sandstones of the St. Veit Klippenzone and the dislodged slices can be regarded as submature to mature (tab.4). For calculating, the original feldspar content was taken into account. The range of values is primarily caused by variable feldspar contents within the samples (see chapter 6.2).

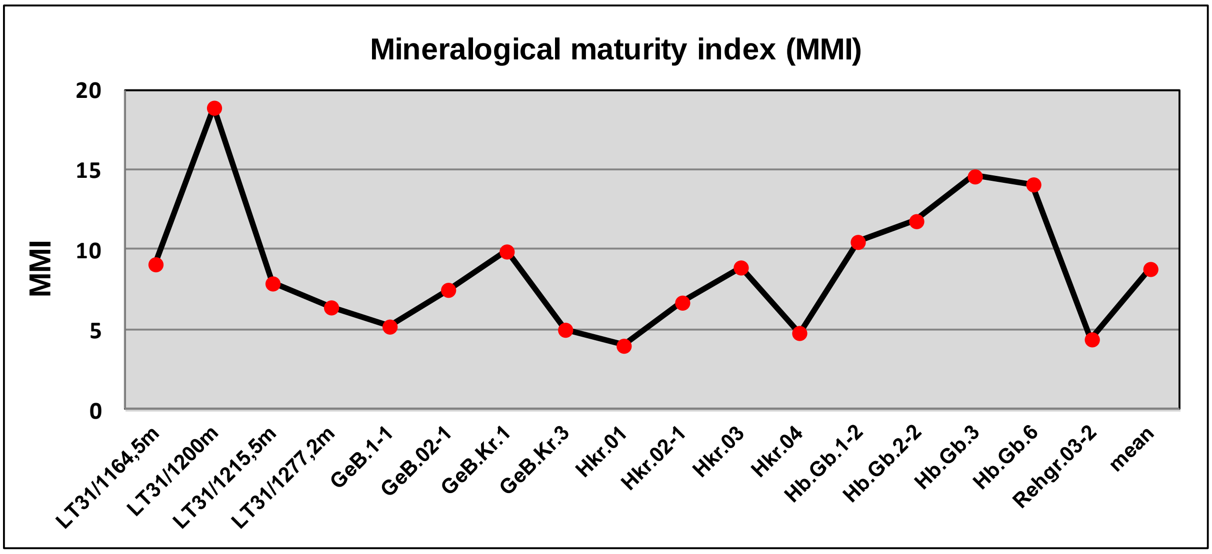

Fig.30 MMI for samples of investigated samples

Generally, it can be said that samples, which include higher amounts of feldspar, (e.g. dislodged slices of Heiligenkreuz) do have a significant lower MMI. All of these sandstones are currently regarded as Late Triassic Keuper sandstones. Therefore, an average of 8.8, what suggests submature (closely to mature) composition, can be calculated. Striking is the fact, that distinct differences in the MMI for different samples sites can be observed. Due to low feldspar content, the dislodged slices of Hinterbrühl seem to have the highest MMI.

	MMI (average)
Lainz tunnel	10,6
Gemeindeberg	6,9
Heiligenkreuz	6,1
Hinterbrühl	12,8

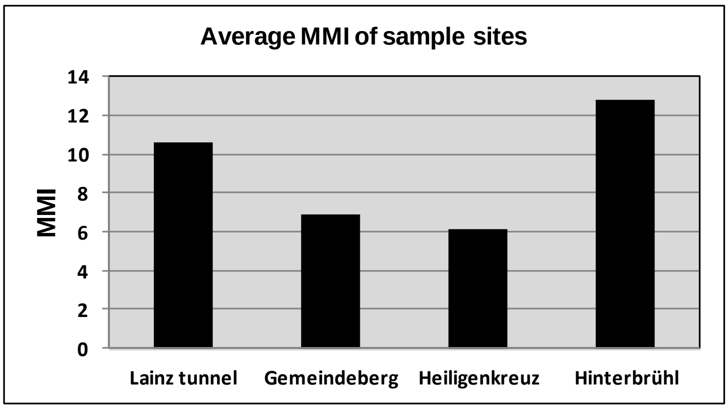

Fig.31 Average MMI of different sample sites of Keuper sandstones; the dislodged slice of Hinterbrühl shows a significantly higher MMI

6.2.9 Petrographic sandstone classification and source rocks

Petrographic sandstone classification after Folk (1970) showed following results: the samples of the St. Veit Klippenzone and the dislodged slices were classified as sublitharenites, litharenites and feldspathic litharenites (fig.32, tab.5). For classification, the original feldspar content was used. In addition, a classification after McBride (1963) was made, which is also commonly used (fig.32). According to this scheme, the samples were classified as sublitharenites, litharenites, lithic subarkoses and feldspatic litharenites. Higher amounts of feldspar led to the classification as lithic subarkose (after McBride 1963) for following samples: 2 sandstones of the dislodged slices of Heiligenkreuz, 1 dislodged slice of Rehgras and 1 sample of Ober St. Veit. The dislodged slices of Hinterbrühl were classified as sublitharenites and litharenites in both schemes. The spread in composition between the samples is mainly caused by grain size effects. Very coarse-grained samples tend to have significantly higher amounts of lithic fragments, mainly consisting of Qp and mica.

Sample	sample site	correlation	after Folk (1970)	after McBride (1963)
LT31/1164,5m	Lainz tunnel	St. Veit Klippenzone	sublitharenite	sublitharenite
LT31/1200m	Lainz tunnel	St. Veit Klippenzone	sublitharenite	sublitharenite
LT31/1215,5m	Lainz tunnel	St. Veit Klippenzone	sublitharenite	sublitharenite
LT31/1277,2m	Lainz tunnel	St. Veit Klippenzone	litharenite	litharenite
GeB.1-1	Gemeindeberg	St. Veit Klippenzone	feldpathic litharenite	lithic subarkose
GeB.02-1	Gemeindeberg	St. Veit Klippenzone	litharenite	litharenite
GeB.Kr.1	Gemeindeberg	St. Veit Klippenzone	litharenite	litharenite
GeB.Kr.3	Gemeindeberg	St. Veit Klippenzone	feldpathic litharenite	feldpathic litharenite
Hkr.01	Heiligenkreuz	dislodged slice	feldpathic litharenite	lithic subarkose
Hkr.02-1	Heiligenkreuz	dislodged slice	feldpathic litharenite	lithic subarkose
Hkr.03	Heiligenkreuz	dislodged slice	sublitharenite	sublitharenite
Hkr.04	Heiligenkreuz	dislodged slice	feldpathic litharenite	feldpathic litharenite
Hb.Gb.1-2	Hinterbrühl	dislodged slice	litharenite	litharenite
Hb.Gb.2-2	Hinterbrühl	dislodged slice	litharenite	litharenite
Hb.Gb.3	Hinterbrühl	dislodged slice	sublitharenite	sublitharenite
Hb.Gb.6	Hinterbrühl	dislodged slice	litharenite	litharenite
Rehgr.03-2	Rehgras	dislodged slice	feldpathic litharenite	lithic subarkose

Tab.6 Results for petrographic sandstone classification; note the slight differences between the schemes

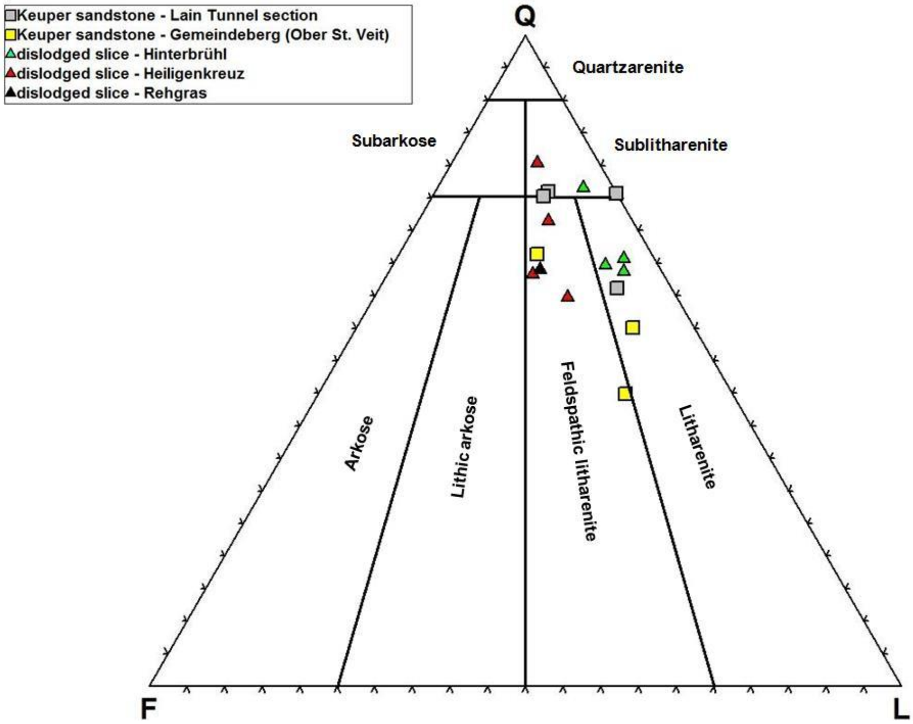

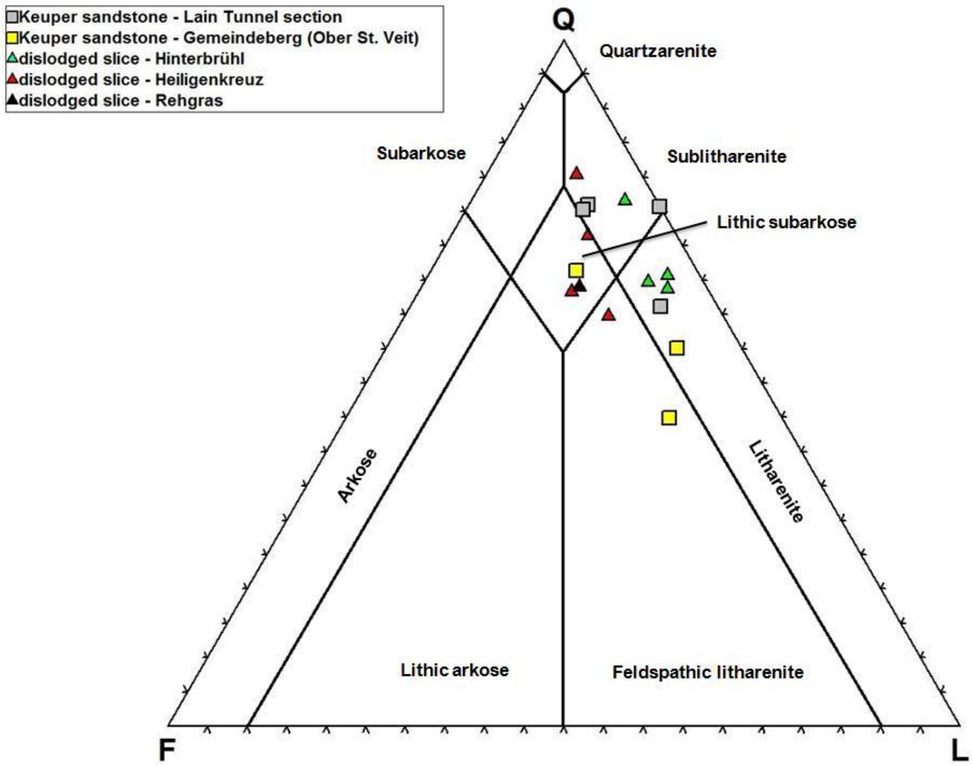

Fig.32 Petrographic sandstone classification; upper fig.: classification after Folk (1970); lower fig.: classification after McBride (1963); note the slight differences between the schemes

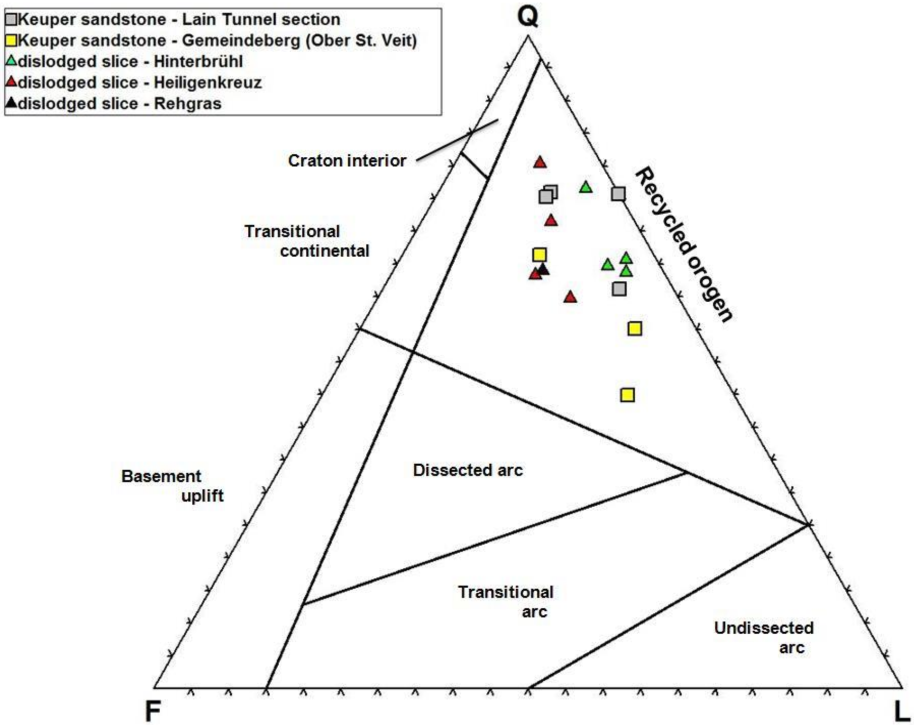

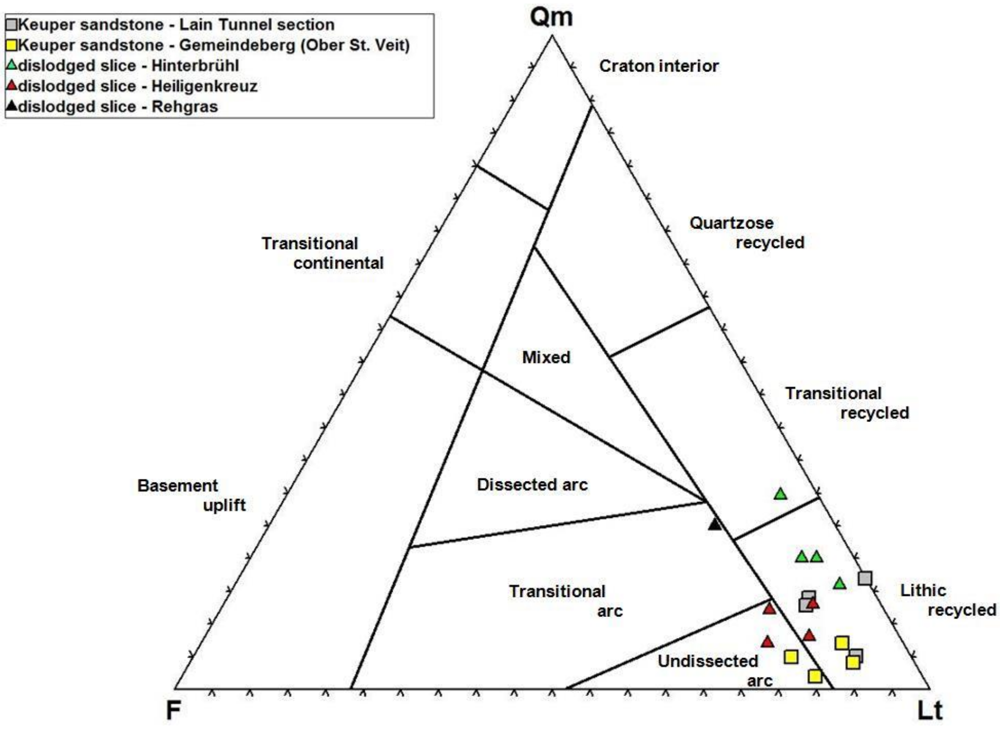

Fig.33 Petrographic provenance analysis after Dickenson and Suszeck (1983);

The results, illustrated by ternary QtFL and QmFLt –plots, indicate a recycled orogen as probable provenance for the investigated samples

A QtFL-plot after Dickinson (1985) indicates a recycled orogen as provenance for the St. Veit Kippenzone sandstones and the dislodged slices of Lower Austria (fig. 33). According to Dickinson and Suszeck (1979, 1985), three major types of orogenic provenances are distinguished: 1. Subduction complexes, mainly composed of uplifted oceanic and/or ophiolithic material. High chert contents are considered as a key signal for sediments derived from subduction complexes. These complexes form structural heights within arch-trench systems. The clastic material is deposited either towards the arc into forearc basins or into the trench along the subduction complex itself. 2. Collision orogens. Collision-derived sediments are mainly composed of material from nappes and thrust sheets, which originally form sedimentary sequences along and near proceeding continental margins. Depositional environments are adjacent oceanic basins (as turbidites), foreland basins and complexly formed basins along the suture belt. 3. Foreland uplifts. This type includes recycled material from fold-thrust belts, which is deposited within adjacent foreland basins also flanking either arc or collision orogens. It is assumed, that fold-thrust belts act as a barrier to clastic influx from nearby arc or collision orogen-provenances. Therefore, sediments derived from foreland-uplift provenances are typically composed of sedimentary successions within the fold-thrust belts.

It is also known, that besides these three main active tectonic settings, orogenic belts, as structural heights, can form big river systems, which are capable of transporting recycled material into distant basins of various kinds of tectonic settings (e.g. Potter 1978).

In general, recycled orogen-derived sediments include various proportions of material from cratonic, arkosic, sedimentary or/and volcanoclastic source rocks, also influenced by metamorphism. This is expressed by e.g. various amounts of lithic fragments, feldspar or varying proportions of Qm/Qp (Dickenson 1985).

The treatment of Qp is crucial for provenance analysis, as the examined samples show high levels of Qp, strongly suggesting a metamorphic source. High degrees of undulatory extinction within the counted Qm-grains support this observation. However, polycrystallinity of quartz and undulatory extinction can be significantly affected by diagenetic processes like compaction (Dickenson 1985).

A QmFLt-plot discriminates provenance terrains with the emphasis on the source rock (fig.33). Large amounts of Qp within the counted samples led to plotting within the “lithic recycled” field of the recycled orogen block. However, it must be noted, that, according to Dickinson (1985) and Dickinson and Suszek (1979) Qp is chiefly associated with the presence of chert, an indicator for sandstones derived from e.g. subduction complexes. Chert only occurs occasionally within the samples (see chapter 6), therefore, it is the opinion by the author of this thesis, that the QmFLt-plot does not reflect accurately the source rocks of the investigated samples.

According to Young (1976), different appearances of Qp can be used for the determination of source rocks. Triple grains junctions within Qp are characterized by non-undulose, strain-free polyhedral subgrains and are associated with medium to high-grade metamorphic source rocks (e.g. gneisses). These grains are considered as “stable” by reflecting a balance with surrounding pressure and temperature conditions in the former rock. An elongated subgrain-fabric, a strong indicator of deformation, is preferably associated with low to medium-grade metamorphic rocks (e.g.schists). Sutured subgrain boundaries are also a result of deformation. Qp with different subgrain sizes, elongated subgrains, subgrains with undulatory extinction are considered as “unstable” and reflect a transition state between the “old” and the “new” crystal. These grains represent the most common types within the samples and are associated with low-grade metamorphism.
Bohemian lamellae within Qm (which are very rare) are an indicator for metamorphic stress. Rounded Qm, seldom with traces of an ancient quartz cement (e.g.fig. 22, G) are a strong indicator for a sedimentary source (e.g. Pettijohn 1975).

Assuming, that the climate was a primary control factor (which only applies under certain conditions) for the composition, the presence of Qp within sandstones can be used to reconstruct palaeoclimatic settings (Suttner and Dutta 1986). Unstable polycrystalline/polymineralic fragments strongly tend to decompose under wet, humid conditions leading to the enrichment of stable Qp within the sample. High amounts of Qp and high mineralogical maturity suggest a humid climate during the deposition for the investigated samples (fig.34).

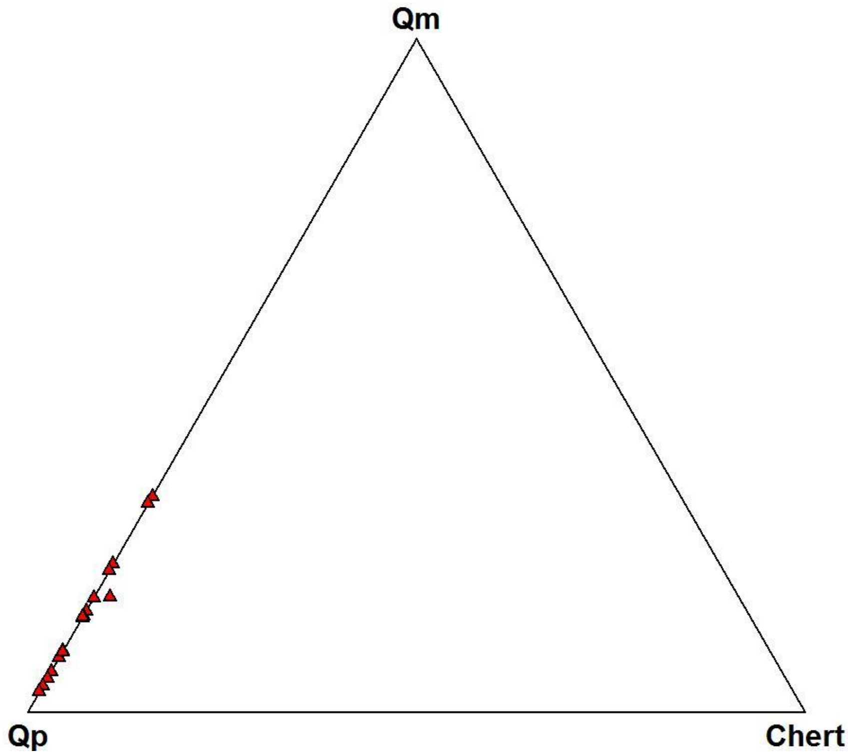

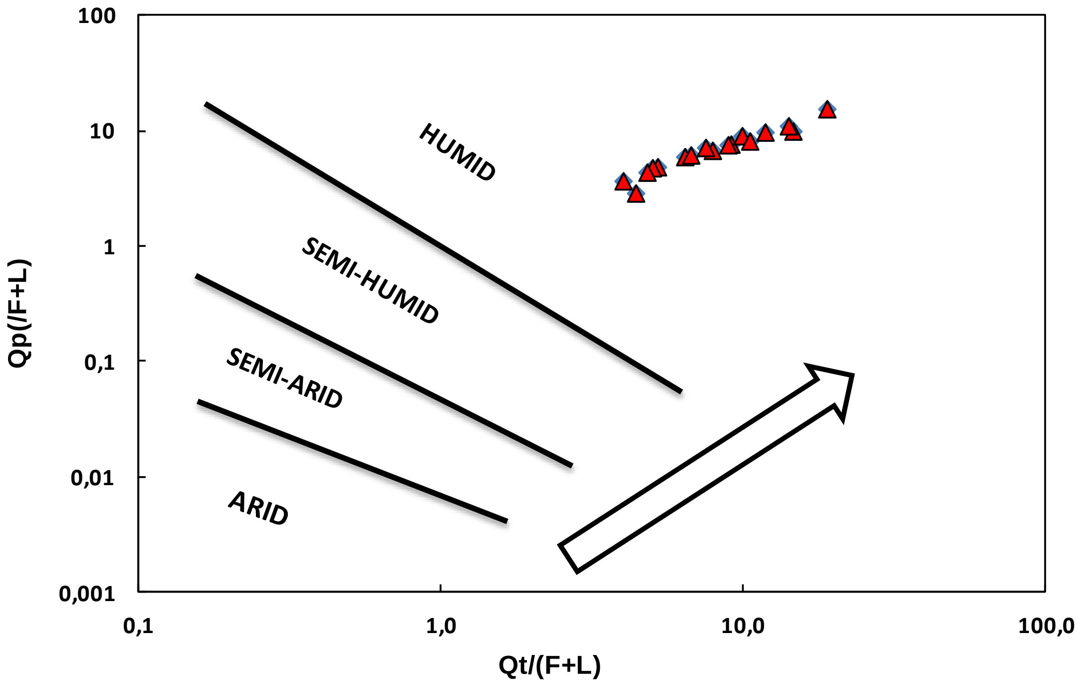

Fig.34 upper fig.: relations of monocrystalline, polycrystalline and microcrystalline (chert) quartz within the samples; lower fig.: palaeoclimatic conditions as a function of polycrystallinity of quartz. High amounts of Qp and high mineralogical maturity strongly indicate a humid climate during deposition; the arrow indicates a rise in temperature (after Suttner and Dutta 1986) 6.2.10

6.2.10 Liassic-Doggerian Gresten sandstones

Thin section analysis shows well to poorly sorted, fine to very coarse grained samples, consisting of Qm and Qp, feldspar (K-feldspar and plagioclase), mica and different lithic fragments. Amounts of feldspar vary strongly between the samples.

1. The Liassic – Doggerian Gresten sandstone, which was taken nearby **Ybbsitz**, shows a well sorted, fine to medium grained fabric of Qm, high amounts of feldspar (potassium feldspar and plagioclase), detrital mica and felsic rock fragments (mainly composed of feldspar) (fig.29 A - D). Qp only occurs occasionally. K-feldspar is more common than plagioclase. An angular to subangular grain shape dominates.

2. The Liassic Gresten sandstone of **Pechgraben** (Weyer) is predominantly poorly sorted, very coarse-grained and with high amounts of Qp (fig.35 E, F). The subgrain-fabric of Qp-grains mostly appears irregular. Inclusions of mica within Qp were also detected. Grain sizes over 2mm are very common. Striking is the fact, that no feldspar was detected, which is in accordance to XRD-analysis (see chapter 6.1.4). Qm is rare. Calcite cementation is also very common. Due to its quartz-rich nature and similar appearance compared to the Keuper sandstones, this sample was chosen for geochemical comparison.

3. The sample of **Waidhofen** appears poorly sorted, calcite-cemented with high amounts of Qp and lithic fragments, which mainly consist of aggregates of Qp and feldspar (fig.35 H) and felsic rock fragments (fig.35 J). K-feldspar and plagioclase (fig.35 I) are very common. Overall, the rock looks very similar to the sample of Pechgraben and was also used for geochemical analysis.

4. The Liassic Gresten sandstone/conglomerate of **Ybbs/Waidhofen** shows a poorly sorted fabric of Qm, Qp, feldspar (K-feldspar, plagioclase) within a brownish clay matrix (fig.35 K-N). Qm is more common compared to the other samples. Felsic rock fragments are predominantly composed of feldspar, quartz and mica.

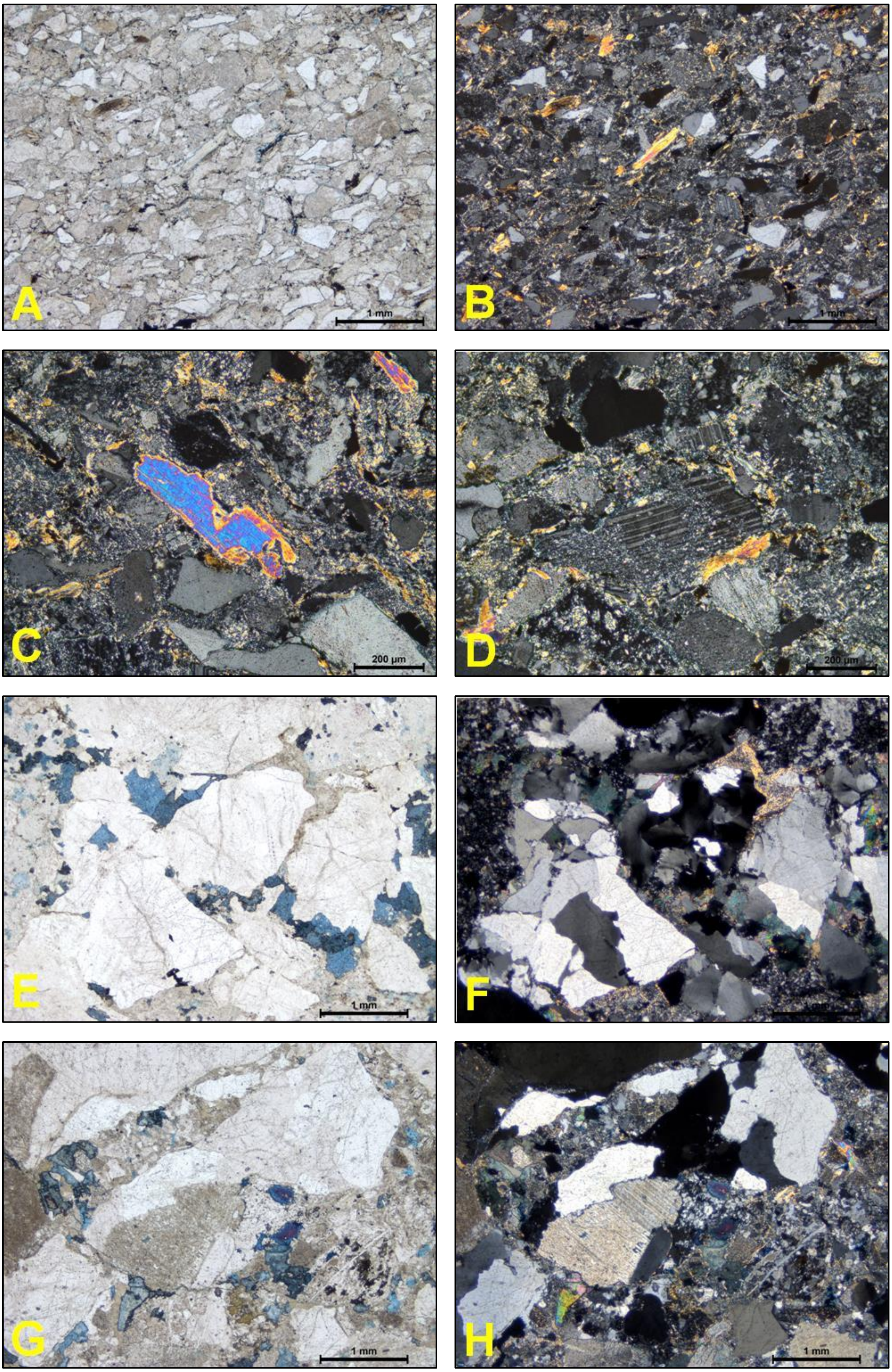
A
1 mm
B
1 mm
C
200 µm
D
200 µm
E
1 mm
F
G
1 mm
H
1 mm

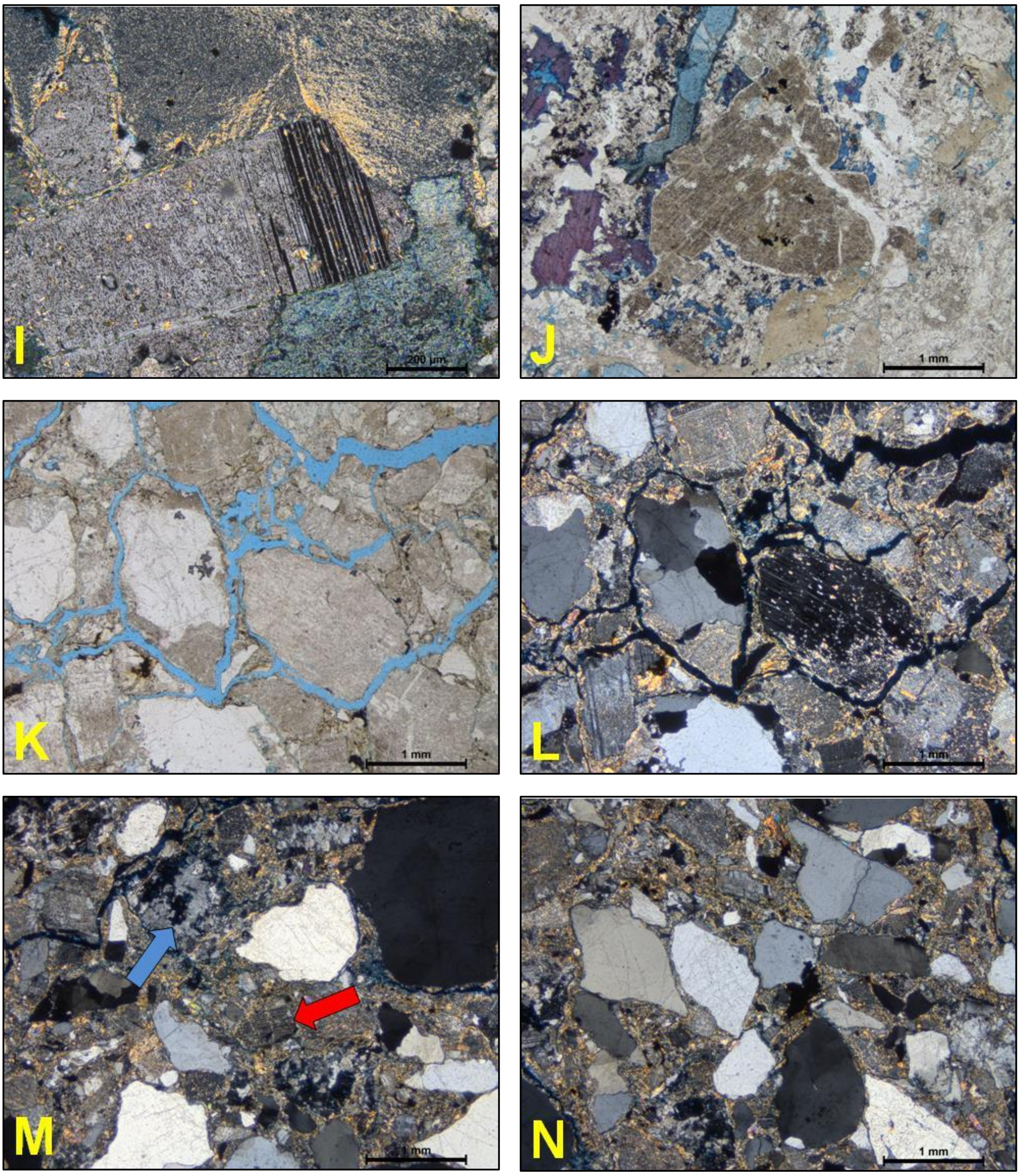

Fig.35 (previous page) A (PPL), B (XPL): well sorted, fine to medium grained sample of **Ybbsitz**, Qm and feldspar are dominant, C (XPL): detrital mica (center), D (XPL): plagioclase (center), quartz, feldspar, mica; E (PPL), (F (XPL): poorly sorted, calcite-cemented, Qp-rich sample of **Pechgraben** (Weyer); G (PPL), H (XPL): poorly sorted sample of **Waidhofen**, center: metamorphic rock fragment, consisting of Qp and plagioclase, I (XPL): plagioclase, J (PPL): center: felsic rock fargment, mainly composed of feldspar; K (PPL), L (XPL): poorly sorted sample of **Ybbs/Waidhofen,** M (XPL): Ybbs/Waidhofen: weathered K-feldspar (blue arrow) and red plagioclase (red arrow) next to Qm and rock fragments, N (XPL): Qm next to feldspar and lithic fragments

6.3 Geochemical analysis

6.3.1 Major and minor element distribution

Nowadays, geochemical analyzes are essential to fully understand the composition, depositional history and provenance of sandstones.

The samples of the St. Veit Klippenzone (GeB.1, GeB.Kr.3) and the dislodged slices (Rehgr.02, Rehgr.03, Hkr.02, Hkr.04, Hb.Gb.3), except the sample of Groisbach (Gr.1-5), show very high SiO_2-contents above 90% (tab.6). The Gresten sandstones of Waidhofen (Gr.S.01) and Pechgraben/Weyer (Gr.S.04) include significant lower SiO_2 amounts of 76,99 and 78,29 %. For the samples which show high amounts of carbonate minerals (Hafnerberg and Groisbach) SiO_2 contents of 8.11 and 5.57 % (Hb.1-1 and Hb.1-2) and 31,68% (Gr.1-5) were analyzed. Quartz is considered to be the main donor for SiO_2 within the samples, whereas chert, feldspar, mica and other silicates provide SiO_2 in lesser amounts. Al_2O_3 and K_2O can be derived from the presence of minerals such as feldspar and mica. The sandstones of Ober St. Veit show Al_2O_3 and K_2O contents of 2.51 - 2.54 and 0.34 – 0.44 %. The quartzite dislodged slices of Lower Austria include Al_2O_3 and K_2O in a range of 1.29 – 3.41% and 0.34 – 1.09%. The dislodged slice of Groisbach shows Al_2O_3 and K_2O contents of 0.84 and 0.08%. Compared to the Keuper sandstones, the Al_2O_3 amounts within the Gresten sandstones are significantly higher: 8.39 and 8.53%. For the samples of Hafnerberg Al_2O_3 contents of 5.29 – 7.91% were observed. Only one Gresten sandstone shows considerable amounts of K_2O of 1.54%. Na_2O is also mainly attributable to the presence of feldspar (plagioclase). Only two samples of dislodged slices of Heiligenkreuz show significant amounts of 1.51 and 1.54%. One Gresten sandstone (Gr.S.01) also contains 1.96% of Na_2O. Contents of Fe_2O_3 and MgO are mainly associated with the presence of lithic fragments or carbonatic cement like siderite and dolomite. Due to the presence of hematite, the samples of Hafnerberg include significant Fe_2O_3 amounts of 1.46 – 3.36%. The Gresten sandstones include iron oxides of 1.47 and 2.06%. MgO contents within the Keuper sandstones are very low: 0.08 – 0.17%, whereas Gresten sandstones show amounts of 1.07 – 1.16%.

Probe:	Rehgr.02	Rehgr.03	Hkr.02	Hkr.04	Hb.Gb.3	Hb.1-1	Hb.1-2	GeB.1	GeB.Kr.3	Gr.S.01	Gr.S.04	Gr.1-5
Init weight:	0,55 g	0,55 g	0,55 g	0,55 g	0,55 g	0,55 g	0,55 g	0,55 g	0,55 g	0,55 g	0,55 g	0,55 g
Flux weight:	5,5 g	5,5 g	5,5 g	5,5 g	5,5 g	5,5 g	5,5 g	5,5 g	5,5 g	5,5 g	5,5 g	5,5 g
Final weight:	6,05 g	6,05 g	6,05 g	6,05 g	6,05 g	6,05 g	6,05 g	6,05 g	6,05 g	6,05 g	6,05 g	6,05 g
LOI:	0,41%	0,68%	0,38%	0,43%	0,32%	38,45%	41,35%	0,78%	0,63%	4,60%	6,80%	29,07%
SiO2	96,18	93,5	92,98	93,64	97,94	8,11	5,57	94,47	94,28	76,99	78,29	31,58
TiO2	0,04	0,14	0,07	0,12	0,03	0,42	0,21	0,06	0,04	0,08	0,2	0,09
Al2O3	1,32	2,82	3,41	3,34	1,29	7,91	5,29	2,51	2,54	8,53	8,39	0,84
Fe2O3	0,55	0,51	0,51	0,48	0,38	3,36	1,46	0,51	0,7	2,06	1,47	1,68
Mn3O4	0	0,01	0,01	0,01	0	0,08	0,09	0	0	0,04	0,02	0,11
MgO	0,09	0,12	0,14	0,13	0,08	17,1	18,79	0,14	0,17	1,07	1,16	0,52
CaO	0,01	0,02	0,1	0,05	0,02	23,79	26,17	0,05	0,07	3,2	3,12	35,51
Na2O	0,12	0,18	1,54	1,51	0,25	0,06	0,07	0,27	0,28	1,96	0,09	0,18
K2O	0,52	1,09	0,39	0,34	0,55	0,44	0,23	0,34	0,44	1,54	0,55	0,08
P2O5	0,01	0,02	0,01	0,02	0	0,05	0,02	0,01	0,01	0	0,08	0,03
SO3	0	0	0,01	0	0	0,01	0,01	0	0,01	0,12	0,03	0,03
V2O5	0	0	0,01	0	0	0,01	0,01	0	0	0	0,01	0,01
Cr2O3	0,05	0,06	0,05	0,04	0,04	0,02	0,01	0,04	0,07	0,03	0,04	0,02
SrO	0	0	0	0	0	0,02	0,01	0	0	0	0	0,07
ZrO2	0,02	0,05	0,03	0,02	0,01	0,02	0,01	0,01	0,01	0,01	0,01	0,02
BaO	0,01	0,02	0,04	0	0,01	0,01	0	0,02	0,04	0,01	0,01	0
NiO	0	0	0	0	0	0,01	0,01	0	0	0	0	0
CuO	0	0	0	0	0	0	0	0	0	0	0	0
ZnO	0	0	0	0	0	0	0	0	0	0	0	0
PbO	0,01	0,01	0,01	0,02	0,02	0	0	0,02	0,01	0,01	0,01	0
HfO2	0,01	0,01	0,01	0,01	0,01	0,01	0,01	0,01	0,01	0,01	0,01	0,01
LOI	0,41	0,68	0,38	0,43	0,32	38,45	41,35	0,78	0,63	4,6	6,8	29,07
Summe	**99,35**	**99,24**	**99,7**	**100,16**	**100,95**	**99,88**	**99,32**	**99,24**	**99,31**	**100,26**	**100,29**	**99,85**

Tab.7 Major and minor elements of measured samples (%)

(Rehgr.02-03: dislodged slice of Rehgras, Hkr.02, 04: dislodged slice of Heiligenkreuz, Hb.Gb.3: dislodged slice of Hinterbrühl (Grillenbühel), Hb.1-1, 1-2: reddish, dolomitic samples of Hafnerberg, GeB.1, GeB.Kr.3: Keuper sandstone of Ober St. Veit (Gemeindeberg), Gr.S.01: Liassic Gresten sandstone of Waidhofen, Gr.S.04: Liassic Gresten sandstone of Pechgraben, Gr.1-5: dislodged slice of Groisbach)

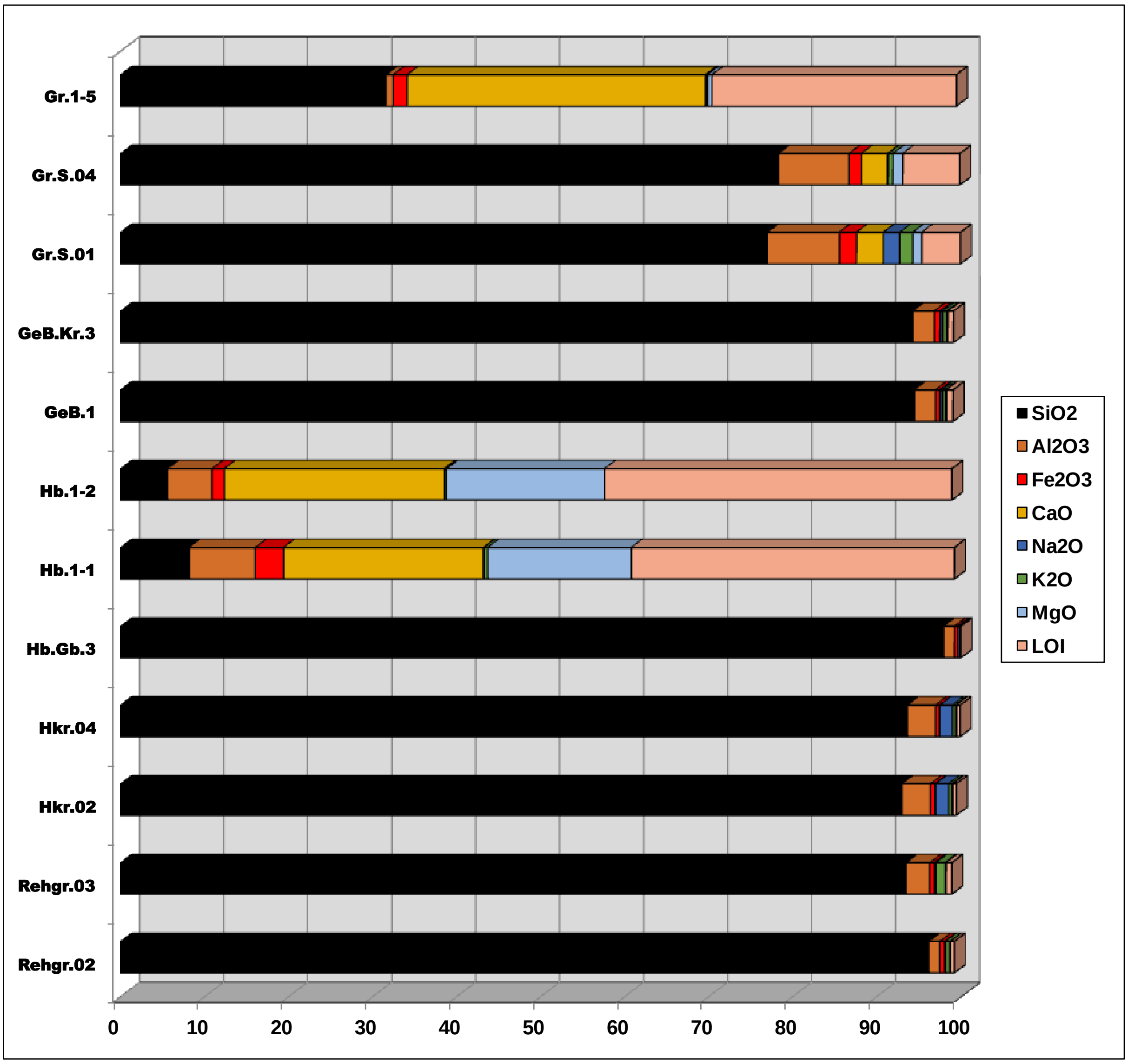

Fig.36 Major and minor element distribution (%)

The two samples of Hafnerberg show MgO contents of 17.1 and 18.79%, which is caused by the presence of dolomite. Generally, CaO is associated with the presence of calcite cement, Ca-rich minerals like dolomite or plagioclase and carbonate fragments (fossils). Significant contents of CaO were measured within the dislodged slice of Groisbach (35.51%), the samples of Hafnerberg (23.79 and 26.17%) and also the Gresten sandstones include notable amounts of 3.12 and 3.2%. Striking is the fact that the measured Keuper sandstones include no CaO at all. Depending on the composition, lithic fragments can be also important donors for SiO_2, Al_2O_3, K_2O, Na_2O, Fe_2O_3, CaO and MgO.

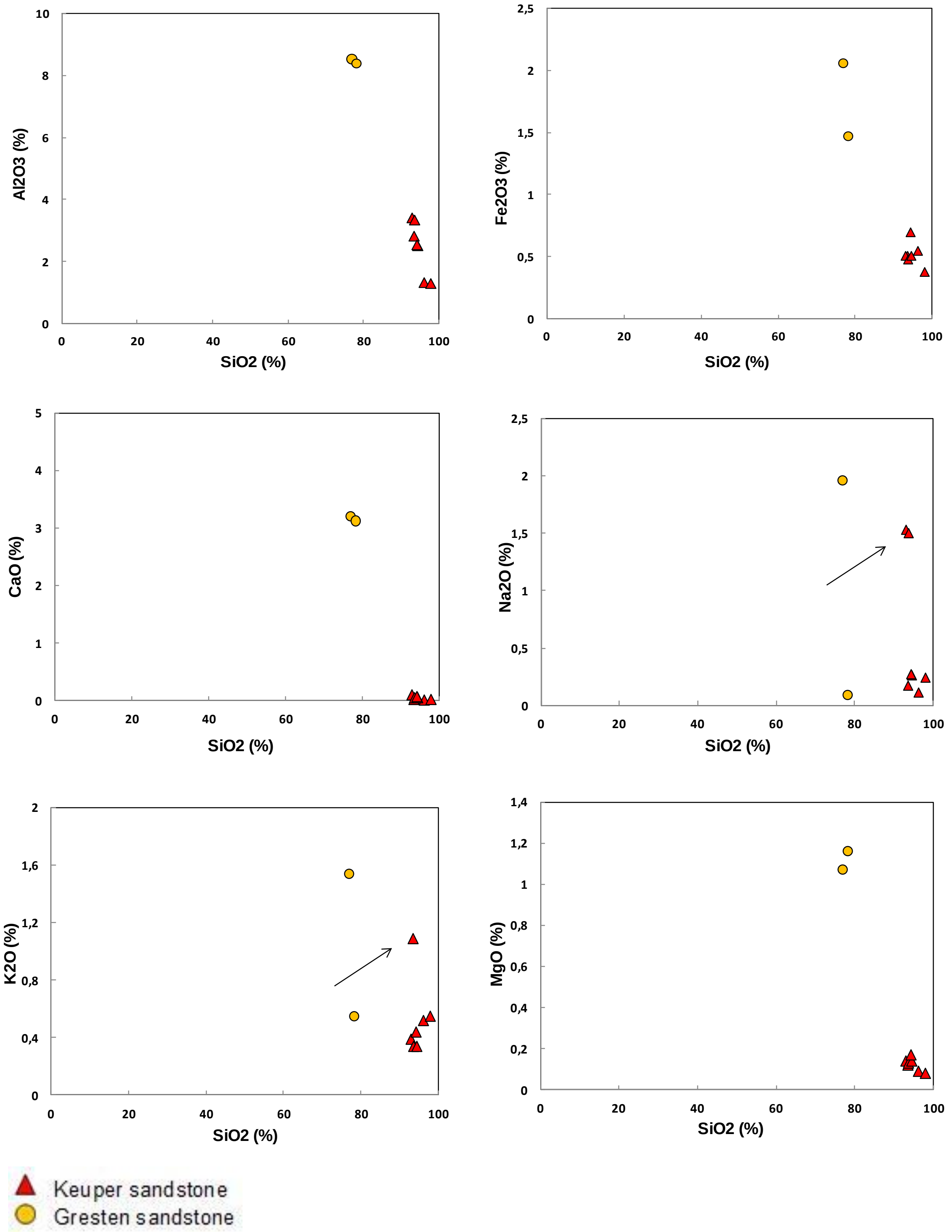

Fig.37 Harker diagrams of major elements for Keuper (dislodged slices and Gemeindeberg sandstones) and Gresten sandstones; Note the missing of CaO within the Keuper sandstones. Two samples of Heiligenkreuz show significant higher amounts of Na2O (black arrow). One sample of Rehgras includes more K2O (black arrow). One sample of the Gresten sandstones shows, compared to the Keuper sandstones, very similar amounts of Na2O and K2O.

The average chemical compositions of the measured samples are shown in table 4. The dislodged slices have an average SiO_2 content of 94.85%, which is nearly identical to the sandstones of Ober St. Veit (94.38%). The Gresten sandstones provide significantly lower average SiO_2 of 77.64%. Al_2O_3 contents between the dislodged slices and the sandstones of Ober St. Veit are also very similar (2.44 and 2.53%). The average Al_2O_3 of the Gresten sandstones is 8.46%, which also show significantly higher amounts of CaO (3.16%) and Fe_2O_3 (1.77%). Calcite cementation was observed in both the dislodged slices and the samples of the Lainz tunnel section, but the very low content of CaO (0.04 and 0.06%) suggests, that the occurrence is rather sporadic within the samples.

The samples were also compared to the average chemical composition of the Upper Continental Crust (UCC) and average sandstones from ocean island arcs (OIC), continental island arcs (CIA), active continental margins (ACM) and passive margins (PM) (tab.7, fig.38). UCC-normalized plotting clearly shows a lesser depletion in major elements within the Gresten sandstones compared to the Keuper sandstones. The dislodged slices and the Gemeindeberg sandstones show significant higher SiO_2 amounts than the average sandstone derived from passive margins, which are considered to reflect high maturity (e.g. Bathia 1983). The Gresten sandstones show a similar average composition compared to average sandstones derived from CIA-, ACM- or PM tectonic settings.

	d.s.	Gb.	Gr.s.	Ucc*	OIC*	CIA*	ACM*	PM*
SiO2	94,85	94,38	77,64	66,60	58,83	70,69	73,86	81,95
TiO2	0,08	0,05	0,14	0,64	1,06	0,64	0,46	0,49
Al2O3	2,44	2,53	8,46	15,40	17,11	14,04	12,89	8,41
Fe2O3	0,49	0,61	1,77	5,04	1,95	1,43	1,30	1,32
CaO	0,04	0,06	3,16	3,59	5,83	2,68	2,48	1,89
Na2O	0,72	0,28	1,03	3,27	4,10	3,12	2,77	1,07
K2O	0,58	0,39	1,05	2,80	1,60	1,89	2,90	1,71
MgO	0,11	0,16	1,12	2,48	3,65	1,97	1,23	1,39

Tab.8 Average geochemical compositions (%) of the dislodged slices (d.s.), Gemeindeberg sandstones (Gb.), Gresten sandstones (Gr.s.), Upper Continental Crust (UCC), ocean island arcs (OIC), continental active margin (CIA), active continental margin (ACM), passive margin (PM);
* data from Rudnick and Gao (2004) and Bhatia (1983)

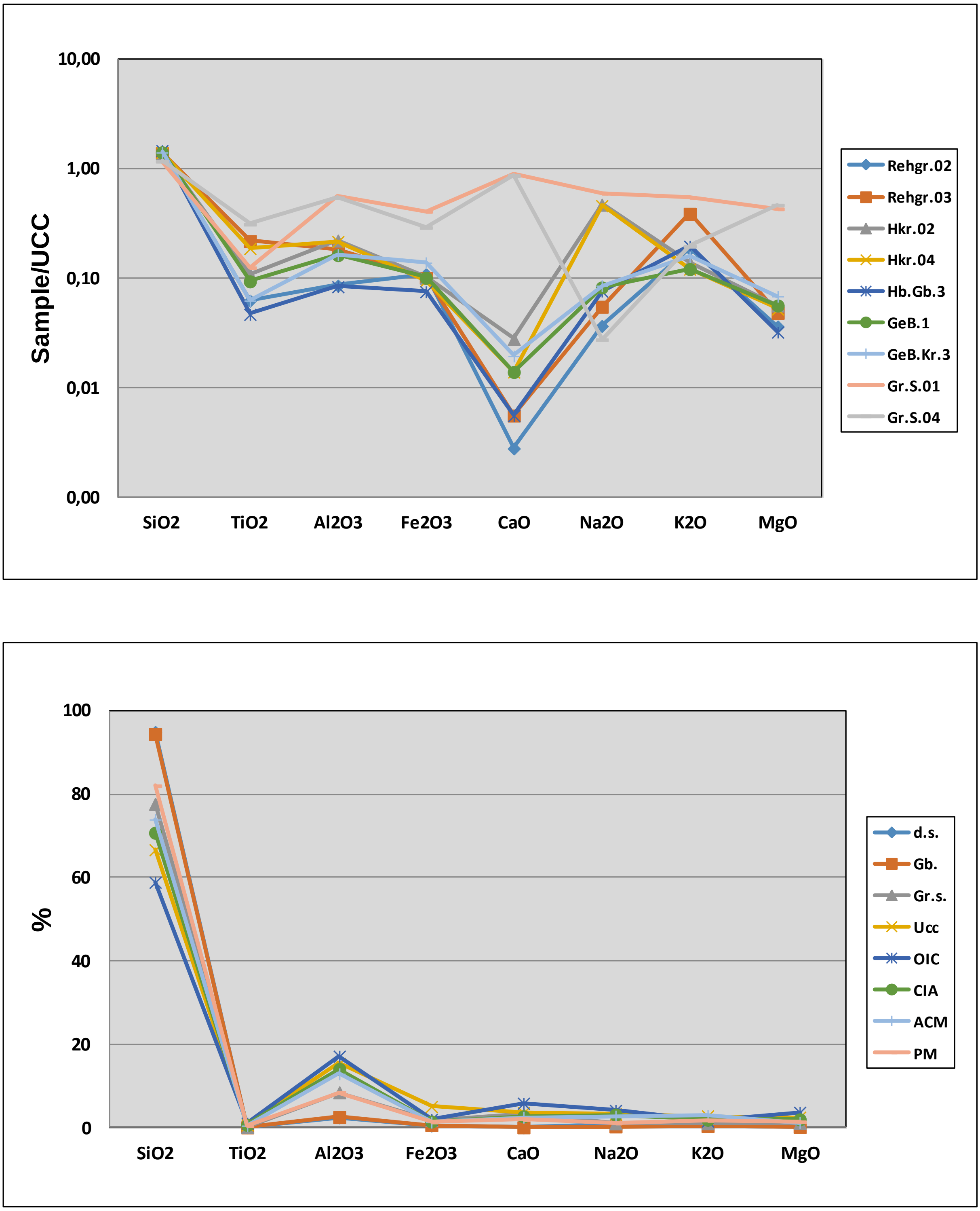

Fig.38 Geochemical results of measured samples; normalized against the Upper Continental Crust (upper figure) and compared to average sandstones from various tectonic settings (lower figure),

(Rehgr.02-03: dislodged slice of Rehgras, Hkr.02, 04: dislodged slice of Heiligenkreuz, Hb.Gb.3: dislodged slice of Hinterbrühl (Grillenbühel), GeB.1, GeB.Kr.3: Keuper sandstone of Ober St. Veit (Gemeindeberg), Gr.S.01: Liassic Gresten sandstone of Waidhofen, Gr.S.04: Liassic Gresten sandstone of Pechgraben

6.3.2 Geochemical sandstone classification and maturity

The use of geochemical data for the classification of sandstones leads in 84% of the cases to matching results with petrographic analysis (Herron 1988). In fact, geochemical data, which are derived from the mineralogy of a sample, can lead to very significant problems for the classification of certain sandstones types like sublitharenites, litharenites and graywackes (e.g. Pettijohn 1963). These rocks are not exactly defined mineralogically, which is caused by the e.g. large spread of possible mineralogical composition for lithic fragments. This is one reason, why geochemical data of sandstones should be used only in conjunction with petrographic results (e.g. Pettijohn 1963).
Geochemical types of sandstones were described and defined by e.g. Pettijohn (1972), Herron (1988) or Lindsay (1999):

1) Quartz arenite: $\log (SiO_2/Al_2O_3) \geq 1.5$
2) Graywacke: $\log (SiO_2/Al_2O_3) < 1$ and $\log (K_2O/Na_2O) < 0$
3) Arkose (subarkose): $\log (SiO_2/Al_2O_3) < 1.5$, $\log (K_2O/Na_2O) \geq 0$,
$\log ((Fe_2O_3+MgO)/(K_2O+Na_2O)) < 0$
4) Lithic arenite: $\log (SiO_2/Al_2O_3) < 1.5$, $\log (K_2O/Na_20) < 0$
$\log ((Fe_2O_3+MgO)/(K_2O+Na_2O)) \geq 0$

Overall, the geochemical sandstone classification is based on following chemical parameters (depending on which of the schemes is used): SiO_2/Al_2O_3, Na_2O/K_2O or K_2O/Na_2O, Fe_2O_3/K_2O. The ratio SiO_2/Al_2O_3 separates quartz arenites from Al-rich intermediate sandstones or shales and is also a strong indicator for the enrichment of SiO_2 due to weathering and transportation processes (e.g. Potter 1978). Therefore, this ratio is also characteristic for the maturity of a sample. The Keuper sandstones show log-ratios between 1.44 and 1.86, which are similar as in quartz arenites (tab.8). The two measured Gresten sandstones show ratios of 0.96 and 0.97, which indicates lower maturity. The Na_2O/K_2O and Fe_2O_3/K_2O are either used in the Pettijohn or the Herron scheme. Na_2O/K_2O separates graywackes and arkoses but is poor for differentiation of lithic fragments and feldspar (Herron 1988). Therefore, Fe_2O_3/K_2O is used for better separation of these two important parameters. This ratio can also be seen as an indicator of mineralogical stability. Under low pressure and temperature, high K- and low Fe-bearing minerals like feldspar and mica form stable components within a wide range of sandstones. Rock fragments, tending to be richer in iron and magnesium are considered to be less stable. Therefore, mature sandstones should have low Fe_2O_3/K_2O ratios. Very mature sandstones like e.g.quartz arenites commonly show very low contents of iron and magnesium. For these rocks, the ratio of Fe_2O_3/K_2O becomes meaningless for geochemical sandstone classification (Herron 1988).

	Rehgr.02	**Rehgr.03**	**Hkr.02**	**Hkr.04**	**Hb.Gb.3**
SiO2	96,18	93,5	92,98	93,64	97,94
Al2O3	1,32	2,82	3,41	3,34	1,29
Fe2O3	0,55	0,51	0,51	0,48	0,38
CaO	0,01	0,02	0,1	0,05	0,02
Na2O	0,12	0,18	1,54	1,51	0,25
K2O	0,52	1,09	0,39	0,34	0,55
MgO	0,09	0,12	0,14	0,13	0,08
log(SiO2/Al2O3)	1,86	1,52	1,44	1,45	1,88
log(Na2O/K2O)	-0,64	-0,78	0,60	0,65	-0,34
log(Fe2O3/K2O)	0,02	-0,33	0,12	0,15	-0,16
log (K2O/Na2O)	0,64	0,78	-0,60	-0,65	0,34

	GeB.1	**GeB.Kr.3**	**Gr.S.01**	**Gr.S.04**
SiO2	94,47	94,28	76,99	78,29
Al2O3	2,51	2,54	8,53	8,39
Fe2O3	0,51	0,7	2,06	1,47
CaO	0,05	0,07	3,2	3,12
Na2O	0,27	0,28	1,96	0,09
K2O	0,34	0,44	1,54	0,55
MgO	0,14	0,17	1,07	1,16
log(SiO2/Al2O3)	1,58	1,57	0,96	0,97
log(Na2O/K2O)	-0,10	-0,20	0,10	-0,79
log(Fe2O3/K2O)	0,18	0,20	0,13	0,43
log (K2O/Na2O)	0,10	0,20	-0,10	0,79

Tab.9 Calculated ratios for geochemical sandstone classification

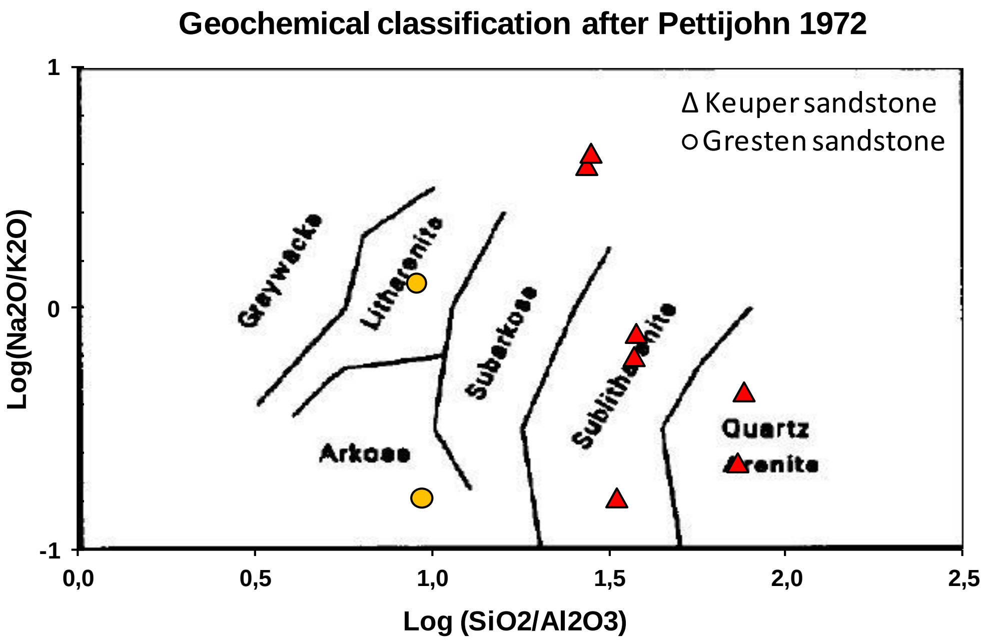

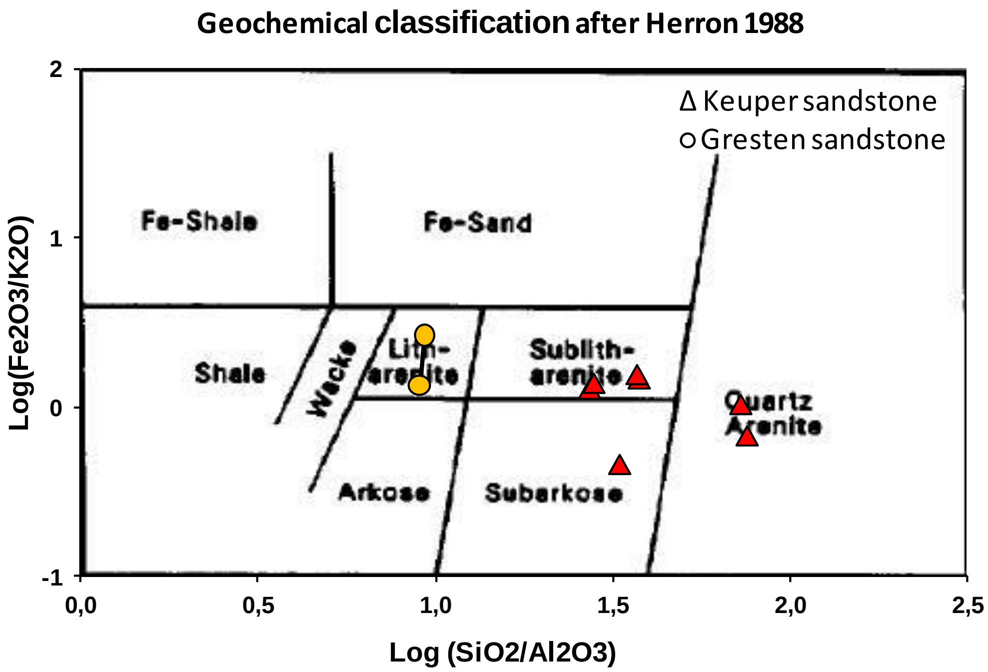

Fig.39 Geochemical sandstone classification after Pettijohn et al. (1972) and Herron (1988)

After this two classification schemes, samples of Keuper sandstones (Gemeindeberg quarzites and dislodged slices) are classified as subarkoses, sublitharenites and quartz arenites. Within the Pettijohn-scheme, the Gresten sandstones plot within the litharenite and arkose field, whereas these rocks are classified as litharenites within the Herron-scheme.

Sandstone classification after Pettijohn (1972) and Herron (1988) led to following results: altogether, the samples, which are regarded as Keuper sandstones, were classified as subarkoses, sublitharenites and quartz arenites (fig.39). The results differ slightly between the two schemes. Within the Pettijohn-scheme, the dislodged slices of Heiligenkreuz (Hkr.02, Hkr.04) were classified as subarkoses. After Herron (1988) these rocks plot within the sublitharenite-field. Two samples of dislodged slices (Rehgras: Rehgr.02, Hinterbrühl: Hb.Gb.3) show very high SiO_2/Al_2O_3-ratios and were classified as quartz arenites. It is interpreted, that high amounts of metamorphic rock fragments, mainly consisting of SiO_2, and quartz cementation led to higher SiO_2/Al_2O_3-ratios (see chapter 6.2). One sample of Rehgras (Rehgr.03) was either classified as sublitharenite (Pettijohn 1972) or as subarkose (Herron 1988). The Gresten sandstones were mainly classified as litharenites. After Pettijohn (1972), the sample of Pechgraben (Gr.S.04) plots within the arkose field.

Sample	sample site	correlation	after Pettijohn (1972)	after Herron (1988)
GeB.1-1	Gemeindeberg	St. Veit Klippenzone	sublitharenite	sublitharenite
GeB.Kr.3	Gemeindeberg	St. Veit Klippenzone	sublitharenite	sublitharenite
Hkr.02	Heiligenkreuz	dislodged slice	subarkose	sublitharenite
Hkr.04	Heiligenkreuz	dislodged slice	subarkose	sublitharenite
Hb.Gb.3	Hinterbrühl	dislodged slice	quartz arenite	quartz arenite
Rehgr.02	Rehgras	dislodged slice	quartz arenite	quartz arenite
Rehgr.03	Rehgras	dislodged slice	sublitharenite	subarkose
Gr.S.01	Waidhofen	Gresten Klippenzone	litharenite	litharenite
Gr.S.04	Pechgraben	Gresten Klippenzone	arkose	litharenite

Tab.10 Results for geochemical sandstone classification

To illustrate the coincidence of mineralogical and geochemical maturity for different samples, a SiO_2/Al_2O_3 vs. Q/(F+RF)-plot was used (Pettijohn 1975). The results show a high coincidence between these two parameters (fig.33). SiO_2 vs. $Al_2O_3 + K_2O + Na_2O$ after Suttner and Dutta (1986) reflects geochemical maturity as a function of climate. (Semi-) humid climatic conditions and high chemical maturity were obtained for the Keuper sandstones, whereas results for two Gresten sandstones indicate semi-arid to semi-humid conditions and significantly lower chemical maturity (fig.40).

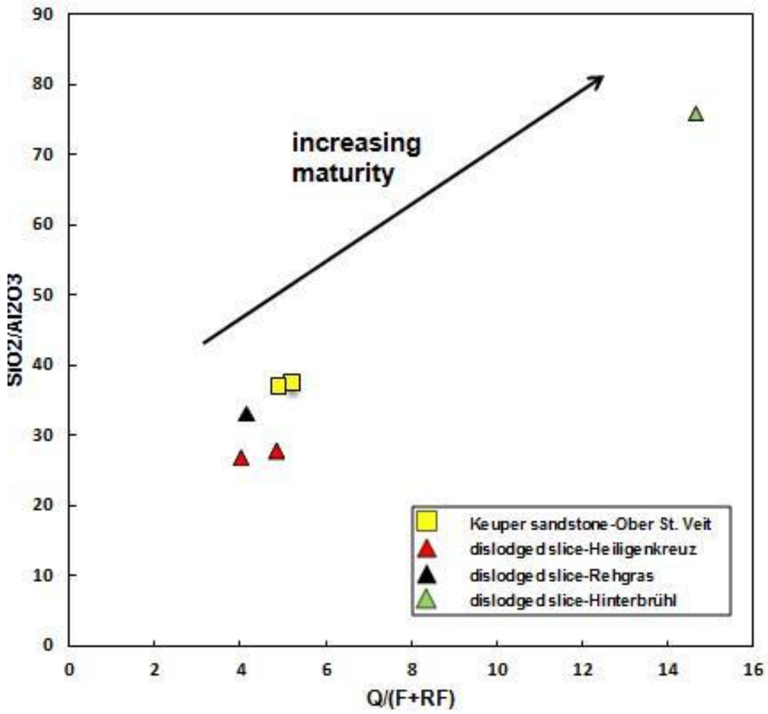

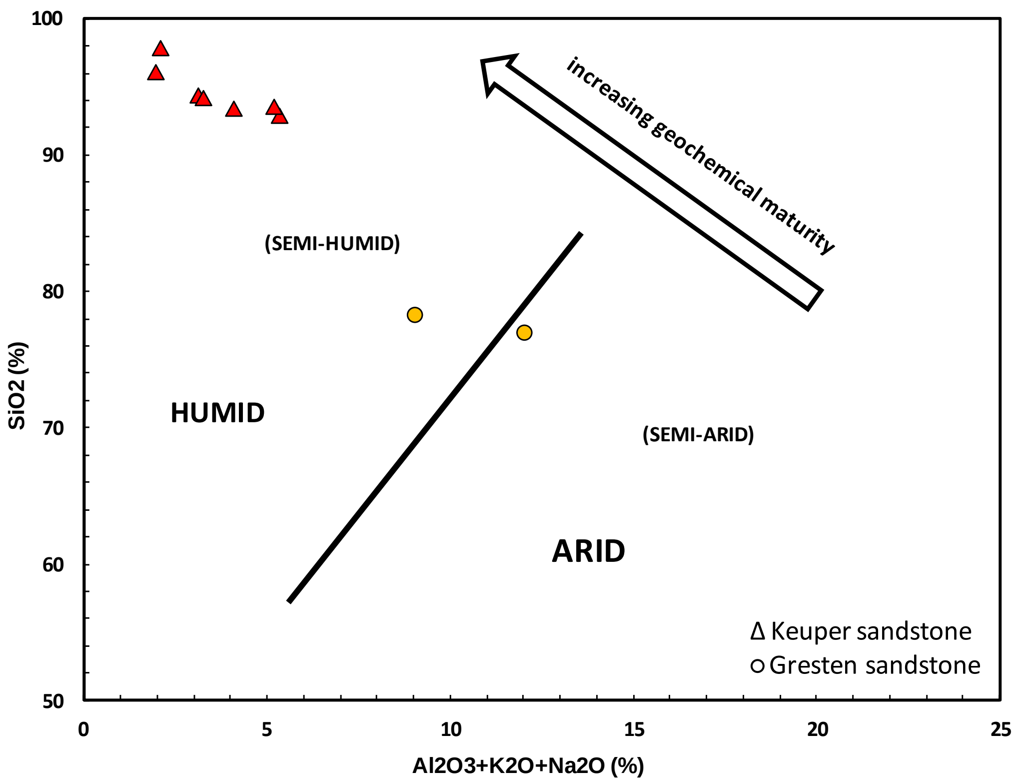

Fig.40 upper fig.: SiO_2/Al_2O_3 vs. Q/(F+RF) – plot for dislodged slices and sandstones of Ober St. Veit suggests high maturity for the dislodged slice of Hinterbrühl (after Pettijohn 1975); lower fig.: bivariant plot after Suttner and Dutta (1986) indicates high chemical maturity for the Keuper sandstones

6.3.3 Chemical weathering indexes (CIA, CIW, PIA)

The chemical index of alteration (CIA), the chemical index of weathering (CIW) and the plagioclase index of alteration (PIA) reflect in different ways the intensity of chemical weathering of sandstones (Nesbitt and Young 1982, Fedo et. al 1995). The basic idea is that these values quantify the removal of mobile or unstable cations like Na, K, Ca relative to immobile or stable residual constituents (Al, Ti) due to chemical weathering of e.g. feldspar. Depending on the deposition history of the rock, these values either reflect weathering processes within the source area, weathering processes during transportation and deposition or weathering after the final deposition. The different indexes are calculated as follows:

1) CIA: $(Al_2O_3 / (Al_2O_3 + CaO^* + Na_2O + K_2O)) \times 100$

2) CIW: $(Al_2O_3 / (Al_2O_3 + CaO^* + Na_2O)) \times 100$

3) PIA: $100 \times (Al_2O_3 - K_2O) / (Al_2O_3 + CaO^* + Na_2O - K_2O))$

* CaO only if incorporated in silicates

	Rehgr.02	Rehgr.03	Hkr.02	Hkr.04	Hb.Gb.3	GeB.1	GeB.Kr.3	Gr.S.01	Gr.S.04
CIA	67,3	68,9	63,9	64,4	61,7	80,4	77,9	56,0	69,1
CIW	91,7	94,0	68,9	68,9	83,8	90,3	90,1	62,3	72,3
PIA	87,0	90,6	66,2	66,5	74,7	88,9	88,2	57,5	71,0

Tab.11 CIA, CIW, PIA - values

CIA-values are interpreted as follows: 50-60: incipient weathering, 60-80: inter-mediate weathering, >80: extreme weathering (Nesbitt and Young 1982). Systematic petrographic observations are essential to properly interpret these dimensionless numbers. In general, values of or near 50 represent unweathered rocks or Upper Continental Crust (unaltered albite, anorthite and potassium feldspar). Fresh basalt has values between 30 and 45. Granites and granodiorites show significantly higher values between 45 and 55. Due to high amounts of clay minerals, average shales have CIA-indexes of 70 – 75. Muscovite shows CIA -values of 75 and illite (and montmorillonite) values between 75 and 85. The CIA-index of kaolinite is 100 (Nesbitt and Young 1982).

The dislodged slices and the Gemeindeberg sandstones show CIA- values between 61 and 81 and therefore reflect intermediate to (almost) extreme chemical weathering (tab.10). It is assumed, that these intensities are primarily caused by post-depositional weathering of feldspar. As examples, the samples of Ober St. Veit (GeB.1, GeB.Kr.3) are cited. Within these samples, chemical weathering of feldspar led to the formation of authigenic kaolinite. Count results clearly illustrate higher contents of kaolinite compared to the dislodged slices (see chapter 6.2), leading to higher CIA-values. Fig. 34 clearly shows the increase of chemical weathering within the samples of Ober St. Veit. CIA-values of the Gresten sandstones reflect intermediate to extreme chemical weathering.

The CIW- and PIA indexes reflect chemical weathering with special emphasis to plagioclase by excluding K_2O. The interpretation is similar to the CIA-index. Also, variations between these values and the CIA reflect compositional variations between the samples (e.g. Cingolani et. al 2003). Except for the dislodged slices of Heiligenkreuz, the values for all the samples are very high indicating extreme weathering of plagioclase. The CIW- and PIA values of the samples of Heiligenkreuz indicate intermediate weathering (tab.10). Higher Na_2O contents within the dislodged slices of Heiligenkreuz are associated with higher amounts of unweathered, perthitic exsoluted K-feldspar. Apparently, that's the reason, why the CIW- and PIA values of these samples are significantly lower. Assuming that the provenance of the samples originally possessed contents of plagioclase, the values may reflect weathering during transportation.

For all samples, CaO was not taken into account for calculation. Both the samples of the Gresten Klippenzone include considerable amounts of calcite cement, which causes higher levels of CaO (see chapter 6.5). Cao levels are higher than the levels of Na_2O, which also indicates that CaO is not derived from albite. Mineralogical investigations have also revealed that the Gresten sandstone of Pechgraben/Weyer (Gr.S.04) does not contain any feldspar due to extreme weathering. The dislodged slices and the sandstones of Ober St. Veit do not include any CaO at all (0.04 and 0.06% in average).

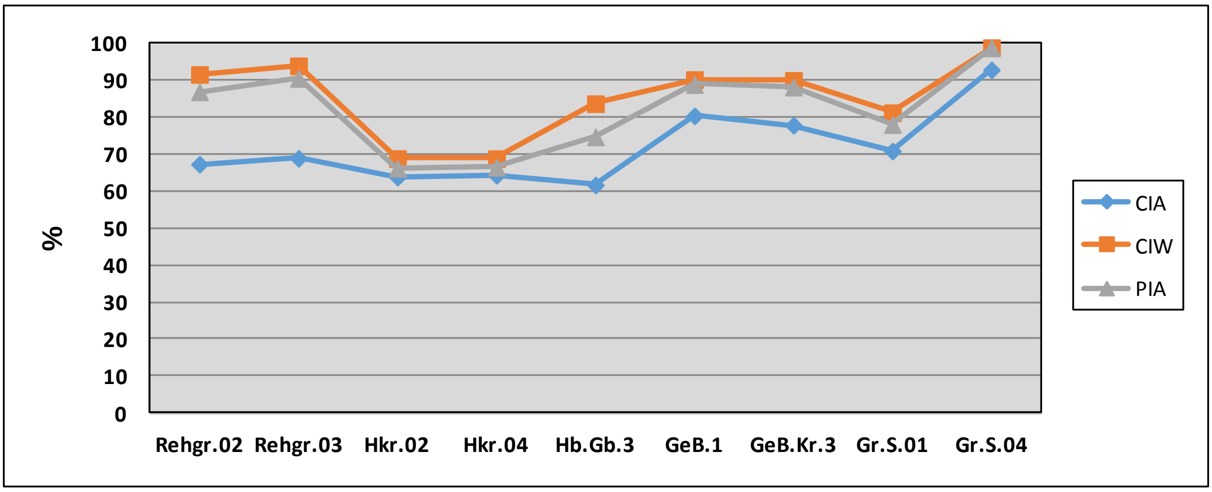

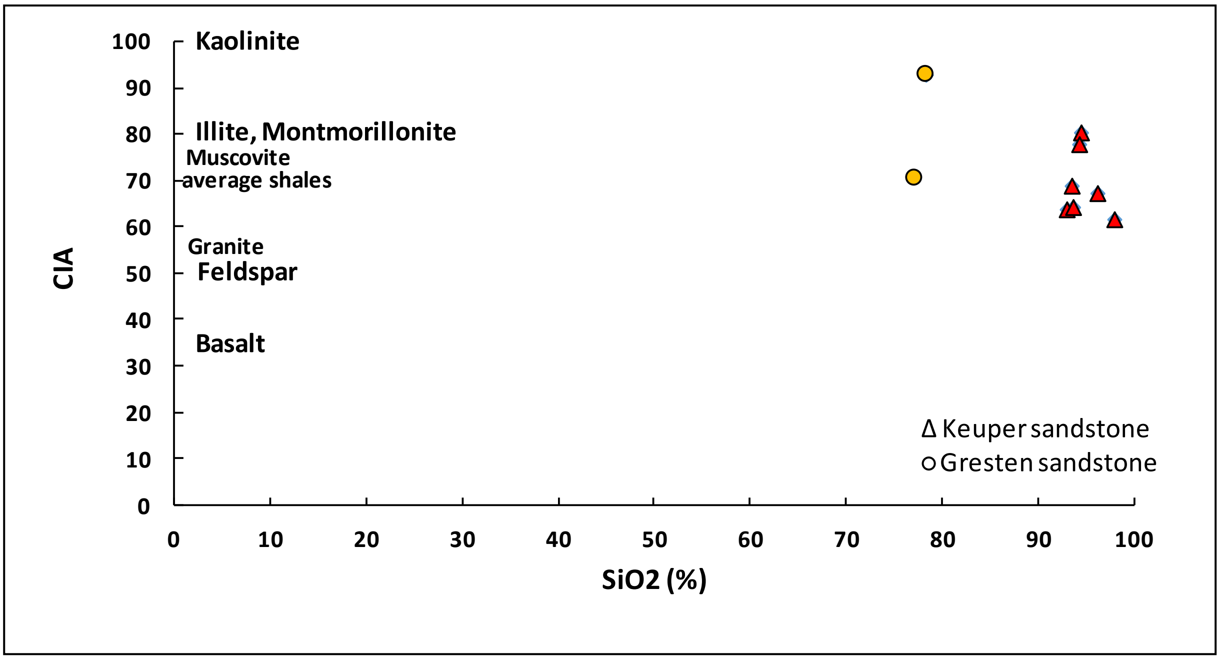

Fig.41 upper fig.: CIA, CIW and PIA values of investigated samples; lower fig.: CIA vs. SiO_2 (after Nesbitt and Young (1982) and modified after Cingolani et. al (2003)) CIA-values: basalt (30-45), feldspar (50), granite (45-55), average shale (70-75), muscovite (75), illite and montmorillonite (75-85), kaolinite and chlorite (100)

6.3.4 Provenance and tectonic setting (major elements)

Discriminant function-plots effectively separate between different groups of provenances by the use of the oxides Al_2O_3, TiO_2, Fe_2O_3, MgO, CaO, Na_2O and K_2O (Roser and Korsch 1988). It is also claimed, that the effect of overlapping between distinctive groups of provenances (mainly caused by grain size effects) can be almost eliminated by using this method. Four groups of provenances are divided: 1. **mafic** (e.g. ocean island arcs), 2.**intermediate** (e.g. mature island arcs), 3.**felsic** (e.g. active continental margin), 4.**recycled** (quartz-rich, granitic-gneissic or sedimentary sources). Maturity rises from type 1 to type 4 and each of these types provides a characteristic geochemical signature. Following 2 discriminant functions were used (after Roser and Korsch 1988):

DF1: $-1.773\ TiO_2 + 0.607\ Al_2O_3 + 0.76\ Fe_2O_3 – 1.5\ MgO + 0.616\ CaO + 0.509\ Na_2O - 1.224\ K_2O – 9.09$

DF2: $0.445\ TiO_2 + 0.07\ Al_2O_3 + 0.25\ Fe_2O_3 – 1.142\ MgO + 0.438\ CaO + 1.475\ Na_2O -1426\ K_2O – 6.861$

	Rehgr.02	Rehgr.03	Hkr.02	Hkr.04	Hb.Gb.3	GeB.1	GeB.Kr.3	Gr.S.01	Gr.S.04
DF1	-8.65	-8.65	-6.60	-6.72	-8.72	-7.74	-7.70	-3.01	-3.68
DF2	-6.07	-5.04	-4.01	-4.11	-5.78	-6.04	-5.96	-1.48	-5.59

Tab.12 Calculated results of discriminant function analyis

The results led to plotting within the provenance type 4, which is associated with quartz-rich sediments of a mature continental provenance indicating a passive margin or intracratonic basin as the tectonic setting (fig.42). This is confirmed by a SiO_2 vs. K_2O/Na_2O – plot which discriminants different tectonic settings by geochemical maturity (Roser and Korsch 1986). Maturity, which is mainly expressed by the content of quartz or SiO_2 increases from active to passive tectonic settings. Samples of dislodged slices and Ober St. Veit plot within the field “PM” indicating a passive margin as the tectonic setting for the investigated Keuper sandstones (fig. 42).

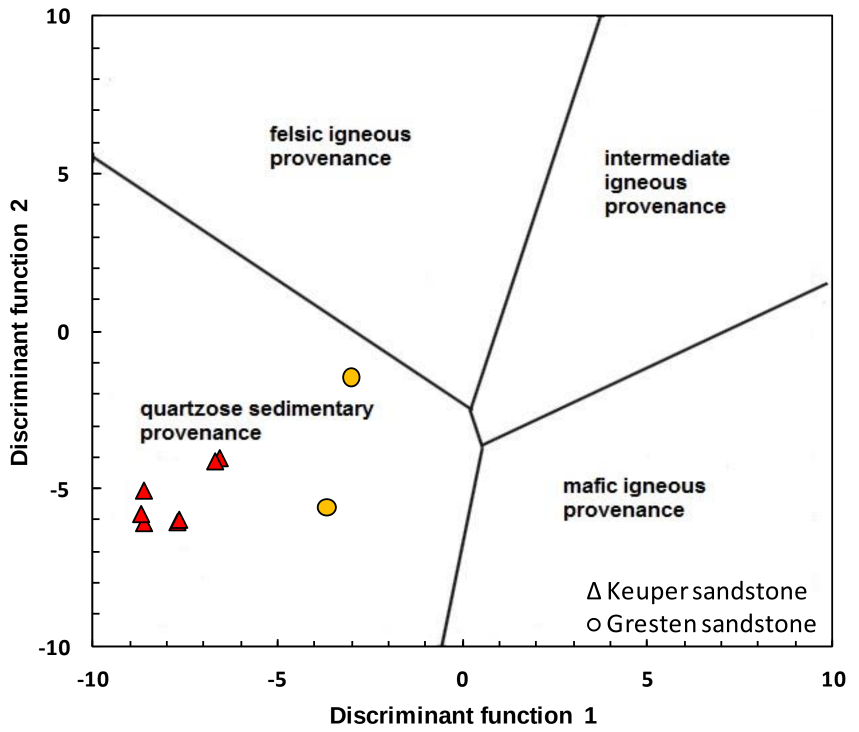

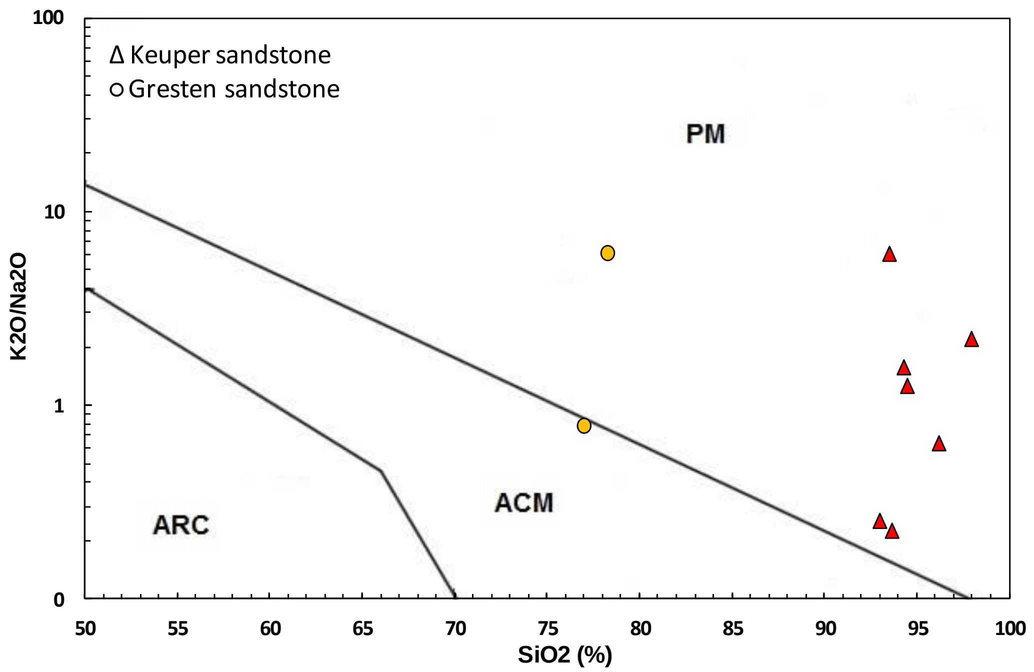

Fig.42 upper fig.: Discriminant-function plot after Roser and Korsch (1988) indicating a continental, recycled, quartz-rich provenance for Keuper and Gresten sandstones; lower fig.: Discrimination of different tectonic settings after Roser and Korsch (1986). Results indicate a passive continental margin for the Keuper sandstones (PM=passive margin, ACM=active continental margin, ARC=ocean island arc)

6.3.5 Trace element analysis (source rocks, sorting and tectonic setting)

Due to their sensitive behaviour to processes like transportation and weathering, major elements alone do not provide reliable data for provenance analysis (e.g. Cingolani 2003). Trace elements like La, Ce, Nd, Y, Th, Zr, Hf Nb, Sc, which are relatively immobile during sedimentary processes, contain characteristic geochemical signatures of their geologic origin (e.g. Bhatia and Crook 1986). However, it is also assumed, that e.g. hydraulic sorting and reworking can lead to variations of trace element distributions due to the enrichment of heavy minerals like zircon, monazite, cr-spinel or apatite (e.g. Cullers et. al 1979). Certain trace elements and their ratios are considered to be characteristic for mafic or felsic sources and the tectonic settings of sandstones. Ferromagnesian elements like Co, Sc, Ni, Cr, V, are generally associated with mafic input (e.g. volcanic rock fragments), whereas HFSE-elements like Zr, Th, Nb, Hf, Y are preferably concentrated in felsic source rocks (e.g. Bhatia and Crook 1986).

The samples are depleted in LIL-, HFSE- and ferromagnesian trace elements with respect to the Upper Continental Crust (UCC) (fig.43). Trace elements, which are superficially associated with mafic sources (Co, Sc, Ni, V) show (in part) a greater depletion than those elements associated with felsic source rocks (Zr, Th, Nb, Hf, Y, La). A striking exception is chromium, which is enriched in both the Keuper- and Gresten sandstones in relation to the UCC. High amounts of chromium in sediments are commonly derived from the presence of chrome spinel, a strong indicator for ophiolithic source rocks (e.g. Mange and Maurer 1991). Chrome spinel was not detected within the heavy mineral fraction (see chapter 6.4), therefore it is assumed that tourmaline acts as an important donor for chromium within the samples.
Uranium is completely missing within the Keuper sandstones. Oxidized (VI) uranium, highly mobile under humid conditions, is preferably enriched within the fine-grained section (e.g. Klepper and Wyant 1957), which is strongly depleted within the Keuper sandstones. Organic or phospatic material, which is also able to absorb released uranium, is also not present within the Keuper sandstones.

		Rehgr.02	Rehgr.03	Hkr.02	Hkr.04	Hb.Gb.3	Hb.1-1	Hb.1-2	GeB.1	GeB.Kr.3	Gr.S.01	Gr.S.04	Gr.1-5
Summe:	(%)	0,70	0,78	0,86	0,81	0,53	38,84	42,41	0,79	0,99	5,97	4,95	75,62
LOI	(%)	0,41	0,68	0,38	0,43	0,32	38,45	41,35	0,78	0,63	4,60	6,80	29,07
Ag	(ppm)	0,00	1,85	1,35	0,50	1,75	1,29	4,12	0,25	1,63	2,82	0,24	1,59
As	(ppm)	8,09	6,38	8,94	7,69	8,83	24,80	13,40	13,42	8,41	9,02	8,76	26,63
Ba	(ppm)	81,10	144,84	303,08	26,88	50,05	14,67	0,00	183,24	267,69	132,65	91,64	2,26
Bi	(ppm)	1,02	0,35	0,57	0,45	0,59	1,17	1,01	0,00	0,67	1,31	1,05	1,74
Br	(ppm)	0,31	0,58	0,73	0,55	0,69	0,50	0,87	0,23	0,45	0,59	0,44	0,99
Ca	(ppm)	204,34	298,31	1100,89	582,72	234,47	343102,10	403209,20	665,76	695,23	35702,99	31009,25	734091,70
Cd	(ppm)	2,40	4,42	4,48	1,78	4,43	2,71	6,43	1,26	4,69	5,94	3,81	5,57
Ce	(ppm)	13,38	18,02	27,57	31,76	17,21	46,74	25,72	21,54	17,27	5,84	24,72	35,65
Co	(ppm)	4,23	4,67	2,98	3,90	1,85	16,04	14,86	4,41	4,79	1,19	4,62	4,35
Cr	(ppm)	285,06	286,11	305,67	297,98	250,87	92,26	50,67	211,60	403,67	184,19	217,09	105,15
Cs	(ppm)	4,50	0,00	3,43	1,71	0,00	5,32	6,05	0,96	0,00	0,74	3,69	10,08
Cu	(ppm)	3,85	4,03	5,50	3,39	2,25	3,55	1,97	3,21	6,15	1,91	6,62	3,06
Fe	(ppm)	5757,05	5154,93	5800,75	5644,99	4332,64	38721,10	16997,01	5904,63	7808,26	22190,39	15428,45	19408,20
Ga	(ppm)	1,73	2,69	3,14	2,86	1,28	9,75	7,20	2,22	2,07	10,59	8,78	0,97
Ge	(ppm)	0,14	0,23	0,40	0,32	0,08	0,00	0,00	0,04	0,31	0,72	1,38	0,00
Hf	(ppm)	1,32	2,24	0,30	0,84	0,47	1,84	1,38	0,01	1,02	0,14	1,21	1,37
Hg	(ppm)	0,00	0,00	0,00	0,00	0,00	0,00	0,00	0,00	0,00	0,00	0,00	0,00
I	(ppm)	0,00	0,00	0,00	0,00	0,00	0,00	0,00	0,00	0,00	0,00	0,00	0,00
La	(ppm)	8,66	9,75	15,21	17,86	8,30	30,96	16,11	10,17	5,16	7,13	16,57	12,32
Mn	(ppm)	29,38	25,79	20,36	26,48	24,61	549,70	657,14	12,53	18,01	255,53	110,36	814,85
Mo	(ppm)	5,09	4,56	5,20	4,96	4,47	1,91	0,71	3,83	7,57	2,44	3,07	1,04
Nb	(ppm)	1,38	3,15	2,31	2,75	1,30	7,14	3,52	1,73	1,88	3,58	6,99	1,03
Nd	(ppm)	10,21	9,76	15,20	15,22	11,96	27,21	19,91	8,80	9,55	8,89	14,92	19,73
Ni	(ppm)	6,38	5,87	7,64	7,20	5,38	72,35	45,71	6,57	10,62	3,92	7,10	4,61
Pb	(ppm)	4,31	6,19	2,38	1,41	3,47	10,75	4,15	8,46	11,06	25,65	26,13	4,72
Rb	(ppm)	14,49	29,01	11,19	9,94	12,84	10,24	4,86	9,89	11,86	71,47	25,34	4,95
Sb	(ppm)	0,00	0,00	0,00	0,00	0,00	0,00	0,00	0,00	0,00	0,00	0,00	0,00
Sc	(ppm)	0,46	0,36	1,11	0,44	0,00	28,80	29,30	0,89	0,56	4,64	5,20	34,50
Se	(ppm)	0,61	0,32	0,80	0,55	0,44	0,55	0,84	0,63	0,54	1,14	0,65	1,45
Sm	(ppm)	0,00	0,00	0,76	0,00	3,03	0,00	1,08	3,38	0,00	0,00	1,42	0,00
Sn	(ppm)	5,26	6,34	6,44	5,99	4,79	4,30	6,52	5,05	6,51	6,61	5,88	2,08
Sr	(ppm)	16,48	26,71	23,04	15,30	9,64	169,24	111,33	16,08	18,99	107,29	104,99	512,48
Ta	(ppm)	0,36	0,00	0,00	0,00	0,00	0,00	0,00	0,33	0,00	0,34	0,09	0,00
Te	(ppm)	0,00	0,00	0,00	0,00	0,00	0,00	0,00	0,00	0,00	0,00	0,00	0,00
Th	(ppm)	3,11	4,92	3,62	4,98	3,89	8,20	4,23	3,79	3,91	5,99	9,08	5,80
Ti	(ppm)	445,58	1573,40	803,55	1237,51	289,81	5156,14	2706,52	680,36	456,13	884,72	2231,85	977,38
Tl	(ppm)	2,23	2,08	3,12	2,50	2,86	3,35	3,53	1,99	2,67	3,99	3,12	4,58
U	(ppm)	0,00	0,00	0,00	0,00	0,00	3,57	2,38	0,00	0,00	1,85	1,99	0,00
V	(ppm)	7,12	8,66	9,39	9,45	4,76	62,78	45,38	9,46	7,97	6,91	20,71	26,32
W	(ppm)	1,92	2,11	1,35	1,74	0,96	0,00	0,53	0,00	1,97	0,81	2,55	0,00
Y	(ppm)	5,01	7,12	6,96	8,40	4,42	26,36	21,56	5,05	5,12	5,87	15,22	10,95
Yb	(ppm)	2,38	2,24	2,96	2,85	3,36	5,34	3,40	3,51	3,24	3,93	3,10	4,17
Zn	(ppm)	4,13	4,95	3,93	2,77	2,52	29,60	22,87	2,25	4,53	7,02	11,90	15,95
Zr	(ppm)	43,97	104,83	49,46	78,97	30,33	129,83	58,37	42,61	42,86	38,83	50,61	51,28

Tab.13 Trace element distribution (ppm) of measured samples

(Rehgr.02-03: dislodged slice of Rehgras, Hkr.02, 04: dislodged slice of Heiligenkreuz, Hb.Gb.3: dislodged slice of Hinterbrühl (Grillenbühel), Hb.1-1, 1-2: reddish, dolomitic samples of Hafnerberg, GeB.1, GeB.Kr.3: Keuper sandstone of Ober St. Veit (Gemeindeberg), Gr.S.01: Liassic Gresten sandstone of Waidhofen, Gr.S.04: Liassic Gresten sandstone of Pechgraben, Gr.1-5: dislodged slice of Groisbach)

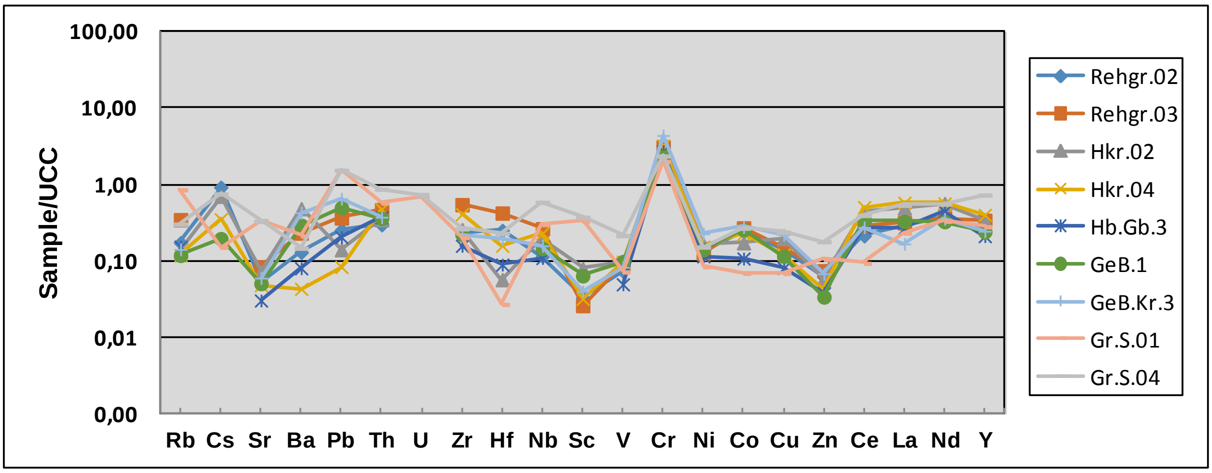

Fig.43 UCC-normalized multi-element diagram for Keuper and Gresten sandstones

La/Sc, Th/Sc, Th/Co, Th/Cr, Cr/Th and La/Co form characteristic ratios within mafic and felsic source rocks and can be used for the determination of the geological origin of clastic sediments (e.g. Cullers 2000).

The results clearly indicate a felsic source, except of the indices which include chromium (tab.13). In strong contrast to the other element ratios, Th/Cr or Cr/Th indicates a mafic derivation for the Keuper and Gresten sandstones (tab.13). No petrographic evidence was found for the presence of Cr-bearing minerals within the samples. It is known, that tourmaline can incorporate chromium, but it seems questionable, that tourmaline alone is responsible for this enrichment. A La/Sc vs. Th/Co - plot after Cullers (2002) clearly illustrates the preferred felsic origin of the investigated samples (fig.44).

Ratios	Keuper and Gresten sandstones (n=9)	felsic origin*	mafic origin*	UCC*
La/Sc	**1.54 – 40.31**	2.5 – 16.3	0.43 – 0.86	2.21
Th/Sc	**1.29 – 13.60**	0.84 – 20.5	0.05 – 0.22	0.79
Th/Co	**0.74 – 5.05**	0.67 – 19.4	0.04 – 1.4	0.63
Th/Cr	**0.01 – 0.04**	0.13 – 2.7	0.018 – 0.046	0.13
Cr/Th	**23.90 – 103.14**	4.00 – 15.00	25 - 500	7.76
La/Co	**1.08 – 5.11**	1.80 – 13.8	0.14 – 0.38	1.76

Tab.14 Range of characteristic elemental ratios from felsic and mafic sources compared to the ratios of Keuper and Gresten sandstones (*data from Cullers (1994) (2000), Cullers et. al (1988), Armstrong – Altrin (2009), Mc Lennan (2001))

To illustrate distinctive differences in important sedimentary processes like sorting and recycling between Keuper and Gresten sandstones, a Zr/Sc vs. Th/Sc – plot after McLennan (1993) was used (fig.44). Zirconium is associated with the presence of zircon and the elemental ratio Zr/Sc implicates the enrichment of zircon due to sedimentary sorting. Thorium, an incompatible element during magmatic differentiation is related to scandium, which is compatible. This ratio indicates magmatic differentiation processes and besides, thorium is also a substituent within zircon. The Keuper sandstones show high Zr/Sc and Th/Sc values related to the UCC (Th/Sc ~ 1) due to recycling and sorting. The Gresten sandstones also indicate certain degrees of sorting but to a significant lesser extent. When interpreting these results, it should be remembered that zirconium and thorium are depleted in contrast to the UCC.

Ferromagnesian trace elements like vanadium and scandium are strongly depleted within mature sandstones (Bhatia and Crook 1986). These elements are associated with the presence of unstable lithic fragments (e.g. volcanic fragments, which are composed of amphibole or pyroxene), which become more and more absent with rising maturity. Since there is a connection between maturity and the tectonic setting of sandstones, ratios of V and Sc can be used to reconstruct palaeo-tectonic settings. Peterson (2009) quoted high resolutions and accuracies of Sc-V plots. Low Sc and V contents led to plotting within the passive margin-field for the Keuper and Gresten sandstones, but near the PM-ACM dividing line for one of the Gresten sandstones (fig.45).

Triplots after Bhatia and Crook (1986) use Th - Sc - Zr (Zr divided by the factor 10) and La - Th - Sc for the discrimination of ancient tectonic settings (fig.45). A passive margin was identified for the Keuper sandstones, which correlates well to previous results. In contrast, the Gresten sandstones plot within the active margin-field and the continental island arc-field, which is caused by significant higher amounts of Sc within these samples (see tab.12).

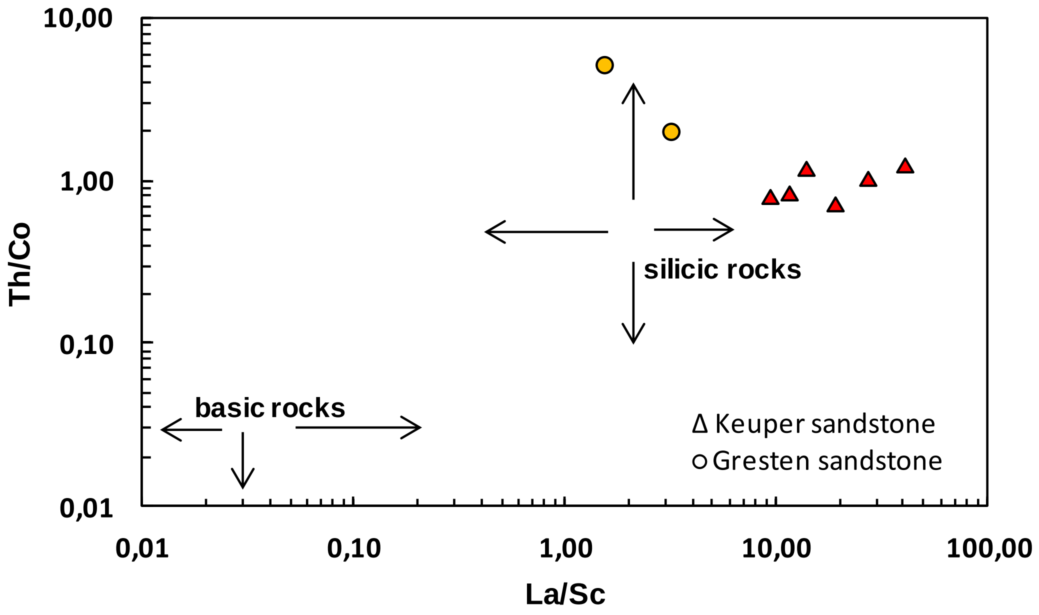

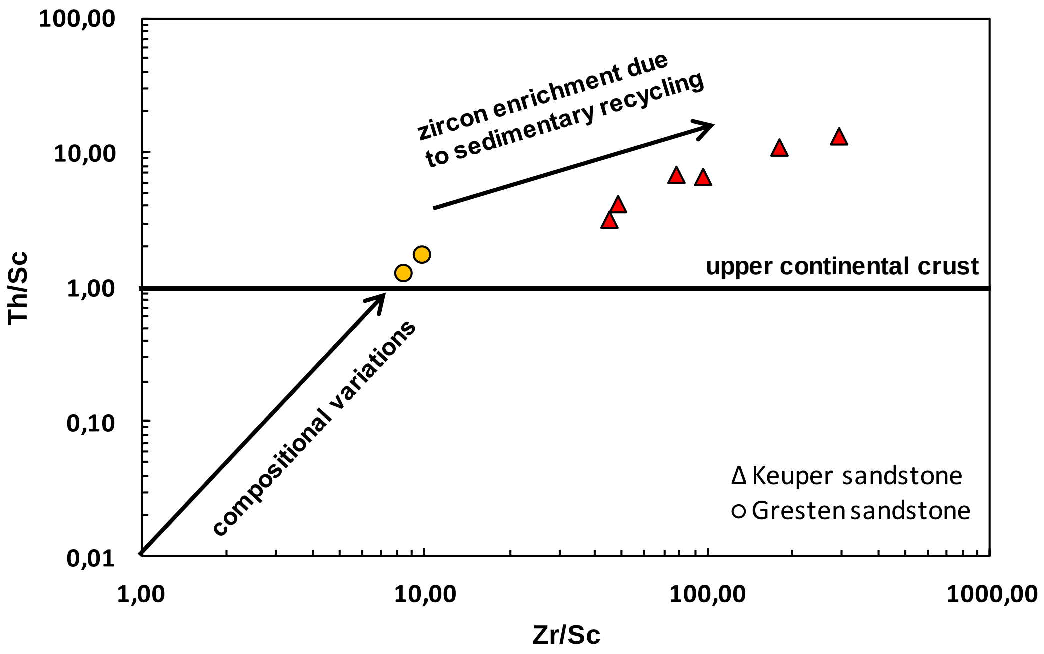

Fig.44 upper fig.: a La/Sc vs. Th/Co-plot after Cullers (2002) suggests a felsic/silicic origin of the Keuper and Gresten sandstones; lower fig.: plot of Zr/Sc versus Th/Sc after McLennan (1993) shows high degrees of sedimentary sorting and recycling for the Keuper sandstones

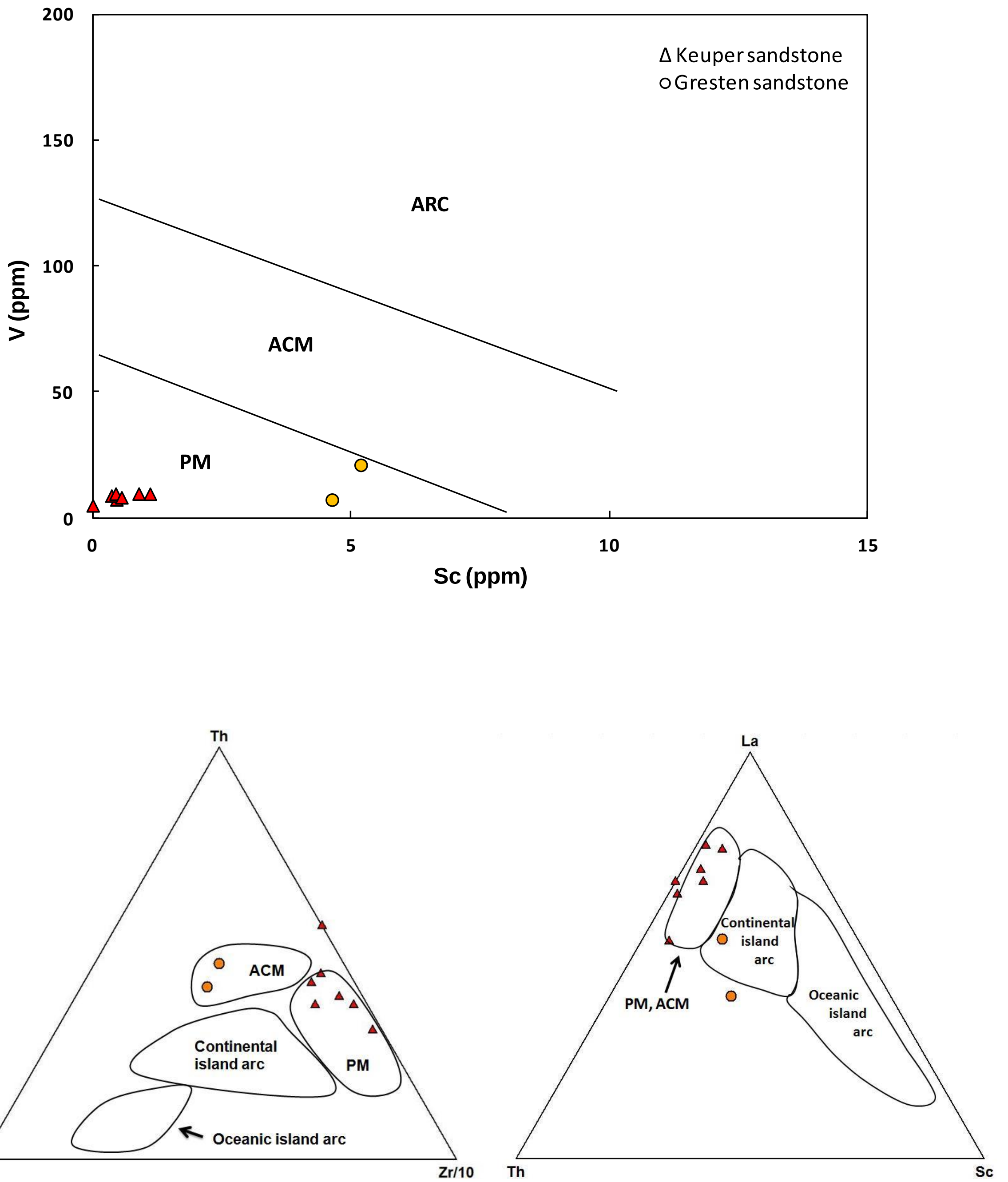

Fig.45 upper fig.: a Sc vs. V – plot after Bathia and Crook (1986) indicates a passiv continental margin for the samples (PM=passive margin, ACM=active continental margin, ARC=island arc; lower fig.: a Th-Sc-Zr/10 and La-Th-Sc triplot after Bhatia and Crook (1986) suggests a passive tectonic regime for the Keuper sandstones and an active continental margin or continental island arc for the Gresten sandstones

6.4 Heavy mineral analysis

6.4.1 Gemeindeberg quartzites

Heavy minerals of three samples of quartzite Gemeindeberg sandstones /con-glomerates were counted (GeB.1, GeB.S.02, GeB.S.03), which led to a total amount of 816 counts (tab.14).

	GeB.1	%	GeB.S.02	%	GeB.S.03	%
zircon	43	18.94	64	23.36	98	31.11
garnet	124	54.63	134	48.91	145	46.03
tourmaline	15	6.61	35	12.77	32	10.16
rutile	33	14.54	30	10.95	34	10.79
monazite	0	0.00	4	1.46	2	0.63
hornblende	4	1.76	3	1.09	1	0.32
anatase	4	1.76	0	0.00	0	0.00
sillimanite	2	0.88	2	0.73	2	0.63
apatite	2	0.88	1	0.36	0	0.00
titanite	0	0.00	1	0.36	0	0.00
Chromespinel	0	0.00	0	0.00	1	0.32
total	**227**	**100.00**	**274**	**100,00**	**315**	**100,00**

Tab.15 Heavy mineral distribution of 3 Gemeindeberg sandstones / conglomerates

Garnet occurs in a range of 46 – 54.6 % within the samples. The grains form irre-gular fragments and often show clearly developed etching structures on the mineral surface. Another key of identification was the total extinction under XPL. Single grains show a pale pink coloration.

Zircon is represented by a range of 18.9 – 31.1 % and was divided by the shape of the grains: euhedral (12.2 – 27.9%), subhedral (0 – 3.1%), anhedral (35.9 – 58.2%), rounded (6.1 – 12.5%), subrounded (18.6 – 34.4%). Fragments of former euhedral or subhedral grains were counted as euhedral or subhedral zircon. Single grains show cloudiness. Inclusions and overgrowths were also investigated.

Tourmaline ranges from 6.6 – 12.8 %. A pleochroism from yellow/pale brown to brown is the most common type. Seldomly a pleochroism of pale grew / colorless to

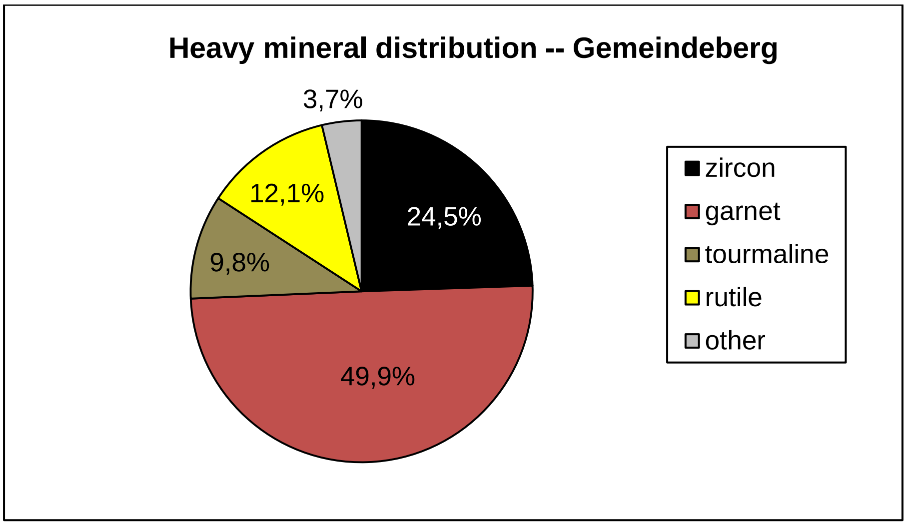

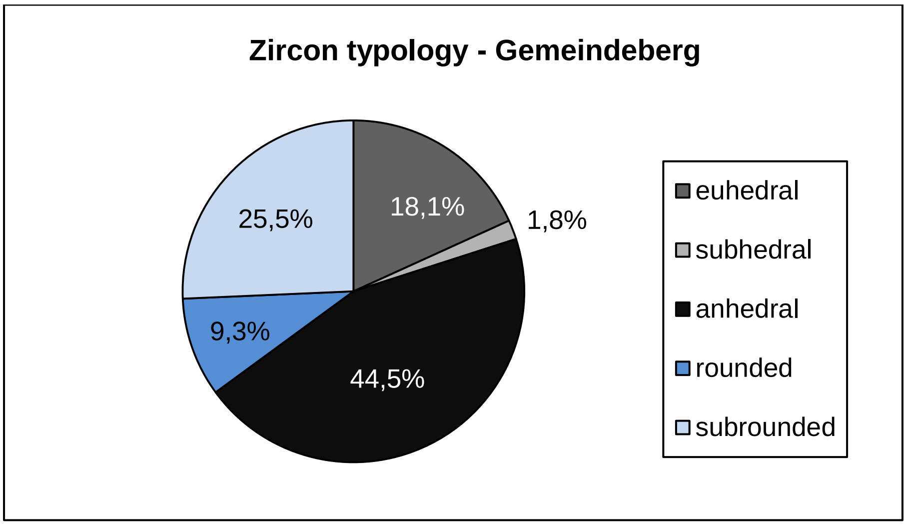

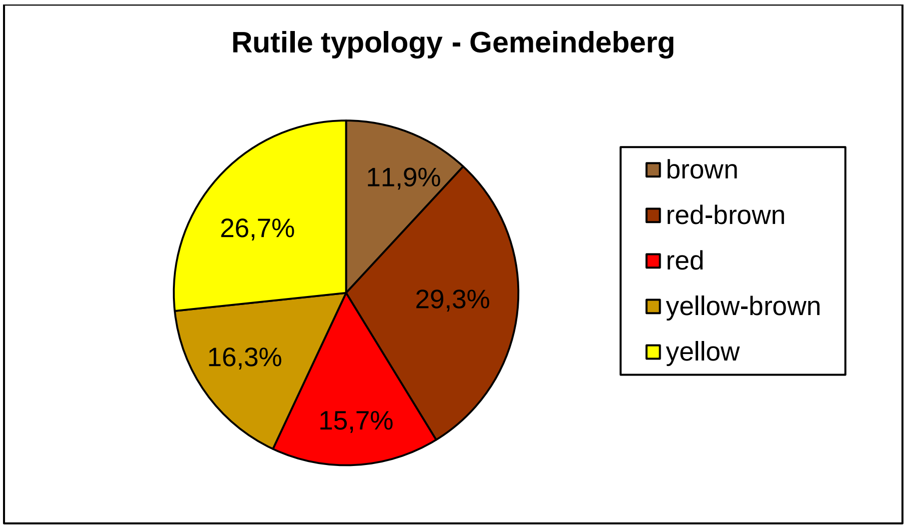

Fig.46 Upper fig.: Average heavy mineral composition of 3 Gemeindeberg quartzites, middle fig.: zircon typology (Gemeindeberg), lower fig.: rutile coloration of the Gemeindeberg quartzites

green was investigated. The shape of the grains appears irregular to subrounded. Columnar tourmaline is very rare (only one count).

Rutile shows a presence of 10.8 – 14.5 % within the samples and was divided by color.: brown: 0 – 32.3%, red – brown: 14.7 – 40%, red: 11.8 – 23.3%, yellow – brown: 10 – 27.3%, yellow: 23.3 – 29.4%.

Other heavy minerals, which only form occurrences of single grains were monazite, hornblende, anatase, sillimanite, apatite, titanite, chrome spinel.

6.4.2 Dislodged slices of Rehgras

Three samples of dislodged quartzites of Rehgras (Rehgr.01, Rehgr. 04. Rehgr. 05) were analyzed according to their heavy mineral content, which led to a total amount of 667 counts (tab. 15).

	Rehgr.01	%	Rehgr.04	%	Rehgr.05	%
zircon	197	50.13	92	41.63	38	57.58
garnet	60	15.27	36	16.29	7	10.61
tourmaline	22	5.60	11	4.98	15	22.73
rutile	61	15.52	46	20.81	4	6.06
monazite	27	6.87	24	10.86	1	1.52
hornblende	17	4.33	2	0.90	0	0.00
anatase	7	1.78	6	2.71	0	0.00
sillimanite	2	0.51	2	0.90	1	1.52
titanite	0	0.00	2	0.90	0	0.00
total	**393**	**100.00**	**221**	**100.00**	**66**	**100.00**

Tab.16 Heavy mineral distribution of 3 dislodged slices of Rehgras

Zircon shows a clear dominance of 41.6 – 57.6%: euhedral (7.6 – 20.6%), subhedral (4.3 – 11.2%), anhedral (22.8 – 37.6%), rounded (15.8 – 23.9%), subrounded (26.4 – 34.2%). Single grains show cloudiness. Overgrowths are quite common. Sporadically, yellow zircon (altogether 7 grains) was detected (fig.50, E).

Garnet occurs as irregular fragments with etching structures in a range of 10.6 – 16.3%. Pale pink coloration of single grains was investigated.

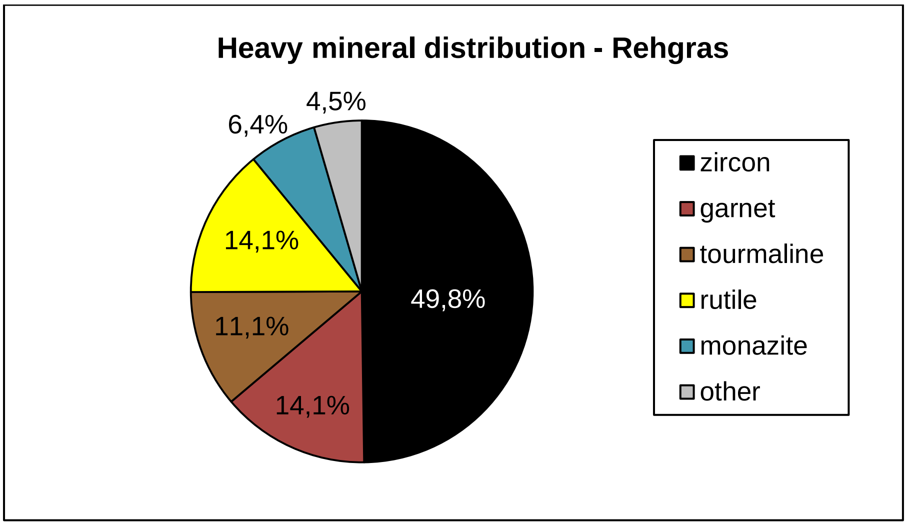

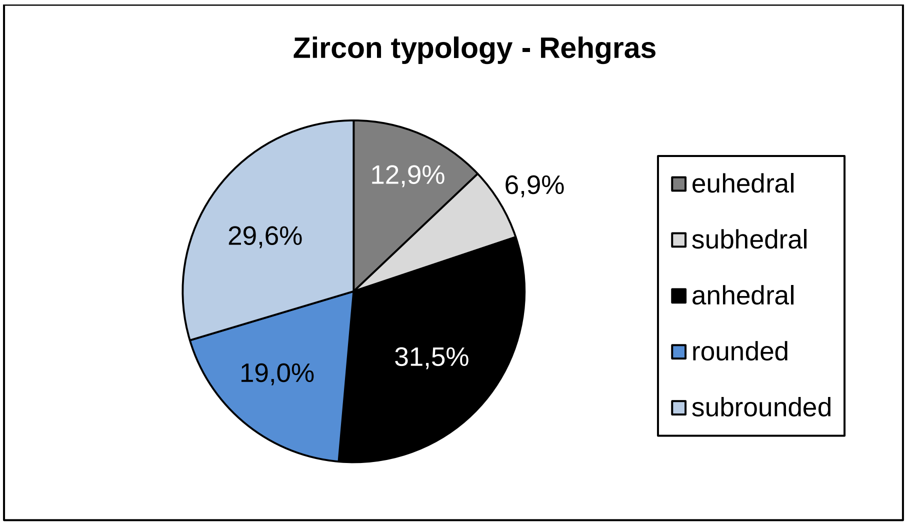

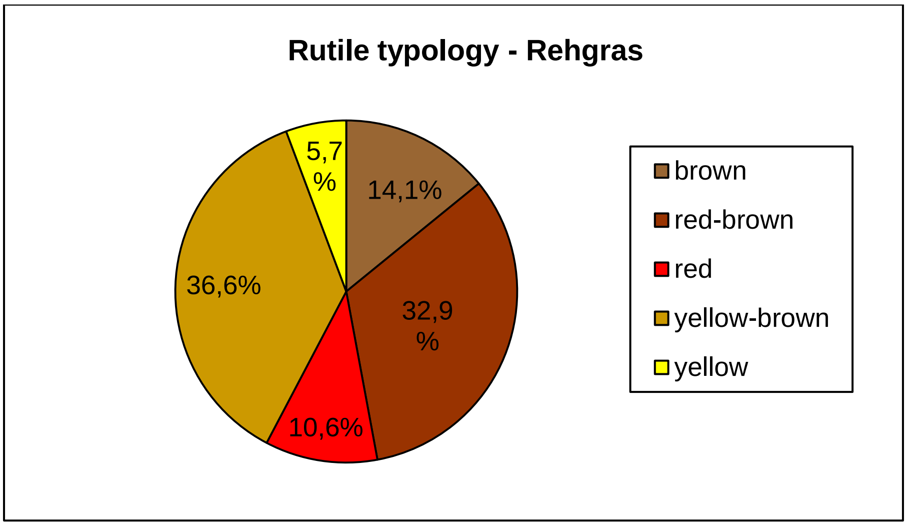

Fig.47 Upper fig.: Average heavy mineral composition of 3 dislodged slices of Rehgras, middle fig.: zircon typology (Rehgras), lower fig.: rutile coloration (Rehgras)

Tourmaline covers a range of 5.0 – 22.7%. The grains show a irregular to sub-rounded shape with yellow to brown pleochroism as the most common type. No columnar tourmaline was investigated.

Rutile, with a range of 6.1 – 20.8, shows following coloration (Rehgr.01, Rehgr.04): brown: 0 – 28.3%, red – brown: 24.6 – 41.3%, red: 6.5 – 14.8%, yellow – brown: 14.7 – 55.7%, yellow: 4.9 – 6.5%.

Monazite represents a occurrence of 1.5 – 10.9%. The grain shape mostly appears subrounded to rounded with brown spots on the mineral surface (fig.51, D).

Other detected minerals were hornblende, anatase, sillimanite, titanite.

6.4.3 Dislodged slices of Heiligenkreuz

Three samples of dislodged slices of Heiligenkreuz (Hkr.01, Hkr.05, Hkr,06) were analyzed according to their heavy mineral content, which led to a total amount of 663 counts (tab.16).

	HKr.01	%	Hkr.05	%	Hkr.06	%
zircon	25	24.75	50	48.54	200	43.67
garnet	24	23.76	9	8.74	41	8.95
tourmaline	35	34.65	19	18.45	57	12.45
rutile	13	12.87	16	15.53	93	20.31
monazite	2	1.98	2	1.94	14	3.06
hornblende	0	0.00	0	0.00	3	0.66
topas	0	0.00	0	0.00	1	0.22
sillimanite	0	0.00	0	0.00	1	0.22
apatite	0	0.00	1	0.97	0	0.00
titanite	0	0.00	0	0.00	2	0.44
tremolite	0	0.00	1	0.97	3	0.66
baryte/celestine	2	1.98	5	4.85	43	9.39
total	**101**	**100.00**	**103**	**100.00**	**458**	**100.00**

Tab.17 Heavy mineral distribution of 3 dislodged slices of Heiligenkreuz

Zircon shows an occurrence of 24.7 – 48.5% within the samples, including following shapes: euhedral (4.0 – 16.0%), subhedral (4.0 – 7.0%), anhedral (34.00 – 52.00%), rounded (8.00 – 19.00%), subrounded (18.00 – 40.00%).

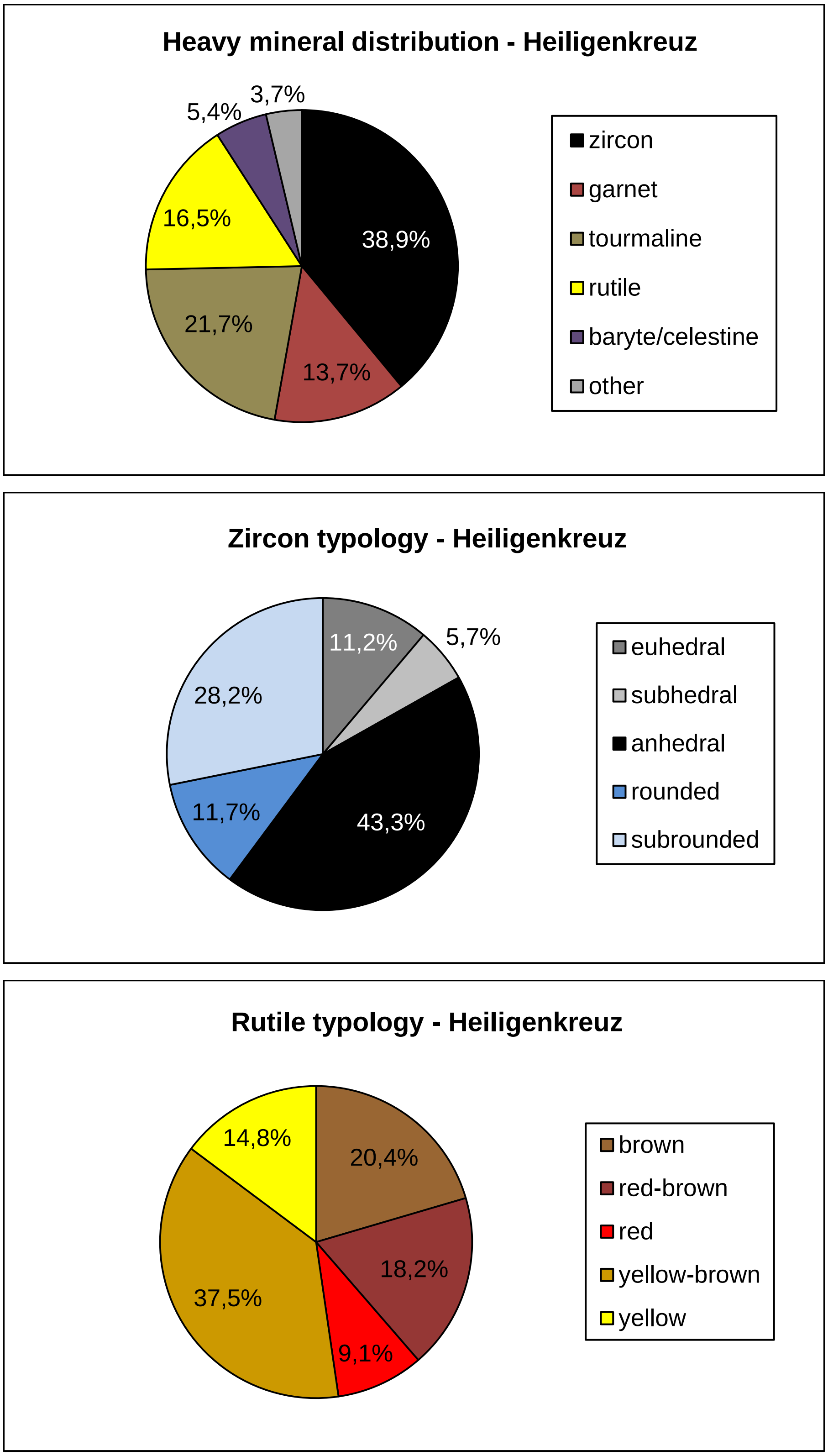

Fig.48 Upper fig.: average heavy mineral composition of 3 dislodged slices of Heiligenkreuz, middle fig.: zircon typology of Heiligenkreuz, lower fig.: coloration of rutile (Heiligenkreuz)

Isolated grains show inclusions and cloudiness. Yellow zircon is very rare (altogether 2 counts).

Garnet occurs within a range of 8.7 – 23.8%. Etching structures on the irregular formed grains are often clearly visible.

Tourmaline shows a frequency of 12.4 – 34.6%. As in the samples of Ober St. Veit and Rehgras, the most common type of pleochroism is from yellow/pale brown to brown. The grains mostly form irregular shapes, but also subrounded grains were detected. Single grains show a pleochroism of colorless/grew to green.

Rutile was devided by color and shows an occurrence of 12.9 – 20.3%: brown: 11.8 – 30.8%, red – brown: 15.4 – 20.4%, red: 0 – 15.4%, yellow – brown: 36.6 – 38.5%, yellow: 0 – 25%.

Other detected heavy minerals, which only occur sporadically, are monazite, hornblende, topas, sillimanite, apatite, titanite, tremolite and baryte/celestine. One sample (Hkr.06) shows significant amounts of baryte/celestine (9.4%).

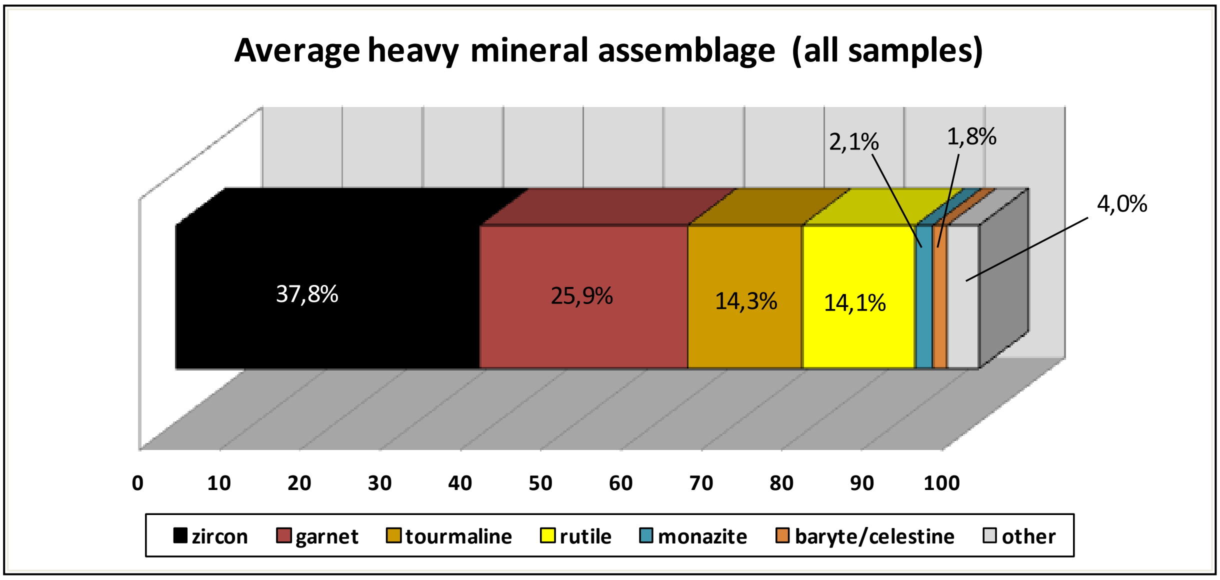

Fig.49 Average heavy mineral assemblage of all counted samples (dislodged slices and sandstones from Ober St. Veit)

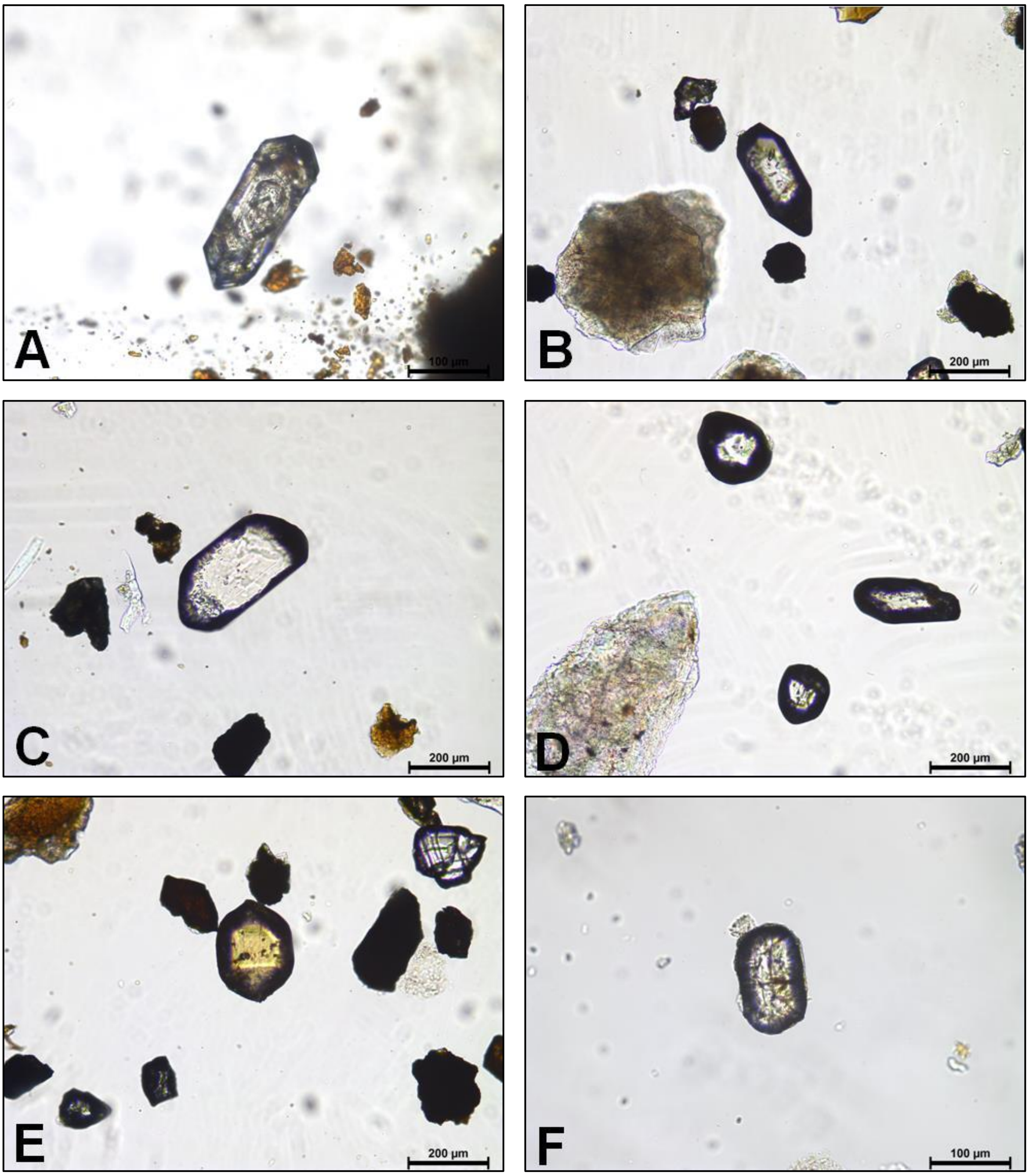

Fig.50 Examples for zircon typology, A: euhedral zircon with growth zoning, B: euhedral zircon with inclusions, C: subhedral zircon, D: rounded zircon, E: rounded, yellow zircon (Rehgras), F: rounded zircon with overgrowths

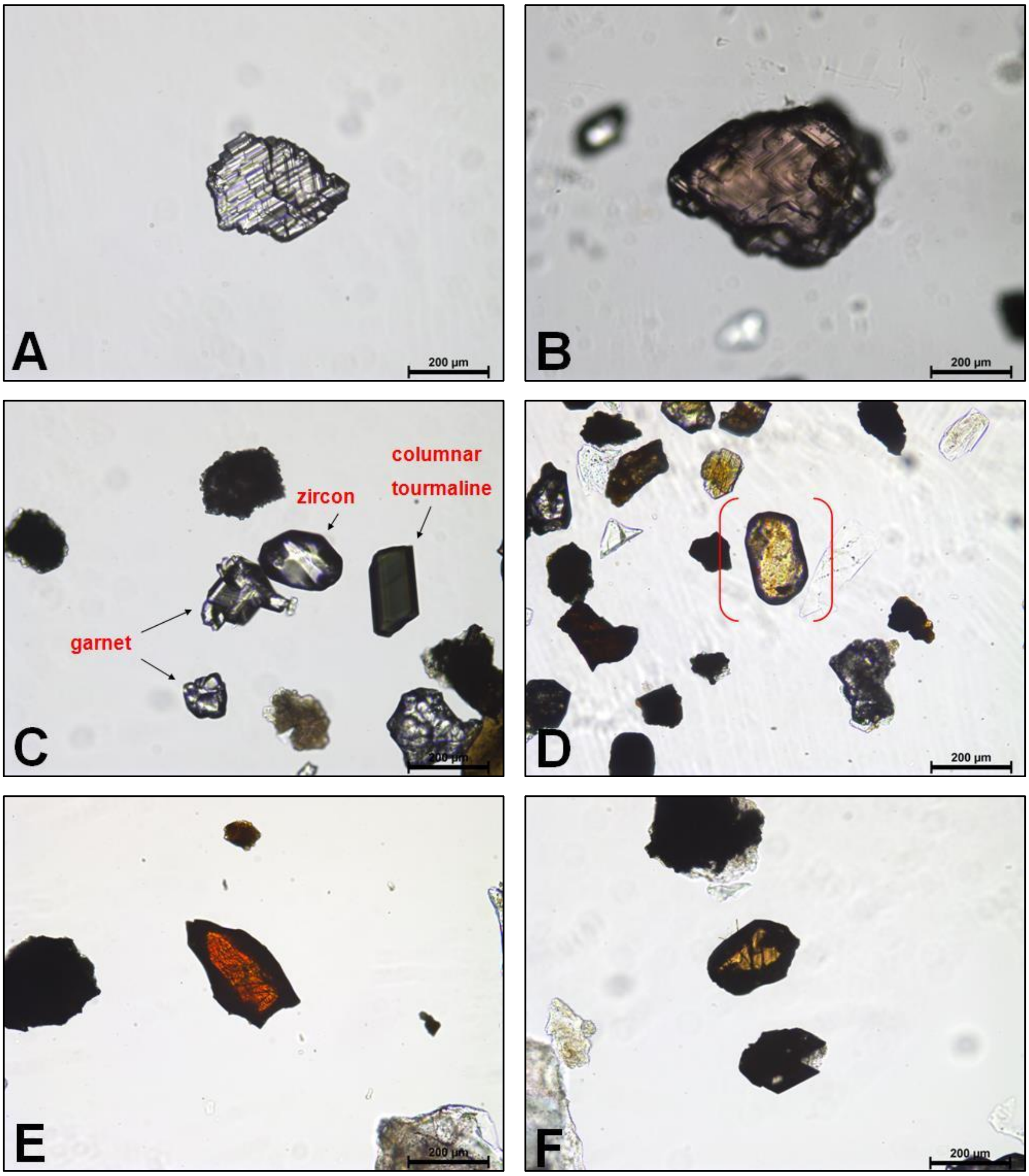

Fig.51 Examples for heavy mineral classification, A: irregular-shaped garnet with etching structures, B: garnet with etching structures and pale, pink coloration, C: garnet, subrounded zircon and green, columnar tourmaline (Gemeindeberg), D: monazite (Rehgras), E: red rutile, F: yellow rutile

6.4.4 ZTR-Index (zircon-tourmaline-rutile index)

The ZTR-index is a strong indicator for the maturity of sandstones (e.g. Hubert 1962). Due to their chemical and mechanical stability, these minerals are strongly enriched within very mature sandstone types like quartz arenites. The amounts of zircon, tourmaline and rutile are related to all non-opaque heavy minerals detected within the sample according to: *(zircon+tourmaline+rutile)*100/ Σ non-opaque heavy m.*

Sample	Sample site	Correlation	ZTR - index (%)
GeB.1	Gemeindeberg (Vienna)	St.Veit Klippenzone	40.1
GeB.S.02	Gemeindeberg (Vienna)	St.Veit Klippenzone	47.1
GeB.S.03	Gemeindeberg (Vienna)	St.Veit Klippenzone	52.1
Rehgr.01	Rehgras	dislodged slice	71.3
Rehgr.04	Rehgras	dislodged slice	67.4
Rehgr.05	Rehgras	dislodged slice	86.4
Hkr.01	Heiligenkreuz	dislodged slice	72.3
Hkr.05	Heiligenkreuz	dislodged slice	82.5
Hkr.06	Heiligenkreuz	dislodged slice	76.4
mean			59.1

Tab.18 Calculated ZTR-indexes (red marked samples did not reach the quantitatively minimum for statistical relevance)

Due to low amounts of heavy minerals, three samples (Rehgr.05, Hkr.01, Hkr.05) did not reach the statistical minimum of 200 counts. The results of these samples must be treated with caution. The samples of Heiligenkreuz (Hkr.01, Hkr.05) do not differ distinctively from the sample, which reached the statistical minimum (Hkr.06), whereas one sample of the dislodged slices of Rehgras (Rehgr.05) shows a significant higher ZTR-index compared to the other two samples (Rehgr.01, Rehgr.04). Because of the low number of only 66 counts (see tab.15), this sample should be treated as not representative. According to Hubert (1962), a ZTR-index of 76 – 100% reflects high maturity. Representative samples show a large range of 40.1 to 76.4%, mainly caused by varying amounts of garnet within the samples. Altogether, an average ZTR-index of 59% was calculated (tab.17), which is significantly higher than the average ZTR-index in e.g. arkoses (42%).

6.4.5 Heavy minerals – source rocks

The table below (derivations after Mange and Maurer (1991) and Shodhganga (2011)) shows the probable provenance of the counted heavy minerals.

Heavy mineral	Probable source rock
euhedral/idiomporhic zircon	igneous rocks
(sub) rounded zircon	(meta-) sedimentary rocks
zoned zircon	igneous rocks (granite)
zircon with overgrowths	paraschists, paragneisses
brown tourmaline	metamorphic rocks
prismatic tourmaline	igneous rocks
garnet	metamorphic rocks
purple garnet	schists, gneisses
rutile	metamorphic rocks, metasediments
monazite	igneous rocks, (sediments)
others	mostly metamorphic

Tab.19 Source rocks of heavy minerals

Zircon shows various types within the samples and due to its high resistance, zircon is regarded as a very high indicator for the provenance of sandstones (e.g. Pettijohn 1975). Zircon typology indicates a mixed provenance mainly consisting of igneous and sedimentary rocks (tab.8). Brown tourmaline and garnet are strongly associated with metamorphic source rocks. Columnar, prismatic tourmaline is very rare within the samples and is derived from igneous rocks like granites. Origin rocks of purple garnet are schists and gneisses. Rutile is mainly derived from metamorphosed argillaceous sediments like schists. Gneisses and amphibolites are also source rocks for rutile. Monazite is an accessory mineral in granitic rocks. Other heavy minerals, which only occur occasionally within the samples, are mainly derived from metamorphic rocks. In summary, the counting results mainly reflect a stable to ultra-stable heavy mineral assemblage, derived from a mixed provenance of igneous, metamorphic and sedimentary rocks.

6.5 Carbonate content determination

Previous results (XRD, petrography and geochemistry) strongly indicate the presence of calcium carbonate within the samples, which was quantified by the use of a Müller – Gastner carbonate bomb. For each sample, a mass of **0,614g** was required (tab. 19).

Sample	Correlation	Sample site	Mass (g)	$CaCO_3$
LT31/1164,5m	St. Veit Klippenzone	Lainz tunnel section	0.613	**0%**
LT31/ 1200m	St. Veit Klippenzone	Lainz tunnel section	0.614-0.615	**11.50%**
LT31/ 1215,5m	St. Veit Klippenzone	Lainz tunnel section	0.616	**0%**
LT31/ 1277,2m	St. Veit Klippenzone	Lainz tunnel section	0.613	**10%**
GeB. 03	St. Veit Klippenzone	Gemeindeberg	0.613-0.614	**0%**
GeB.Kr.02	St. Veit Klippenzone	Gemeindeberg	0.616	**0%**
Rehgr.02	Dislodged slice	Rehgras	0.616	**0%**
Hkr.04	Dislodged slice	Heiligenkreuz	0.614	**0%**
May.01-W	Dislodged slice	Mayerling	0.614-0.615	**0%**
Hb.Gb.3	Dislodged slice	Hinterbrühl	0.613-0.614	**0%**
Gr.1-3	Dislodged slice	Groisbach	0.615	**27%**
Gr.1-4	Dislodged slice	Groisbach	0.613-0.614	**26%**
Gr.1-5	Dislodged slice	Groisbach	0.615-0.616	**61.50%**
Gr.1-7	Dislodged slice	Groisbach	0.613	**81%**
Hb.1-1	Reisalpen nappe	Hafnerberg	0.613	**74%**
Hb.1-2	Reisalpen nappe	Hafnerberg	0.613-0.614	**83%**
Hb.1-3	Reisalpen nappe	Hafnerberg	0.614-0.615	**80%**
Hb.1-6	Reisalpen nappe	Hafnerberg	0.613	**89%**
Gr.S.01	Gresten Klippenzone	Waidhofen	0.615-0.616	**13%**
Gr.S.02	Gresten Klippenzone	Waidhofen	0.616-0.617	**0%**
Gr.S.03	Gresten Klippenzone	Ybbsitz	0.614	**0%**
Gr.S.04	Gresten Klippenzone	Pechgraben	0.615	**14%**

Tab.20 Results of carbonate content determination

Two samples of the Lainz tunnel section show $CaCO_3$ contents of 10 and 11.5% due to calcite cementation. None of the samples of Ober St. Veit include any $CaCO_3$, which again indicates, that calcite cementation within the samples is rather sporadic.

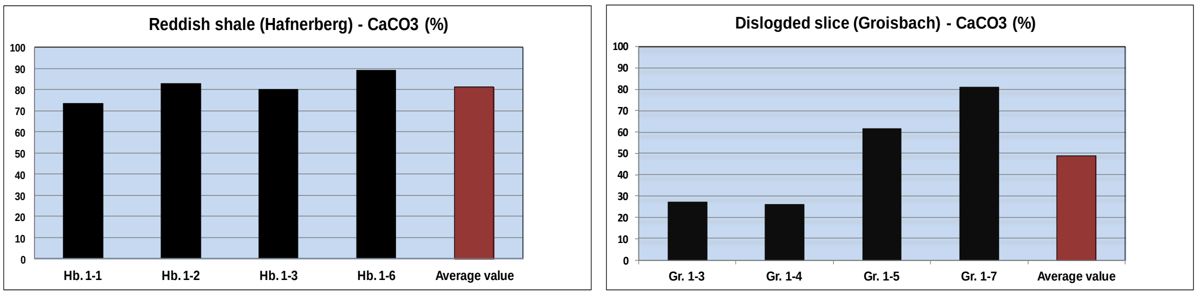

Fig.52 Calcite contents of samples of Hafnerberg (left) and Groisbach (right); mean values are shown by the red bar

For the dislodged slices, only the samples of Groisbach show significant $CaCO_3$ contents between 26 – 81%. The wide range between these values is primarily caused by the inconsistent amount of biogenic particles within the samples (see chapter 6.2.5). It can be assumed, that higher contents of bioclasts led to higher amounts of $CaCO_3$. Due to the dissolution of dolomite, the eye-catching dolo-sparstones western of Hafnerberg show high contents of 74 – 89%. Only the Gresten arkoses of Waidhofen und Pechgraben show carbonate contents of 13 and 14%, whereas the Gresten conglomerate of Waidhofen and the fine-grained Gresten sandstone of Ybbsitz include no carbonate at all. Also, these values are caused by the presence of calcite cement within the samples (see chapter 6.2.9).

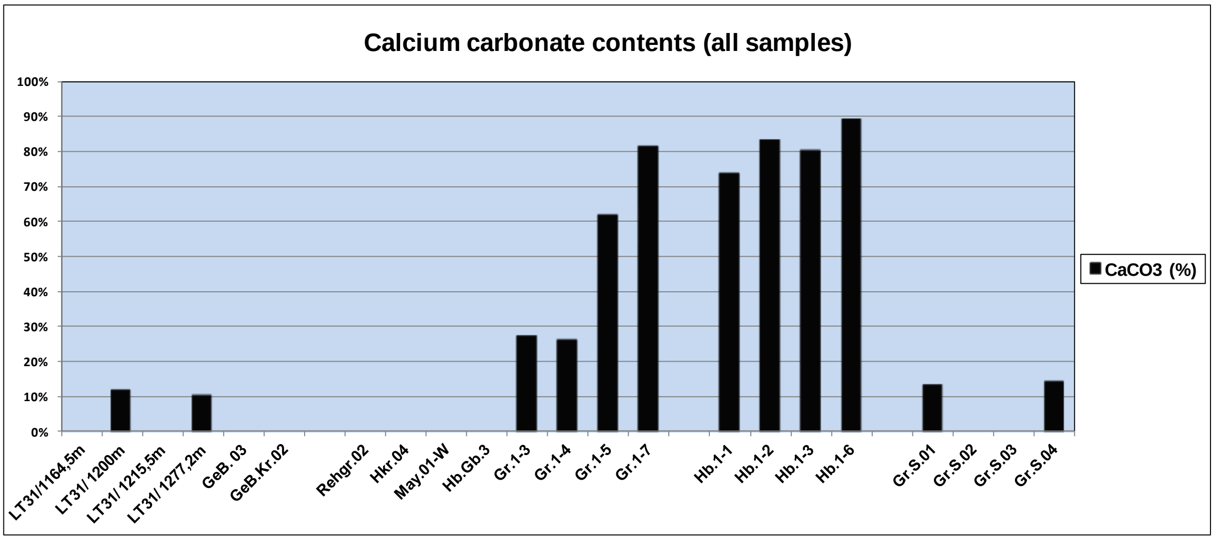

Fig.53 Calcite contents within all samples

7. Discussion

7.1 The dislodged slices and the St. Veit Klippenzone sandstones

Different methods used in this thesis clearly reflect the quartz-rich composition of the rocks, whereas the results of the individual chapters confirm each other successfully. The geochemical results of the collected Keuper sandstones (dislodged slices and St. Veit Klippenzone sandstones of Ober St. Veit) fit very well the results (main-, minor and trace elements) of the Lainz tunnel sandstones. A SiO_2–content of more than 90% and a strong depletion in other main and minor elements in relation to the UCC seems to be a defining characteristic of these stones. Considerable amounts of CaO were detected within the samples of the Lainz tunnel section, whereas the investigated Keuper sandstones collected for this thesis showed no CaO at all. Low CaO and $CaCO_3$ levels are associated with the sporadic appearance of calcite cement within the samples, which is confirmed by petrographic analysis. Ultimately, according to their mineralogy and geochemistry, the dislodged slices of Lower Austria (except the occurrence of Groisbach) can be regarded as almost identical to the sandstones of the St. Veit Klippenzone. The dislodged slices of Groisbach show a different facies development and are likely to be the fossil-rich sandy-marly deposits that Wessely (1976) referred to the Liassic.

The dolosparstones of Hafnerberg show no similarities to the Keuper sandstones and shales of the St. Veit Klippenzone. No direct evidence of the exact age of these rocks could be found although their occurrence within Norian Hauptdolomite infers a Late Triassic age and may explain the predominance of dolomite grains. However, Plöchinger and Salaj (1991) assumed an Upper Cretaceous age without giving any further explanation. More investigations are required to provide a final conclusion about these conspicuous rocks.

The results of the heavy mineral analysis between the individual samples collected for this thesis and the Lainz tunnel sandstones show partially strongly varying ratios of garnet and zircon. In general, the heavy mineral composition of sandstones is a strong function of the different heavy mineral species within the rocks of the source area as well as the extent of physical abrasion during sorting, transportation and deposition. Successive sorting and transport lead to the ultimate enrichment of stable to ultrastable minerals like quartz, zircon, tourmaline and rutile (Hubert 1962). Due to the strong dominance of stable to ultrastable heavy mineral species (and geochemical results) within the samples, Pfersmann (2013) supposed a long, fluvial transport from the north into the alpine depositional realm.

Zircon is a major constituent of all samples. Especially the dislodged slices show a clear zircon-dominance of 39 – 50%, which fits well the results of the Lainz tunnel sandstones (56%). At this point it must be mentioned, that, according to Pfersmann (2013), large amounts of baryte and pyrite strongly handicapped the heavy mineral analyses of the Lainz tunnel sandstones leading to non-representative results. Garnet shows strong varying amounts between the counted dislodged slices and the samples of Ober St. Veit (14 – 50%). The samples of the Lainz tunnel section include amounts of 0 – 11%, leading to an average value of 3%. According to Füchtbauer (1988), considerable amounts of garnet within long-distance transported sandstones strongly indicate deposition under dry climatic conditions. Garnet appears unstable to acidic (ph≤ 5,6) chemical weathering during e.g. humid climates but very stable during diagenesis. It is interpreted, that varying amounts of heavy mineral species like garnet are mainly caused by grain size effects. It is also mentioned here, that only 9 of over 20 treated samples showed notable amounts of heavy minerals, which implies that the heavy mineral distribution within the samples is also rather inconsistent. According to Woletz (1967), Keuper sandstones of the St. Veit Klippenzone, which were exposed at Roter Berg (Norhartgasse), showed a strong dominance of zircon with lesser amounts of rutile, tourmaline, garnet and apatite. At this time, these rocks were interpreted as Liassic Gresten sandstones.

7.2 Source of clastics – probable provenance(s)

Altogether, the results strongly suggest a felsic-silicic origin of the rocks. Petrography, geochemistry and heavy minerals clearly indicate a derivation from igneous rocks (granites), metamorphic rocks (e.g gneisses, metasediments) and older sandstones. Although high levels of Qp suggest a dominance of metamorphic source rocks, it must be assumed that strong compaction has affected the polycrystallinity and shape of the quartz grains. Sandstone classification schemes after Folk (1970) and McBride (1963) identified the samples as litharenites, sublitharenites, feldspathic litharenites and lithic subarkoses. Geochemical classification after Pettijohn (1972) or Herron (1988) resulted in the classification as sublitharenites, subarkoses and quartz arenites. A QFL-plot after Dickenson (1983) showed a recycled orogen as most probable provenance. The samples have an average mineralogical composition of $\mathbf{Q_{88}F_{10}L_2}$, whereas Q includes all quartzose grains. If Qp+mica is treated as a lithic fragment (as quoted by Ingersoll 1988), the average composition consists of $\mathbf{Q_{65}F_{10}L_{25}}$. Overall, these results fit the composition of Triassic Keuper sandstones of the Western Carpathians quite well, but some differences can be observed. According to Al-juboury (2007), Keuper sandstones of Westcarpathian units are pronounced quartz-rich leading to an average composition of $Q_{84}F_7L_9$. Plagioclase, identified by zoning and twinning, is much more common than K-feldspar. Average SiO_2-contents range from 42.1% (Envelope unit of the Tatricum) to 95.1% (Križna Vysoká unit). Considerable amounts of hematite cement and clayey matrix were also detected (8.8 – 18.4%), which are completely missing within the samples investigated for this thesis. The “high” matrix content is partially associated with the weathering of feldspar during diagenesis, which suggests that the feldspar content was originally higher. The samples were deposited under a passive-extensional tectonic regime with lithospheric stretching and crustal thinning. The crystalline cores of the Western Carpathians itself and of the Bohemian Massif were identified as most probable provenance.

Striking is the fact, that the results of this thesis indicate a more uniform composition for the investigated Keuper sandstones compared to Westcarpathian samples, which also could be caused by lower sample numbers. The variety of compositions within Westcarpathian Keuper units is associated with diagenetic changes after deposition, different sedimentation rates and relief-changes within the source area.

By recognizing strong similarities to Westcarpathian Keuper sandstones, a derivation from the crystalline cores of the Bohemian Massif or another stable craton seems possible and should be taken into account for the investigated samples. According to Dickinson (1985), craton-derived quartzose sands are from stable, low-lying granitic and gneissic exposures, also influenced by recycling of overlying sediments. These sands are preferably deposited within craton interiors or at passive continental margins by fluvial transport ultimately leading to very high quartz contents. K-feldspar is much more common than plagioclase, which fits well the mineralogy of the investigated samples. Additionally, intense (humid) weathering and a low relief are required for the formation of first-cycle very quartz-rich sediments (Dickinson 1985).

Generally, the samples investigated for this study show much in common with sandstones whose compositions are derived from long, fluvial transport. According to Potter (1978), following important parameters are characteristic for long-distance, fluvial transported sandstones:

- mostly lithic arenites in composition with an average feldspar content of 12%
- wide range of lithic fragments; stable metamorphic grains often show average contents of 25%
- more Qm than Qp
- moderately to well sorted
- river sands are deficient in clay matrix
- average geochemical composition between arkoses and quartz arenites
- grain shape: rather angular→ quartz grains in rivers round very slowly, except in high-gradient mountain streams
- <u>modern river sands of tectonic passive coastlines</u>: very high quartz contents, richer in K-feldspar than plagioclase, high ZTR-indexes, free of volcanic clasts, from stable cratonic sources

Mineralogical maturity and the stable to ultrastable heavy mineral assemblage detected within the samples indicate long fluvial transport, most probably from northern regions. Additionally, trace element analysis (e.g. a plot of Zr/Sc versus Th/Sc after McLennan (1993)) suggests high degrees of sedimentary sorting and recycling and a passive margin as tectonic setting. This agrees well with the assumed tectonics within the depositional realm of the Northern Calcareous Alps during the Late Triassic (e.g. Lein 1985, Mandl 2000). Nowadays, the existence of wide-spreading river systems, which formed large deltas with barrier islands and lagoons within the Central European Basin during the Triassic, is overall accepted (e.g. Wurster 1964, Paul et al. 2009). Also, connections from the Germanic Basin to the western Tethys are assumed. Based on zircon-fission track data, Köppen and

Carter (2000) mentioned a European-wide fluvial transport system, which linked the Fennoscandian Shield to the central Germanic basin (Schilfsandstein Formation) and the Tethyan depositional realm (Lunzsandstein Formation) during Carnian times. This “Nordic Keuper” concept for Triassic sediment series of the Northern Calcareous Alps was already proclaimed by Behrens (1972). According to Behrens (1972), Lunz sandstones show a strong correlation to the Germanic Schilfsandstein Formation. The mineralogy of Lunz sandstones contains quartz and feldspar in equal quantities. Feldspar grains consist of orthoclase, microcline and plagioclase. Grain sizes are predominantly 63-125 µm. Also, the rocks contain considerable amounts of plant remains. The heavy mineral assemblage mainly consists of apatite, zircon, tourmaline, rutile, chrome spinel and various amounts of garnet, which is largely similar to the investigated Keuper sandstones.

According to Pfersmann (2013), no indications for the exact age of the Lainz tunnel sandstones could be found. However, due to petrological and geochemical evidence, a Late Triassic age was assumed. Keuper sandstones and shales of the Northern Calcareous Alps mainly form intercalations within the Hauptdolomit, which represent Norian age (e.g. Faupl 2003). Considering a renewed transgression of the western Tethys during the Rhaetian, which ended successive clastic influx into the Tethyan realm (e.g. Mandl 2000), a Carnian to Norian age of the samples seems very probable.

According to Paul et al. (2009), analyzes (K/Ar ages of mica) of (possible) comparative samples of the Germanic basin revealed, that clastic transport during the Late Triassic (Lower to Middle Keuper) mainly occurred from the Caledonian mountain ranges west of the Fennoscandian Shield. Paul et al. (2009) interpreted the Fennoscandian Shield at these times as “low land”, which did not supply any clastic material. The Caledonides were lifted up due to subsequent exhumation. These tectonic movements were probably caused by the Viking graben-system. For deposits of the Upper Keuper (Rhaetian Exter Formation), a different source area was located. These occurrences were derived from Panafrican sources in southeast Poland or Slovakia. Other potential source areas, e.g. the Rhenish or the London-Brabant Massif, did not provide significant amounts of clastic material (Paul et al.

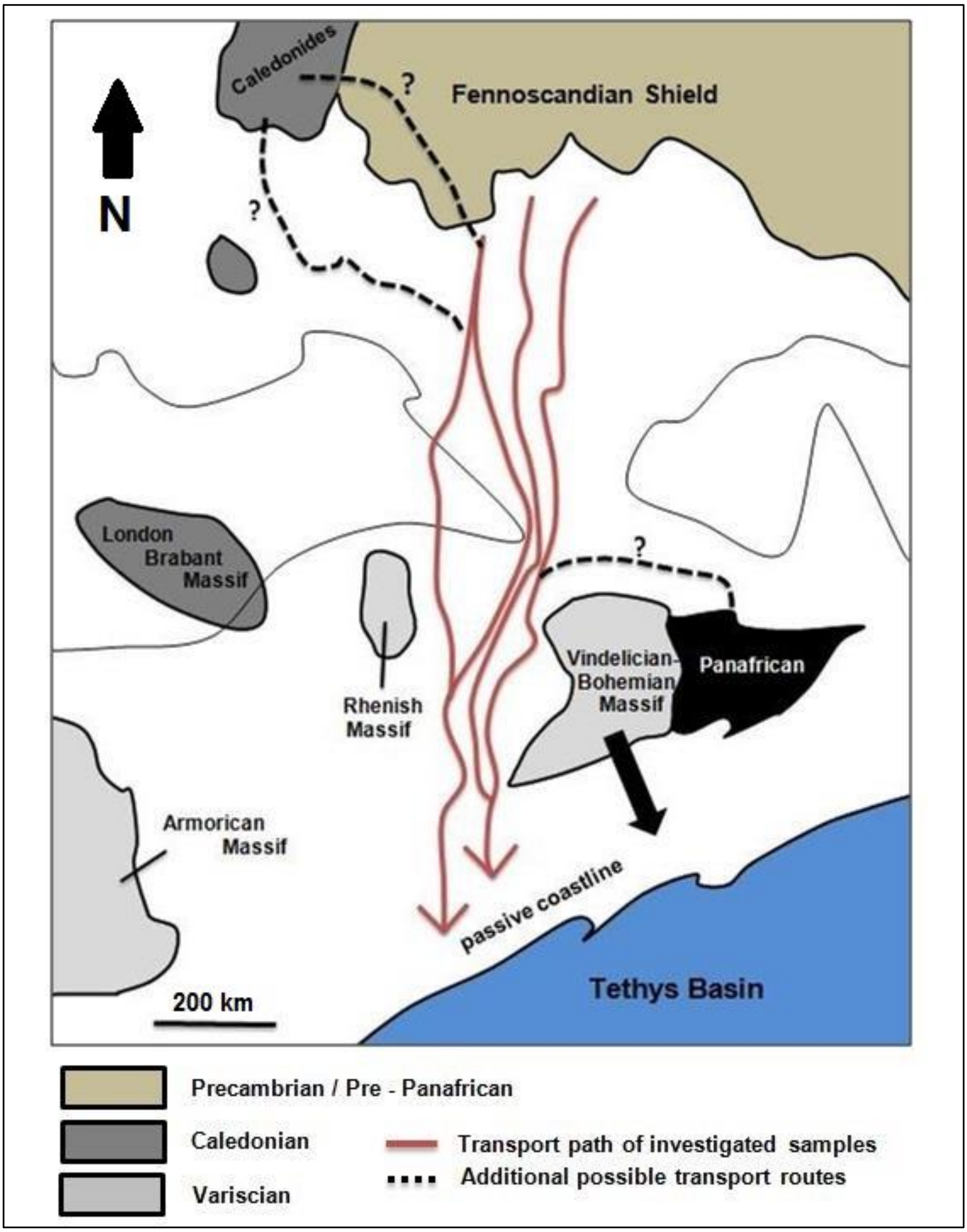

Fig.54 Simplified palaeogeographic sketch showing the assumed transport of clastic material of the investigated Keuper sandstones during the Late Triassic

2009). By considering the “Nordic-Keuper” concept proclaimed by Behrens (1972) and Köppen and Carter (2000) and the results obtained for this thesis, a long fluvial transport from northern regions, most probably from the Fennoscandian Shield, must be assumed for large parts of the investigated units. Possible additive transport routes, as illustrated by Germanic Keuper sediments, should be kept in mind (fig. 54).

The Fennoscandian Shield occupies large areas of Finland, NW Russia, Norway, Sweden and is the largest exposed area of Precambrian rocks in Europe. This area is also characterized by diverse complex orogenic events during the Paleoproterozoic, Meso-, Neoproterozoic and Phanerozoic leading to a large variety of crystalline and sedimentary rocks (e.g. Lahtinen 2012).

7.3 Climate – a main control factors of composition?

In general, the modal composition of sandstones is mainly derived from the tectonic setting during the time of deposition, whereas provenance, transport, weathering, climate and diagenesis are also considered to be important secondary parameters (Dickenson 1985). However, within recent times, climatic conditions have become recognized as a key factor for understanding the composition of sandstones. One question to be clarified for this hypothesis is whether the climate had a significant influence on the composition of the samples. Analyzes strongly suggest that deposition occurred under semi-humid to humid climates. According to Al-juboury (2007), a semi-arid to semi-humid climate is assumed during the deposition of Westcarpathian Keuper sandstones. Climate fluctuations within the Alpine-Carpathian realm during the Keuper period were mainly indicated by sea-level oscillations of the western Tethys (e.g. Wurster 1964). Within the Germanic basin, arid to semi-arid climatic conditions are dominant, expressed by the deposition of sabkhas, gypsum and salt during the e.g. lower and upper part of the Middle Keuper. Humid intermezzos (e.g. Stuttgart Formation) led to the formation of large river systems, which transported clastic material from Scandinavia to Switzerland and further south into the Tethys (e.g. Paul et al. 2009). Pluvial events are also assumed during Carnian times. With the beginning of the Jurassic, a climate-shift from warm semi-arid/arid to hot - humid in the Tethyan domain was observed (e.g. Iqbal et al. 2018). In general, a relation between the climate and the formation of large braided river systems can be assumed.

According to Suttner and Dutta (1986), following (optimal) conditions must be fulfilled for the preservation of climatic signatures within sandstones:

- derivation: phaneritic crystalline rocks (e.g. granites, gneisses)
- transportation: less than 100 km in streams of medium to low gradient
- deposition: low-order streams and associated alluvial environments
- diagenesis: early cementation at shallow burial depths

Strong compaction and the formation of significant amounts of secondary porosity as it was investigated within the samples only occur at great burial depths (Schmidt and McDonalds 1979). Also, due to mineralogical and geochemical results, it must be assumed that the samples were transported over large distances. Altogether, these facts suggest that rather long transportation and the tectonic setting were main control factors for the composition and not climatic conditions. Diagenesis, expressed by significant amounts of quartz and calcite cement within some of the samples, influenced the composition. The effects of (postdepositional) weathering should also not be forgotten.

7.4 Keuper and Gresten sandstones – a comparison

In early stages of research, the Keuper sandstones of the St. Veit Klippenzone and the dislodged slices were commonly interpreted as early Jurassic Gresten sandstones (see chapter 3.2). A closer comparison might clarify some differences between these rocks. Overall, the start of the Jurassic was marked by the continuous transgression of the Vindelician-Bohemian Massif by the western Tethys leading to characteristic sedimentary successions. In northern areas, fluviatile coarse –grained arkoses were deposited on Variszian-crystalline rocks (Basal series, Liassic-Doggerian). With ongoing transgression, this shallow water development (deltas) continued into a marine-terrigenous facies (seam complex, Doggerian)). Taken together, this characteristic sequence is known as “Gresten beds” of the Helvetic Gresten Klippenzone (Faupl 1975, 2003). Upper Jurassic sediments (Malmian-Neokom) are predominantly carbonatic.

In general, the Gresten zone samples of Waidhofen (Ybbs), Ybbsitz (between Waidhofen and Gresten) and the Pechgraben area (nearby the Leopold Buch Memorial) show a significant lower mineralogical and geochemical maturity, which might be a result of shorter transportation and a different (more active) tectonic setting. Geochemical classification resulted in the classification as arkoses and lithic arenites. A higher diversity of mineralogy compared to Keuper sandstones was also observed by Pfersmann (2013). Additionally, according to Pfersmann (2013), the Gresten sandstones showed higher contents of CaO, MgO, P_2O_3 and Sr, which are associated with marine environments. Al_sO_3 and Fe_2O_3 contents were also higher. These observations fit well the results gained for this thesis (see chapter 6.3). Faupl (1975) described early Jurassic (Liassic – Doggerian) sandstones of the Gresten Klippenzone as mainly coarse-grained arkoses, subarkoses and (sub)litharenites. The highest quartz-content is 78%. Qp becomes more common as Qm with rising grain size within the samples. Mostly, amounts of plagioclase exceed the amounts of K-Feldspar. Rock fragments mainly appear as aggregates of quartz and feldspar. Plant remains were also investigated. Another striking difference may be that, due to the presence of index fossils (e.g. arietites), in some cases, the exact age of the rocks could be determined. According to Faupl (2003) the crystalline basement rocks itsself were identified as source rocks for the clastic material. Unfortunately, due to very high amounts of opaque minerals, the results of the heavy mineral analysis are not representative. However, non-opaque heavy minerals detected within early Jurassic Gresten sandstones mainly consist of zircon, tourmaline, rutile and lesser amounts of apatite and garnet (Faupl 1975).

Overall, these petrographic results gained by Faupl (1975) fit the observations done for this thesis well. A modern provenance analysis, which includes petrographic and geochemical data of more (15-20) samples of Gresten sandstones, could provide a final contribution to this matter.

	Triassic Keuper sandstones	Liassic Gresten sandstones
Mineralogy	quartz, feldspar (K-feldspar), mica, lithic fragments (mainly composed of quartz)	quartz, feldspar (K-feldspar, plagioclase) mica, lithic fragments (polymineralic)
Grain size	medium - (very) coarse	fine - (very) coarse
Geochemistry	very high SiO_2-contents above 90% strong depletion in other main or minor elements	SiO_2-contents: 77-78%, Al_2O_3: 8 - 9% higher Fe_2O_3, MgO, CaO contents
Mineralogical classification	sublitharenite, litharenite, feldspathic litharenite, lithic subarkose	arkose, subarkose sublitharenite (after Faupl 1975)
Geochemical classification	sublitharenite, subarkose, quartz arenite	litharenite, arkose
cement	quartz, calcite	quartz, calcite
matrix	none	clay
log (SiO_2/Al_2O_3)	1.44 - 1.88	0.96 - 0.97
tectonic setting	passive continental margin	passive continental margin, active continental margin, cont. island arc
heavy minerals	zircon, garnet, tourmaline, rutile, monazite, others	mainly opaque (zircon, tourmaline, rutile, apatite, garnet) (after Faupl 1975)

Tab.21 Characteristic parameters of Keuper and Gresten sandstones

8. Conclusion

Systematic investigations of Late Triassic Keuper sandstones from the eastern part of the Austrian Eastern Alps led to following final conclusions:

1) The occurrence of the Gemeindeberg (Ober St. Veit) and the dislodged slices of Lower Austria can be regarded as almost identical to the Late Triassic St. Veit Klippenzone sandstones of the Lainz tunnel section. Petrographic sandstones classification identified the rocks as sublitharenites, litharenites, feldspathic lith-arenites and lithic subarkoses. The samples show an average mineralogical composition of $Q_{88}F_{10}L_{2}$ respectively $Q_{65}F_{10}L_{25}$. Geochemically, the rocks were clas-sified as sublitharenites, subarkoses and quartz arenites. According to their mineralogical maturity index (MMI), the rocks can be regarded as submature to mature. Additionally, the samples show CIA-values between 61 and 81, which reflect intermediate to extreme post-depositional weathering of feldspar.

2) The primary control factors for composition were long fluvial transport and a passive tectonic setting. A recycled orogen was identified as most probable provenance. Mineralogical and geochemical results strongly indicate a derivation from quartzose igneous, metamorphic and sedimentary rocks. Based on the results of this thesis and a literature review, a derivation from northern regions, most probably from the Fennoscandian Shield must be assumed.

3) Due to the lack of any index-fossils within the samples, no exact age of the rocks could be determined. Assuming that the samples represent Late Triassic Keuper sediments, a Carnian to Norian age is very likely. This also compares nicely to the Carpathian Keuper of proven Late Triassic age.

4) Overall, the Keuper sandstones from the St. Veit Klippenzone and the dislodged slices of Lower Austria show much in common with Westcarpathian Keuper sandstones, especially with samples from the Vysoká unit of the Križna nappe system. Striking differences are also noticeable, expressed by the strong dominance

of plagioclase within the feldspar-section and the presence of clayey matrix within the Westcarpathian Keuper units. Altogether, a derivation from the Bohemian Massif seems to also be possible for the investigated Keuper sandstones and should be taken into account.

5) The early Jurassic sandstones from the “Gresten beds” of the Gresten Klippen-zone show a different mineralogical and geochemical composition leading to lower maturity and a different tectonic setting during the time of deposition. Geochemically, the rocks were classified as litharenites and arkoses. Due to the strong limitation of the number of samples, further, more detailed investigations are required.

9. References

Al-juboury, A. 2007: Petrography and major element geochemistry of Late Triassic Carpathian Keuper sandstones: Implications for provenance. Bulletin de l'Institut Scientifique, Rabat, section Sciences de la Terre, 2007, n 29, 1-14.

Armstrong-Altrin, J.S. (2009): Provenance of sands from Cazones, Acapulco, and Bahía Kino beaches, Mexico. Rev Mex Cien Geol 26: 764–782.

Behrens, M., 1973: Schwermineralverteilung und Sedimentstrukturen in den Lunzer Schichten. Jb. Geol. B.-A.,116.

Bhatia, M.R., 1983: Plate tectonics and geochemical composition of sandstones. J. Geol. 91, 611–627.

Bhatia, M.R., Crook, K.A.W., 1986: Trace element characteristics of graywackes and tectonic setting discrimination of sedimentary basins. Contributions to Mineralogy and Petrology 92, 181–193.

Cullers, R. L. (2000): The geochemistry of shales, siltstones and sandstones of Pennsylvanian–Permian age, Colorado, USA: Implications for provenance and metamorphic studies. Lithos 51, 181–203.

Dickinson, W.R., Suczek, C.A., 1979: Plate tectonic and sandstone composition. Bull. Am. Assoc. Petrol. Geol. 63, 2164–2172.

Dickinson, W.R., 1985: Interpreting provenance relations from detrital modes of sandstones. In: Zuffa, G. (Ed.), Provenance of Arenites. Reidel, Dordrecht, pp. 333–361.

Faupl, P., 1975: Kristallinvorkommen und terrigene Sedimentgesteine in der Grestener Klippenzone (Lias-Neokom) von Ober- und Niederösterreich, Jb. Geol. B.-A. Bd.118, S.1-74 Wien 1975

Faupl, P., 2003. Historische Geologie. 2. Aufl. Wien (Fakultas UTB).

Fedo, C.M., Nesbitt, H.W. and Young, G.M. (1995): Unraveling the Effects of Potassium Meta-somatism in Sedimentary Rocks and Paleosols, with Implications for Paleoweathering Conditions and Provenance. Geology, 23, 921-924.

Flügel, E., 2002: Microfacies of carbonate rocks: analysis, interpretation and application, Springer 2002

Folk, R.L., 1974: Petrology of Sedimentary Rocks. Hemphill Publication Co., Austin, Texas.

Fuchs W., 1985: Großtektonische Neuorientierung in den Ostalpen und Westkarpaten unter Ein-beziehung plattentektonischer Gesichtspunkte, Jb.Geol.B.-A., ISSN 0016-7800, Band 127, Heft 4, S.571-631, Wien 1985

Griesbach, C.L., 1869. Die Klippen im Wiener Sandsteine. Jahrb. d. k. k. geol. R.-A., XIX. Bd., S. 217.

Golonka, Jan, and Frank J. Picha, 2006, Introduction, in J. Golonka and F. J. Picha, The Carpathians and their foreland: Geology and hydrocarbon resources: AAPG Memoir 84, p. 1 – 9.

Häusler, H., Plasienka, D., Polak, M., 1993: Comparison of mesozoic successions of the Central Eastern Alps and the Central Western Carpathians, Jb. Geol. B. –A., ISSN 0016 – 7800, Band 136, Heft 4, 715-739, Wien 1993

Hertweck, G.: Die Geologie der Ötscherdecke im Gebiet der Triesting und der Piesting und die Frage der alpin-karpatischen Abbiegung in den niederösterreichischen Kalkalpen. — Mitt. Ges. Geol. Bergbaustud. Wien, 12, (1961), Wien 1961.

Herron, M.M., 1988: Geochemical classification of terrigenous sands and shales from core or log data. J. Sediment. Petrol. 58, 820–829.

Hochstetter, E.W.v., 1897. Die Klippe von St. Veit bei Wien. Jahrb. d. k. k. geol. R.-A., XLVII., 95.

Hubert, J. T.: Zircon-tourmaline-rutile maturity index and interdependence of the composition of heavy minerals assemblages with the gross composition and texture of sandstones. J. Sed pet., 1962; 32:440–450.

Iqbal, S., Wagreich, M., Jan, I., Kuerschner W., Gier S., (2018): A southern hemisphere record of climate change during theTriassic-Jurassic transition: Evidence for hot house climate from the Salt Range, Pakistan

Ingersoll, R.V., Bullard, T.F., Ford, R.L., Grimm, J.P., Pickle, J.D., Sares, S.W., 1984. The effect of grain size on detrital modes: a test of the Gazzi-Dickinson point-counting method. J. Sediment. Petrol. 46, 620–632.

Janoschek, R., Küpper, H. & Zirkl, E.J., 1956. Beiträge zur Geologie des Klippenbereiches bei Wien. Mitt. Österr. Geol. Ges., 47, 235-308.

Klepper, M.R., and Wyant, D.G., 1957, Notes on the geology of uranium: U.S. Geological Survey Bulletin 1046-F, p. 87–147

Kröll et. al 1993: Erläuterungen zu den Karten über den Untergrund des Wiener Beckens und der angrenzenden Gebiete, Geol. Bundesanstalt, Wien 1993, 16-19

Lahtinen, R. 2012: Main geological features of Fennoscandia. Geological Survey of Finland, Special Paper 53, 13–18,

Lein, R., 1987: Evolution of the Northern Calcareous Alps during Triassic times. - In: FLÜGEL, H. & FAUPL, P (eds.): Geodynamics of the Eastern Alps, 85-102, Wien (Deuticke).

Lindsay, D. 1999: An evaluation of alternative chemical classifications of sandstones, USGS, 1999

Mandl G.W. 2000: The Alpine sector of the Tethyan shelf - Examples of Triassic to Jurassic sedimentation and deformation from the Northern Calcareous Alps - Mitt. Geol. Ges., ISSN 0251 – 7493, 92 (1999), 61-77, Wien 2000.

Mange u. Maurer 1991: Schwerminerale in Farbe, Stuttgart: Enke 1991, 41-43, 45-46, 107-108, 128-129

McBride, E., F., 1963: A classification of modern sandstones; J. Sed pet., Vol. 33, No.3, 664-669, 1963.

McLennan, S.M., Hemming, S., McDaniel, D.K., Hanson, G.N., 1993: Geochemical approaches to sedimentation, provenance and tectonics. In: Johnsson, M.J., Basu, A. (Eds.), Processes Controlling the Composition of Clastic Sediments, Geological Society of America, Special Papers 285, pp. 21–40.

McLennan, S. M. (2001): Relationships between the trace element composition of sedimentary rocks and upper continental crust. Geochemistry Geophysics Geosystems **2**, paper number 2000GC000109, April 20, 2001.

Nesbitt, H.W., Young, G.M., 1982: Early Proterozoic climates and plate motions inferred from major element chemistry of lutites. Nature 199, 715–717.

Nwajide, C.S., and Hoque, MProblem of classification and maturity. Evaluation of a diagnostically altered fluvial Sandstone. Geologic on Nujibouw,1985; vol.64 p 67-70.

Oberhauser, R.1980: Der geologische Aufbau Österreichs, Wien, New York: Springer 1980.

Paul, J., Wemmer, K. & Wetzel, F. 2009: Keuper (Late Triassic) sediments in Germany – indicators of rapid uplift of Caledonian rocks in southern Norway. *Norwegian Journal of Geology,* vol. 89, pp 193-202, Trondheim 2009, ISSN 029-196X.

Peterson, John Aaron, "Geochemical Provenance of Clastic Sedimentary Rocks in the Western Cordillera: Utah, Colorado, Wyoming,and Oregon." (2009), All Graduate Theses and Dissertations. 439.

Pettijohn, F., Potter, P., & Siever, R. (1972): Sands and Sandstones. Springer-Verlag. New York. 618.

Pettijohn, F.J. (1975): Sedimentary Rocks. 2nd Edition, Harper and Row Publishers, New York, 628 p.

Pfersmann, G., 2013: Stratigraphy, lithofacies and geochemistry of the St. Veit Klippenzone and the Flysch units from the Lainz tunnel, Vienna, Vienna 2013

Prey, S., 1975. Neue Forschungsergebnisse über Bau und Stellung der Klippenzone des Lainzer Tiergartens in Wien (Österreich). Ver. Geol. Bundesanst., 1975, 1-15.

Roser, B.P. and Korsch, R.J.,1986: Determination of tectonic setting of sandstone-mudstone suites using SiO2 content and K2O/Na2O ratio. J. Geol. 94, 635–650.

Roser, B.P. and Korsch, R.J.,1988: Provenance signatures of sandstone-mudstone suites determined using discriminant function analysis of major-element data. Chemical Geology, 67, 119-139.

Rudnick, R. L., & Gao, S. (2003) The Composition of the Continental Crust. In *Treatise on* Geochemistry. Elsevier–Pergamon, Oxford–London. Vol. 3, p. 1-64.

Rychliñski, T. 2008: Facies development and sedimentary enviroments of the Carpathian Keuper deposits from the Tatra Mountains, Poland and Slovakia. *Annales Societatis Geologorum Poloniae*, 78: 1–18.

Schmidt, V. and D.A. McDonald 1979: The role of secondary porosity in the course of sandstone dia-genesis. Society of Economic Paleontologists and Mineralogists, Special Publication no. 26, p. 175-208.

Suttner, L. J., and Dutta, P. K.: Alluvial sandstone composition and paleoclimate. I. Framework mineralogy. J. Sed. Petrol. 1986; 56, 329–345.

Tollmann, A.: Tektonische Karte d. nördlichen Kalkalpen, 1. Teil: Der Ostabschnitt. — Mitt. Geol. Ges. Wien, 59. Bd., 1966, H. 2, Wien 1967.

Tollmann, A.: Der karpatische Einfluß am Ostrand der Alpen. — Mitt. Geol. Ges. Wien, 64. Bd., 1971, Wien 1972.

Trauth, F., 1930. Geologie der Klippenregion von Ober-St.Veit und des Lainzer Tiergartens. Mitteilungen der Geologischen Gesellschaft in Wien, 21 (1928), 35-132.

Wessely, G.: Ein Fossilfundpunkt im Lias von Groisbach (N.-Ö.) und seine geologische Stellung. - Verh. Geol. B.-A., 1967/1-2, 37-50, Wien 1967.

Wessely,G.: Rand und Untergrund des Wiener Beckens - Verbindungen und Vergleiche. - Mitt. Geol. Ges. Wien, 66/67 (1973-74), 265-287, Wien 1975.

Wessely,G.: Bericht 1992 über geologische Aufnahmen in den Kalkalpen auf Blatt 57 Neulengbach - Verh. Geol. B.-A.,1992, 566-567, Wien 1992

Wessely,G.: The Calcareous Alps below the Vienna Basin in Austria and their structural and facial development in the Alpine-Carpathian border zone, Geologica Carpathia, 43,6, December, Bratislava 1992, 347-353

Wurster, P. 1964: Geologie des Schilfsandsteins. Mitteilungen des Geologischen Staatsinstitutes Hamburg *13*, 1-144.

Young, S.W., 1976: Petrographic textures of detrital polycrystalline quartz as an aid to interpreting crystalline source rocks. J. Sediment. Petrol. 46, 595–603.

10. Appendix

10.1 XRD-results

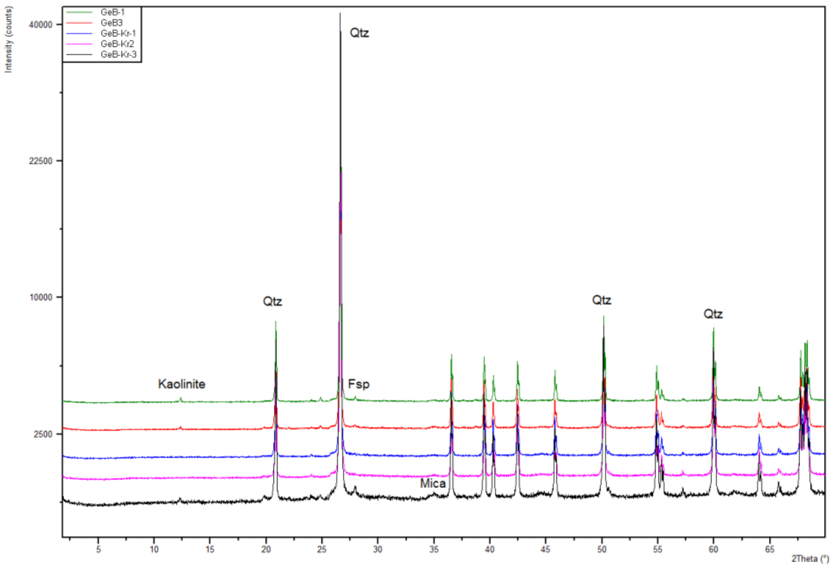

Appendix 1: X-ray patterns of 5 Gemeindeberg (Ober St.Veit) sandstones

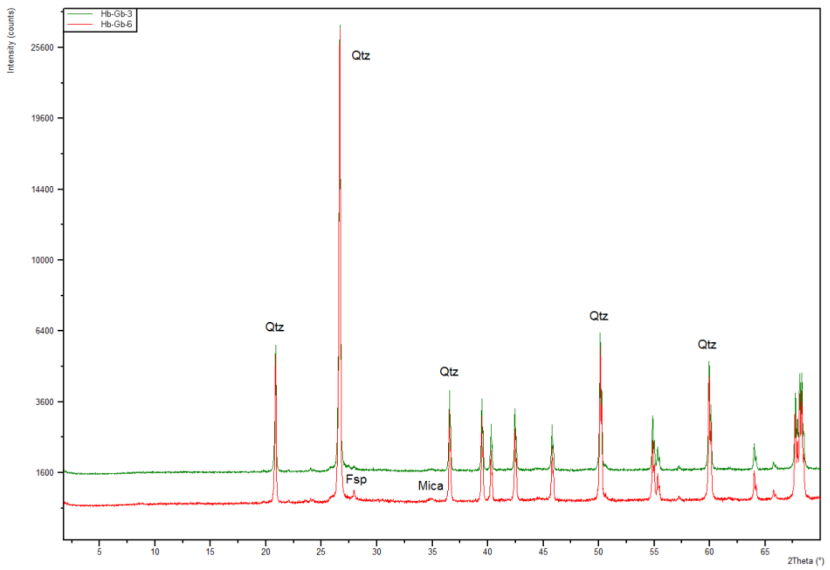

Appendix 2: X-ray patterns of 2 dislodged slices of Hinterbrühl (Lower Austria)

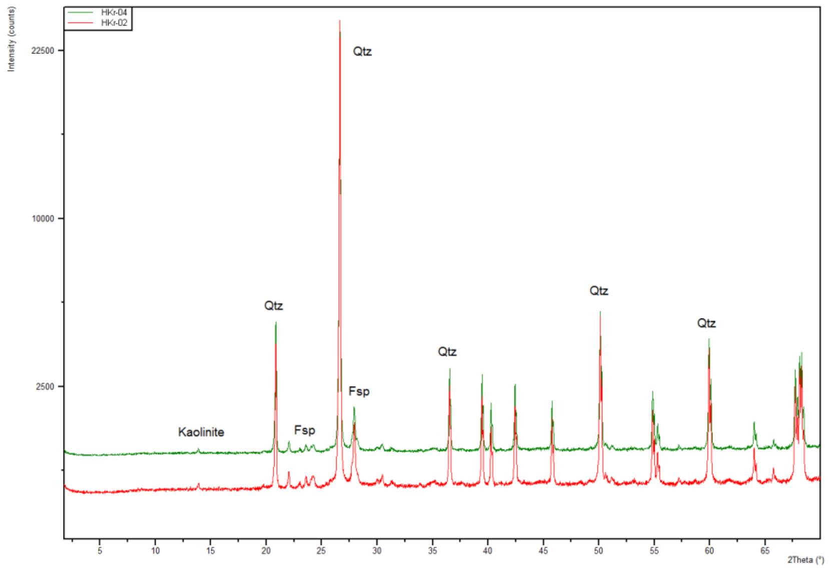

Appendix 3: X-ray patterns of 2 dislodged slices of Heiligenkreuz (Lower Austria)

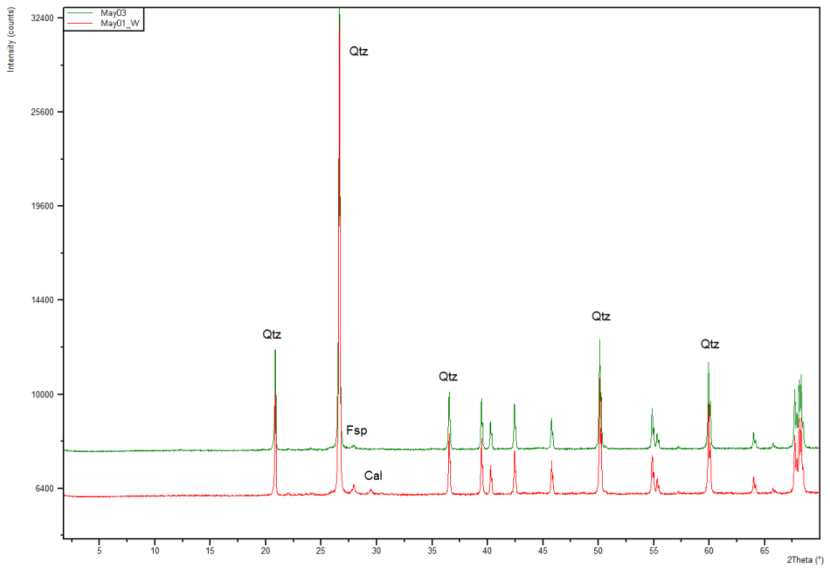

Appendix 4: X-ray patterns of 2 dislodged slices of Mayerling (Lower Austria)

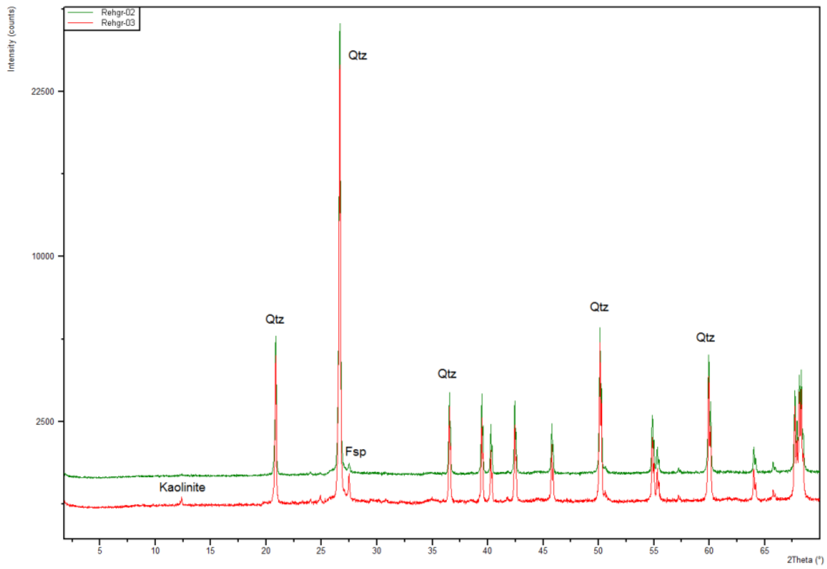

Appendix 5: X-ray patterns of 2 dislodged slices of Rehgras (Lower Austria)

10.2 Gazzi Dickinson point counting

Sample	1164,5m	%	%(gesamt)	1200m	%	%(gesamt)	1215,5m	%	%(gesamt)	1277,2m	%	%(gesamt)
Qm (slight u.ex), <10°	7	16,28	2,24	8	15,09	2,51	1	2,38	0,30	2	11,76	0,61
Qm (undul. ex.), >10°	36	83,72	11,50	45	84,91	14,11	41	97,62	12,42	15	88,24	4,60
Total	**43**	**100,00**	**13,74**	**53**	**100,00**	**16,61**	**42**	**100,00**	**12,73**	**17**	**100,00**	**5,21**
Qp2	24	10,08	7,67	28	11,52	8,78	28	11,16	8,48	13	5,04	3,99
Qp3	11	4,62	3,51	12	4,94	3,76	16	6,37	4,85	6	2,33	1,84
Qp>3	203	85,29	64,86	203	83,54	63,64	207	82,47	62,73	239	92,64	73,31
**Qp elong.*	2	0,84	0,64	8	3,29	2,51	3	1,20	0,91	2	0,78	0,61
**Qp tripple. gr. b.*	5	2,10	1,60	29	11,93	9,09	6	2,39	1,82	9	3,49	2,76
**(+mica (Lm))*	44	18,49	14,06	63	25,93	19,75	43	17,13	13,03	80	31,01	24,54
Total	**238**	**100,00**	**76,04**	**243**	**100,00**	**76,18**	**251**	**100,00**	**76,06**	**258**	**100,00**	**79,14**
Fsp.	4	26,67	1,28	0	0,00	0,00	4	16,67	1,21	1	4,76	0,31
Fsp (exsolution l.)	1	6,67	0,32	1	100,00	0,31	4	16,67	1,21	1	4,76	0,31
Sec. Por. (Relicts of F.)	10	66,67	3,19	0	0,00	0,00	16	66,67	4,85	19	90,48	5,83
Total	**15**	**100,00**	**4,79**	**1**	**100,00**	**0,31**	**24**	**100,00**	**7,27**	**21**	**100,00**	**6,44**
grain replacive kaolinite	0		0,00	0		0,00	0		0,00	0		0,00
Chert	0		0,00	6		1,88	0		0,00	1		0,31
Mica	1		0,32	1		0,31	0		0,00	1		0,31
Sec. Porosity	14		4,47	0		0,00	8		2,42	2		0,61
Lithic fragments												
***Felsic fr.**	2	100,00	0,64	2	13,33	0,63	2	40,00	0,61	6	23,08	1,84
***Ls**	0		0,00	11	73,33	3,45	1	20,00	0,30	17	65,38	5,21
***Lm**	0		0,00	2	13,33	0,63	2	40,00	0,61	3	11,54	0,92
Total	**2**	**100,00**	**0,64**	**15**	**100,00**	**4,70**	**5**	**100,00**	**1,52**	**26**	**100,00**	**6,13**
Total	**313**		**100,00**	**319**		**100,00**	**330**		**100,00**	**326**		**98,16**

Appendix 6: Count results of 4 Lainz tunnel sandstones (St. Veit Klippenzone)

Sample	Geb.1-1	%	%(gesamt)	Geb.02-1	%	%(gesamt)	Geb.Kr.1	%	%(gesamt)	Geb.Kr.3	%	%(gesamt)
Qm (slight u.ex), <10°	2	12,50	0,60	1	8,33	0,33	1	4,17	0,30	1	12,50	0,31
Qm (undul. ex.), >10°	14	87,50	4,18	11	91,67	3,59	23	95,83	7,01	7	87,50	2,15
Total	**16**	**100,00**	**4,78**	**12**	**100,00**	**3,92**	**24**	**100,00**	**7,32**	**8**	**100,00**	**2,46**
Qp2	13	4,92	3,88	7	2,71	2,29	15	5,49	4,57	11	4,21	3,38
Qp3	13	4,92	3,88	10	3,88	3,27	14	5,13	4,27	8	3,07	2,46
Qp>3	238	90,15	71,04	241	93,41	78,76	244	89,38	74,39	242	92,72	74,46
**Qp elong.*	1	0,38	0,30	2	0,78	0,65	6	2,20	1,83	4	1,53	1,23
**Qp tripple. gr. b.*	5	1,89	1,49	37	14,34	12,09	28	10,26	8,54	13	4,98	4,00
**(+mica (Lm))*	61	23,11	18,21	102	39,53	33,33	118	43,22	35,98	124	47,51	38,15
Total	**264**	**100,00**	**78,81**	**258**	**100,00**	**84,31**	**273**	**100,00**	**83,23**	**261**	**100,00**	**80,31**
Fsp.	2	11,11	0,60	4	33,33	1,31	1	10,00	0,30	5	25,00	1,54
Fsp (exsolution l.)	1	5,56	0,30	2	16,67	0,65	1	10,00	0,30	1	5,00	0,31
Sec. Por. (Relicts of F.)	15	83,33	4,48	6	50,00	1,96	8	80,00	2,44	14	70,00	4,31
Total	**18**	**100,00**	**5,37**	**12**	**100,00**	**3,92**	**10**	**100,00**	**3,05**	**20**	**100,00**	**6,15**
grain replacive kaolinite	20		5,97	0		0,00	2		0,61	6		1,85
Chert	0		0,00	0		0,00	1		0,30	1		0,31
Mica	1		0,30	0		0,00	0		0,00	1		0,31
Sec. Porosity	14		4,18	13		4,25	15		4,57	20		6,15
Lithic fragments												
*Felsic fr.	0	33,33	0,00	0		0,00	0	0,00	0,00	0		
*Ls	1	66,67	0,30	7	63,64	2,29	2	66,67	0,61	5	62,50	1,54
*Lm	1		0,30	4	36,36	1,31	1	33,33	0,30	3	37,50	0,92
Total	**2**	**100,00**	**0,60**	**11**	**100,00**	**3,59**	**3**	**100,00**	**0,91**	**8**	**100,00**	**2,46**
Total	335		100,00	306		100,00	328		100,00	325		100,00

Appendix 7: Count results of 4 Gemeindeberg sandstones (St. Veit Klippenzone)

Sample	Hb.Gb.1-2	%	%(gesamt)	Hb.Gb.2-2	%	%(gesamt)	Hb.Gb.3	%	%(gesamt)	Hb.Gb.6	%	%(gesamt)
Qm (slight u.ex), <10°	1	1,61	0,32	1	2,00	0,31	2	2,15	0,64	2	2,94	0,58
Qm (undul. ex.), >10°	61	98,39	19,61	49	98,00	15,31	91	97,85	29,07	66	97,06	19,02
Total	**62**	**100,00**	**19,94**	**50**	**100,00**	**15,63**	**93**	**100,00**	**29,71**	**68**	**100,00**	**19,60**
Qp2	41	18,47	13,18	28	11,43	8,75	28	14,00	8,95	56	21,88	16,14
Qp3	27	12,16	8,68	29	11,84	9,06	27	13,50	8,63	34	13,28	9,80
Qp>3	154	69,37	49,52	188	76,73	58,75	145	72,50	46,33	166	64,84	47,84
**Qp elong.*	8	3,60	2,57	2	0,82	0,63	4	2,00	1,28	3	1,17	0,86
**Qp tripple. gr. b.*	24	10,81	7,72	10	4,08	3,13	10	5,00	3,19	25	9,77	7,20
**(+mica, Fsp(Lm))*	84	37,84	27,01	86	35,10	26,88	57	28,50	18,21	104	40,63	29,97
Total	**222**	**100,00**	**71,38**	**245**	**100,00**	**76,56**	**200**	**100,00**	**63,90**	**256**	**100,00**	**73,78**
Fsp.	15	75,00	4,82	8	66,67	2,50	11	73,33	3,51	2	14,29	0,58
Fsp (exsolution l.)	4	20,00	1,29	3	25,00	0,94	3	20,00	0,96	5	35,71	1,44
Sec. Por. (Relicts of F.)	1	5,00	0,32	1	8,33	0,31	1	6,67	0,32	7	50,00	2,02
Total	**20**	**100,00**	**6,43**	**12**	**100,00**	**3,75**	**15**	**100,00**	**4,79**	**14**	**100,00**	**4,03**
grain replacive kaolinite	0		0,00	0		0,00	0		0,00	0		0,00
Chert	0		0,00	0		0,00	0		0,00	0		0,00
Mica	0		0,00	0		0,00	0		0,00	0		0,00
Sec. Porosity	2		0,64	1		0,31	0		0,00	5		1,44
Lithic fragments												
*Felsic fr.	0	33,33	0,00	0		0,00	4	80,00	1,28	2	50,00	0,58
*Ls	0	66,67	0,00	7	58,33	2,19	1	20,00	0,32	2	50,00	0,58
*Lm	5		1,61	5	41,67	1,56	0	0,00	0,00	0	0,00	0,00
Total	**5**	**100,00**	**1,61**	**12**	**100,00**	**3,75**	**5**	**100,00**	**1,60**	**4**	**100,00**	**1,15**
Total	311		100,00	320		100,00	313		100,00	347		100,00

Appendix 8: Count results of 4 dislodged slices of Hinterbrühl (Lower Austria)

Sample	Hkr.01	%	%(gesamt)	Hkr.02-1	%	%(gesamt)	Hkr.03	%	%(gesamt)	Hkr.04	%	%(gesamt)
Qm (slight u.ex), <10°	2	8,33	0,62	2	8,00	0,63	6	14,29	1,89	4	10,53	1,24
Qm (undul. ex.), >10°	22	91,67	6,79	23	92,00	7,28	36	85,71	11,32	34	89,47	10,53
Total	**24**	**100,00**	**7,41**	**25**	**100,00**	**7,91**	**42**	**100,00**	**13,21**	**38**	**100,00**	**11,76**
Qp2	14	5,98	4,32	15	6,00	4,75	24	9,92	7,55	6	2,64	1,86
Qp3	14	5,98	4,32	12	4,80	3,80	20	8,26	6,29	14	6,17	4,33
Qp>3	206	88,03	63,58	223	89,20	70,57	198	81,82	62,26	207	91,19	64,09
**Qp elong.*	8	3,42	2,47	7	2,80	2,22	4	1,65	1,26	4	1,76	1,24
**Qp tripple. gr. b.*	11	4,70	3,40	14	5,60	4,43	23	9,50	7,23	18	7,93	5,57
**(+mica,)(Lm))*	56	23,93	17,28	52	20,80	16,46	34	14,05	10,69	75	33,04	23,22
Total	**234**	**100,00**	**72,22**	**250**	**100,00**	**79,11**	**242**	**100,00**	**76,10**	**227**	**100,00**	**70,28**
Fsp.	25	43,10	7,72	13	36,11	4,11	14	50,00	4,40	24	52,17	7,43
Fsp (exsolution l.)	30	51,72	9,26	20	55,56	6,33	13	46,43	4,09	22	47,83	6,81
Sec. Por. Within F.	3	5,17	0,93	3	8,33	0,95	1	3,57	0,31	0	0,00	0,00
Total	**58**	**100,00**	**17,90**	**36**	**100,00**	**11,39**	**28**	**100,00**	**8,81**	**46**	**100,00**	**14,24**
grain replacive kaolinite	0			0			0			0		
Chert	1		0,31	0			2		0,63	0		
Mica	0			0			0			3		0,93
Sec. Porosity	1		0,31	1		0,32	0			3		0,93
Lithic fragments												
***Felsic fr.**	2	33,33	0,62	0			1	25,00	0,31	0		
***Ls**	4	66,67	1,23	3	75,00	0,95	2	50,00	0,63	2	33,33	0,62
***Lm**	0			1	25,00	0,32	1	25,00	0,31	4	66,67	1,24
Total	**6**	**100,00**	**1,85**	**4**	**100,00**	**1,27**	**4**	**100,00**	**1,26**	**6**	**100,00**	**1,86**
Total	**324**		**100,00**	**316**		**100,00**	**318**		**100,00**	**323**		**100,00**

Appendix 9: Count results of 4 dislodged slices of Heiligenkreuz (Lower Austria)

Sample	Rehgr.03-2	%	%(gesamt)
Qm (slight u.ex), <10°	2	2,25	0,57
Qm (undul. ex.), >10°	87	97,75	24,72
Total	**89**	**100,00**	**25,28**
Qp2	42	21,65	11,93
Qp3	21	10,82	5,97
Qp>3	131	67,53	37,22
**Qp elong.*	2	1,03	0,57
**Qp tripple. gr. b.*	5	2,58	1,42
**(+mica, Fsp(Lm))*	56	28,87	15,91
Total	**194**	**100,00**	**55,11**
Fsp.	19	57,58	5,40
Fsp (exsolution l.)	3	9,09	0,85
Sec. Por. (Relicts of F.)	11	33,33	3,13
Total	**33**	**100,00**	**9,38**
grain replacive kaolinite	4		1,14
Chert	0		0,00
Mica	1		0,28
Sec. Porosity	18		5,11
Lithic fragments			
***Felsic fr.**	6	33,33	1,70
***Ls**	7	66,67	1,99
***Lm**	0		0,00
Total	**13**	**100,00**	**3,69**
Total	**352**		**100,00**

Appendix 9: Count results of 1 dislodged slice of Rehgras (Lower Austria)

10.3 Calculations (Point counting)

	Qm	Qp	Chert	summe	Qm (%)	Qp (%)	Chert (%)
LT31/1164,5m	43	238	0	281	15,3	84,7	0,0
LT31/1200m	53	243	6	302	17,5	80,5	2,0
LT31/1215,5m	42	251	0	293	14,3	85,7	0,0
LT31/1277,2m	17	258	1	276	6,2	93,5	0,4
GeB.1-1	16	264	0	280	5,7	94,3	0,0
GeB.02-1	12	258	0	270	4,4	95,6	0,0
GeB.Kr.1	24	273	1	298	8,1	91,6	0,3
GeB.Kr.3	8	261	1	270	3,0	96,7	0,4
Hkr.01	24	234	1	259	9,3	90,3	0,4
Hkr.02-1	25	250	0	275	9,1	90,9	0,0
Hkr.03	42	242	2	286	14,7	84,6	0,7
Hkr.04	38	227	0	265	14,3	85,7	0,0
Hb.Gb.1-2	62	222	0	284	21,8	78,2	0,0
Hb.Gb.2-2	50	245	0	295	16,9	83,1	0,0
Hb.Gb.3	93	200	0	293	31,7	68,3	0,0
Hb.Gb.6	68	256	0	324	21,0	79,0	0,0
Rehgr.03-2	89	194	0	283	31,4	68,6	0,0

Appendix 10: calculations for a Qm-Qp-chert triplot

Sample	MMI (Q/(F+L))	Qp/(F+L)
LT31/1164,5m	9,1	7,7
LT31/1200m	18,9	15,6
LT31/1215,5m	7,9	6,8
LT31/1277,2m	6,4	6,0
GeB.1-1	5,2	4,9
GeB.02-1	7,5	7,2
GeB.Kr.1	9,9	9,1
GeB.Kr.3	5,0	4,8
Hkr.01	4,0	3,7
Hkr.02-1	6,7	6,2
Hkr.03	8,9	7,6
Hkr.04	4,8	4,4
Hb.Gb.1-2	10,5	8,2
Hb.Gb.2-2	11,8	9,8
Hb.Gb.3	14,6	10,0
Hb.Gb.6	14,1	11,1
Rehgr.03-2	4,4	2,9

Appendix 11: calculations for a Qp(/F+L) vs. Qt/(F+L) plot after Suttner and Dutta (1986)

Sample	sample site	correlation	Qm (%)	F (%)	Lt (%)	summe
LT31/1164,5m	Lainz tunnel	St. Veit Klippenzone	13,7	9,3	76,7	99,7
LT31/1200m	Lainz tunnel	St. Veit Klippenzone	16,6	0,3	82,8	99,7
LT31/1215,5m	Lainz tunnel	St. Veit Klippenzone	12,7	9,7	77,6	100,0
LT31/1277,2m	Lainz tunnel	St. Veit Klippenzone	5,2	7,1	85,3	97,6
GeB.1-1	Gemeindeberg	St. Veit Klippenzone	4,8	15,5	79,4	99,7
GeB.02-1	Gemeindeberg	St. Veit Klippenzone	3,9	8,2	87,9	100,0
GeB.Kr.1	Gemeindeberg	St. Veit Klippenzone	7,3	8,2	84,2	99,7
GeB.Kr.3	Gemeindeberg	St. Veit Klippenzone	2,5	14,2	82,8	99,4
Hkr.01	Heiligenkreuz	dislodged slice	7,4	18,2	74,4	100,0
Hkr.02-1	Heiligenkreuz	dislodged slice	7,9	11,7	80,4	100,0
Hkr.03	Heiligenkreuz	dislodged slice	13,2	8,8	78,0	100,0
Hkr.04	Heiligenkreuz	dislodged slice	11,8	15,2	72,1	99,1
Hb.Gb.1-2	Hinterbrühl	dislodged slice	19,9	7,1	73,0	100,0
Hb.Gb.2-2	Hinterbrühl	dislodged slice	15,6	4,1	80,3	100,0
Hb.Gb.3	Hinterbrühl	dislodged slice	29,7	4,8	65,5	100,0
Hb.Gb.6	Hinterbrühl	dislodged slice	19,6	5,5	74,9	100,0
Rehgr.03-2	Rehgras	dislodged slice	25,3	15,6	58,6	99,5
mean			12,8	9,6	77,3	99,7

Appendix 12: calculations for the Qm-F-Lt triplot after Dickinson and Suszeck (1983)

10.4 Geochemical calculations

	Geb.1-1	Geb.Kr.3	Hkr.02	Hkr.04	Hb.Gb.3	Rehgr.03-2
Q/(F+RF)	5,19	4,89	3,97	4,82	14,65	4,16
SiO2/Al2O3 (%)	37,64	37,12	27,27	28,04	75,92	33,16

Appendix 13: calculations for a Q/(F+RF) vs. SiO_2/Al_2O_3 plot after Pettijohn (1975)

	Rehgr.02	Rehgr.03	Hkr.02	Hkr.04	Hb.Gb.3	GeB.1	GeB.Kr.3	Gr.S.01	Gr.S.04
SiO2	96,18	93,5	92,98	93,64	97,94	94,47	94,28	76,99	78,29
Al2O3+K2O+Na2O	1,96	4,09	5,34	5,19	2,09	3,12	3,26	12,03	9,03

Appendix 14: calculations (%) for a SiO_2 vs. $Al_2O_3+K_2O+Na_2O$ plot after Suttner and Dutta (1986)

	Rehgr.02	Rehgr.03	Hkr.02	Hkr.04	Hb.Gb.3	GeB.1	GeB.Kr.3	Gr.S.01	Gr.S.04
K2O/Na2O	0,64	6,06	0,25	0,23	2,20	1,26	1,57	0,79	6,11
SiO2	96,18	93,50	92,98	93,64	97,94	94,47	94,28	76,99	78,29

Appendix 15: calculations (%) for a K_2O/Na_2O vs. SiO_2 plot after Roser and Korsch (1986)

	Rehgr.02	Rehgr.03	Hkr.02	Hkr.04	GeB.1	GeB.Kr.3	Gr.S.01	Gr.S.04
La/Sc	18,86	26,94	13,74	40,31	11,44	9,28	1,54	3,19
Th/Co	0,74	1,06	1,22	1,28	0,86	0,82	5,05	1,97

Appendix 16: calculations (ppm) for a La/Sc vs. Th/Co plot after Cullers (2002)

	Rehgr.02	Rehgr.03	Hkr.02	Hkr.04	GeB.1	GeB.Kr.3	Gr.S.01	Gr.S.04
Zr/Sc	95,79	289,59	44,68	178,25	47,93	77,08	8,38	9,73
Th/Sc	6,78	13,60	3,27	11,23	4,26	7,04	1,29	1,75

Appendix 17: calculations (ppm) for a Zr/Sc vs. Th/Sc plot after McLennan (1993)

	Rehgr.02	Rehgr.03	Hkr.02	Hkr.04	Hb.Gb.3	GeB.1	GeB.Kr.3	Gr.S.01	Gr.S.04
Th	39,1	31,2	37,4	37,4	56,2	42,4	44,7	41,3	47,0
Sc	5,8	2,3	11,4	3,3	0,0	9,9	6,4	31,9	26,9
Zr/10	55,2	66,5	51,1	59,3	43,8	47,7	48,9	26,8	26,2
total	100,0	100,0	100,0	100,0	100,0	100,0	100,0	100,0	100,0

Appendix 18: calculations (%) for a Th-Sc-Zr/10 triplot after Bathia and Crook (1986)

	Rehgr.02	Rehgr.03	Hkr.02	Hkr.04	Hb.Gb.3	GeB.1	GeB.Kr.3	Gr.S.01	Gr.S.04
La	70,8	64,9	76,3	76,7	68,1	68,5	53,6	40,2	53,7
Th	25,5	32,7	18,1	21,4	31,9	25,5	40,6	33,7	29,4
Sc	3,8	2,4	5,6	1,9	0,0	6,0	5,8	26,1	16,9
total	100,0	100,0	100,0	100,0	100,0	100,0	100,0	100,0	100,0

Appendix 19: calculations (%) for the La-Th-Sc triplot after Bhatia and Crook (1986)

11. List of samples

Sample	Sample site	Correlation	Lithology
LT31/1164,5m	Lainz tunnel	St. Veit Klippenzone	sandstone
LT31/1200m	Lainz tunnel	St. Veit Klippenzone	sandstone/conglomerate
LT31/1215,5m	Lainz tunnel	St. Veit Klippenzone	sandstone
LT31/1277,2m	Lainz tunnel	St. Veit Klippenzone	sandstone
GeB.1	Vienna,Ober St. Veit (Gemeindeberg)	St. Veit Klippenzone	sandstone
GeB.2	Vienna,Ober St. Veit (Gemeindeberg)	St. Veit Klippenzone	sandstone/conglomerate
GeB.3	Vienna,Ober St. Veit (Gemeindeberg)	St. Veit Klippenzone	sandstone/conglomerate
GeB.4	Vienna,Ober St. Veit (Gemeindeberg)	St. Veit Klippenzone	sandstone/conglomerate
GeB.Kr.1	Vienna,Ober St. Veit (Gemeindeberg)	St. Veit Klippenzone	sandstone
GeB.Kr.2	Vienna,Ober St. Veit (Gemeindeberg)	St. Veit Klippenzone	sandstone
GeB.Kr.3	Vienna,Ober St. Veit (Gemeindeberg)	St. Veit Klippenzone	sandstone/conglomerate
GeB.Kr.4	Vienna,Ober St. Veit (Gemeindeberg)	St. Veit Klippenzone	sandstone/conglomerate
Hb.Gb.1	Hinterbrühl (Lower Austria), "Grillenbühel"	dislodged slice	sandstone
Hb.Gb.2	Hinterbrühl (Lower Austria), "Grillenbühel"	dislodged slice	sandstone
Hb.Gb.3	Hinterbrühl (Lower Austria), "Grillenbühel"	dislodged slice	sandstone
Hb.Gb.4	Hinterbrühl (Lower Austria), "Grillenbühel"	dislodged slice	sandstone
Hb.Gb.5	Hinterbrühl (Lower Austria), "Grillenbühel"	dislodged slice	sandstone
Hb.Gb.6	Hinterbrühl (Lower Austria), "Grillenbühel"	dislodged slice	sandstone
Hb.Gb.7	Hinterbrühl (Lower Austria), "Grillenbühel"	dislodged slice	sandstone
Hb.Gb.8	Hinterbrühl (Lower Austria), "Grillenbühel"	dislodged slice	sandstone
Hb.Gb.9	Hinterbrühl (Lower Austria), "Grillenbühel"	dislodged slice	sandstone
Hkr.01	Heiligenkreuz (Lower Austria)	dislodged slice	sandstone
Hkr.02	Heiligenkreuz (Lower Austria)	dislodged slice	sandstone
Hkr.03	Heiligenkreuz (Lower Austria)	dislodged slice	sandstone
Hkr.04	Heiligenkreuz (Lower Austria)	dislodged slice	sandstone
Hkr.05	Heiligenkreuz (Lower Austria)	dislodged slice	sandstone
Hkr.06	Heiligenkreuz (Lower Austria)	dislodged slice	sandstone
May.01	Mayerling (Lower Austria), "Kritschenkogel"	dislodged slice	sandstone
May.02	Mayerling (Lower Austria), "Kritschenkogel"	dislodged slice	sandstone/conglomerate
May.03	Mayerling (Lower Austria), "Kritschenkogel"	dislodged slice	sandstone/conglomerate
May.04	Mayerling (Lower Austria), "Kritschenkogel"	dislodged slice	sandstone/conglomerate
Rehgr.01	Rehgras (Lower Austria)	dislodged slice	sandstone/conglomerate
Rehgr.02	Rehgras (Lower Austria)	dislodged slice	sandstone/conglomerate
Rehgr.03	Rehgras (Lower Austria)	dislodged slice	sandstone/conglomerate
Rehgr.04	Rehgras (Lower Austria)	dislodged slice	sandstone/conglomerate
Rehgr.05	Rehgras (Lower Austria)	dislodged slice	sandstone/conglomerate
Rehgr.06	Rehgras (Lower Austria)	dislodged slice	sandstone/conglomerate
Rehgr.07	Rehgras (Lower Austria)	dislodged slice	sandstone/conglomerate
Gr.1-1	Groisbach (Lower Austria)	dislodged slice	marly sandstone
Gr.1-2	Groisbach (Lower Austria)	dislodged slice	marly sandstone

Gr.1-3	Groisbach (Lower Austria)	dislodged slice	marly sandstone
Gr.1-4	Groisbach (Lower Austria)	dislodged slice	marly sandstone
Gr.1-5	Groisbach (Lower Austria)	dislodged slice	marly sandstone
Gr.1-6	Groisbach (Lower Austria)	dislodged slice	marly sandstone
Hb.1-1	Hafnerberg	Reisalpen nappe	dolosparstone
Hb.1-2	Hafnerberg	Reisalpen nappe	dolosparstone
Hb.1-3	Hafnerberg	Reisalpen nappe	dolosparstone
Hb.1-4	Hafnerberg	Reisalpen nappe	dolosparstone
Hb.1-5	Hafnerberg	Reisalpen nappe	dolosparstone
Hb.1-6	Hafnerberg	Reisalpen nappe	dolosparstone
Hb.1-7	Hafnerberg	Reisalpen nappe	dolosparstone

12. List of figures

13. List of tables